

CHAPETR 4

RESULTS AND DISCUSSION

This chapter describes various results obtained for various investigations carried out. An attempt has also been made to discuss these results in order to provide convincing reasons for the studied performed.

4.1 Preliminary Pharmacognostic Studies

4.1.1 Morphological evaluation

Enicostemma hyssopifolium

It is glabrous perenial herb of 15-20 inch height.

Leaves: Numerous, cauline and ramal, opposite, linear.

Inflorescence: Axillary, cluster all around the stem.

Flower: Small, white, complete.

Fruit: Glabrous ,smooth base, slightly arrowed.

Seed: Numerous, minute, subglobose.

The photographs of the plant and aerial parts are shown in figure 6.



Figure 6 *Enicostemma hyssopifolium* herb.

Gymnema Sylvestre

It is twinning woody climber running over the tops of high trees.

Leaves: Opposite, ovate.

Inflorescence: Lateral umbellate cymes.

Flower: Complete, actinomorphic.

Fruit: Paired, rigid.

Seed: Numerous narrowly ovoid oblong.

The photographs of plants are shown in figure 7.



Figure 7 *Gymnema sylvestre* twig

Tinospora cordifolia

It is woody, extensive deciduous, glabrous twinner with glabrous branches

Leaves: Alternate, cordate

Inflorescence: Axillary, pseudo raceme

Flower: Green, minute, unisexual

Fruit: Drupes

Seed: White, heart shaped, warty.

Photographs are shown in figure 8.



Figure 8 *Tinospora cordifolia* twinner, climbing on neem tree.

Eclipta alba

It is an annual, erect or prostrate entirely pubescent herb.

Leaves: Opposite, sessile, usually oblong, 2.5 - 7.5 cm long leaves with appressed hairs.

Inflorescence: Axillary, terminal, solitary

Flower: Floral heads 6-8 mm in diameter, solitary, white; achene compressed and narrowly winged.

Fruit: Triquetrous, often empty. Photographs are shown in figure 9.



Figure 9 A herb of *Eclipta alba*

4.1.2 Microscopic evaluation

4.1.2.1 *Enicostemma hyssopifolium* Leaf

It is isobilateral leaf.

Epidermis: A single layer of thin walled, rectangular parenchyma with a thick cuticle layer.

Lamina region consists of round or polygonal parenchymatous cells. Some of the cells contain brown matter inside.

Above the lower epidermis 2-6 layers of collenchymatous cells were present in midrib.

In the centre of mid rib, an arc shaped vascular bundle was present with,

Xylem: Lignified vessels present towards upper epidermis.

Phloem: Just below the xylem vessels.

4.1.2.2 *Enicostemma hyssopifolium* stem

Epidermis: It consists of single layer of epidermal cells with thick cuticle.

Cortex: Outer cortex about 2-3 layers consists of collenchyma that are small oval to round shaped cells. Inner cortex which is 7-8 layers consists of large oval to irregular cortical parenchyma.

Phloem: It is present towards both side of xylem and contains colorless, irregular parenchyma.

Xylem: It forms a continuous band thereby appearing like a ring and contains xylem vessels and scanty xylem parenchyma.

Pith: Large and made up of thin walled undignified big polygonal to round parenchyma cells with intercellular spaces.

Microscopic photographs of leaf and stem of *E. hyssopifolium* are presented in figure 10 and 11 respectively.

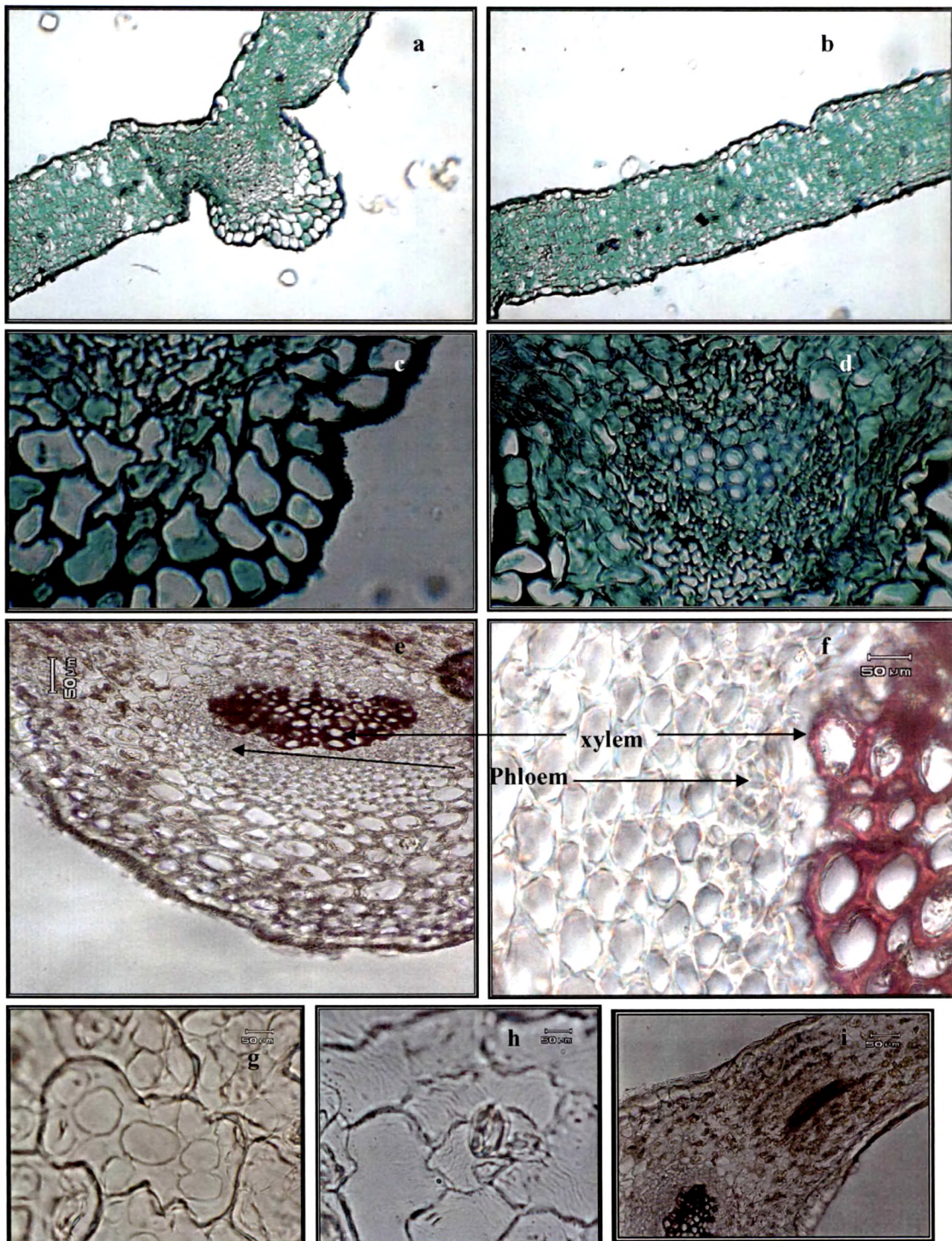


Figure 10 Microscopy of transverse section of *E. hyssopifolium* leaf (a) through midrib (100X) (b) lamina (100X) (c) collenchymatous cells below lower epidermis (d) vascular bundle (e) lower epidermis with collenchyma and vascular bundle (400X) (f) phloem and xylem vessels (400X) (g) surface preparation, palisade cells (h) anisocytic stomata (i) brown matter in lamina cells.

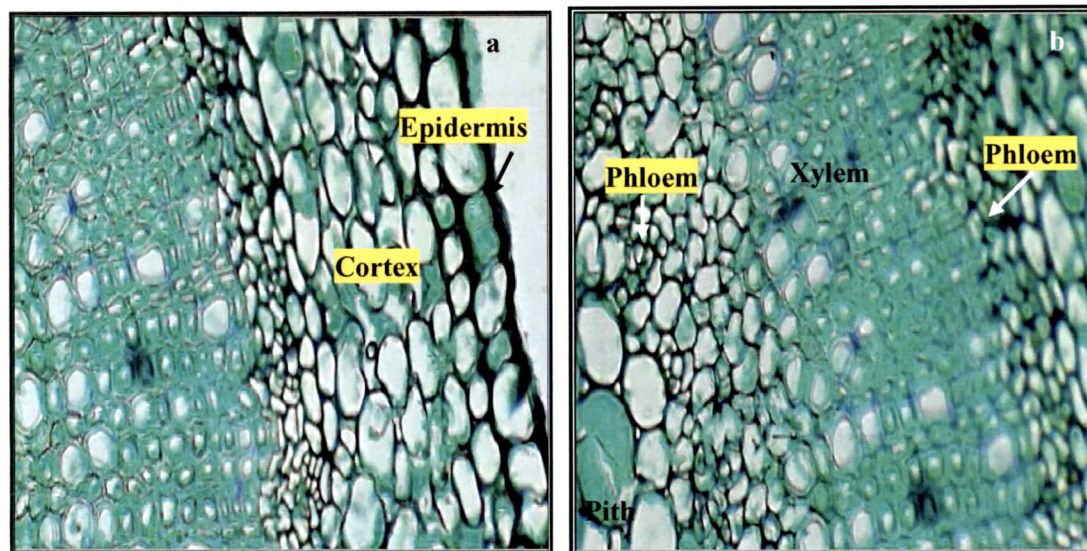


Figure 11 Microscopy of transverse section of *E. hyssopifolium* stem.

4.1.2.3 *Gymnema sylvestre* leaf

It is dorsiventral leaf. The transverse section of the leaf was divided in to two regions, lamina and midrib region.

Epidermis: A single layer of thin walled, rectangular parenchyma with a thick cuticle layer. Upper and lower, both the epidermis shows the presence of multicellular covering trichomes (3-5 cells) which are uniseriate. Trichomes are unligified in nature.

Lamina region consists of round or polygonal parenchymatous cells. Some of the cells contain brown matter inside. Below the upper epidermis are present a single layer of palisade cells which are narrow and elongated in nature containing chloroplast. Below the palisade there is a presence of spongy parenchyma. In spongy parenchyma there can be seen a rossete of calcium oxalate. Next appears lower epidermis which is similar to the upper epidermis. Both Upper and lower epidermis shows the presence of anomocytic stomata.

Midrib: Upper and lower epidermis also extends into midrib region where as palisade do not extend in to the midrib region. Below the upper epidermis and above the lower epidermis (3-5 layers in case of upper epidermis, 2-3 layers in the case of lower epidermis) are present layers of collenchyma. In the centre of the midrib there present well developed bicollateral vascular bundle which is of arch shaped. The photo micrograph of transverse section of leaf and few microscopic diagnostic features are shown in figure 12 and 13.

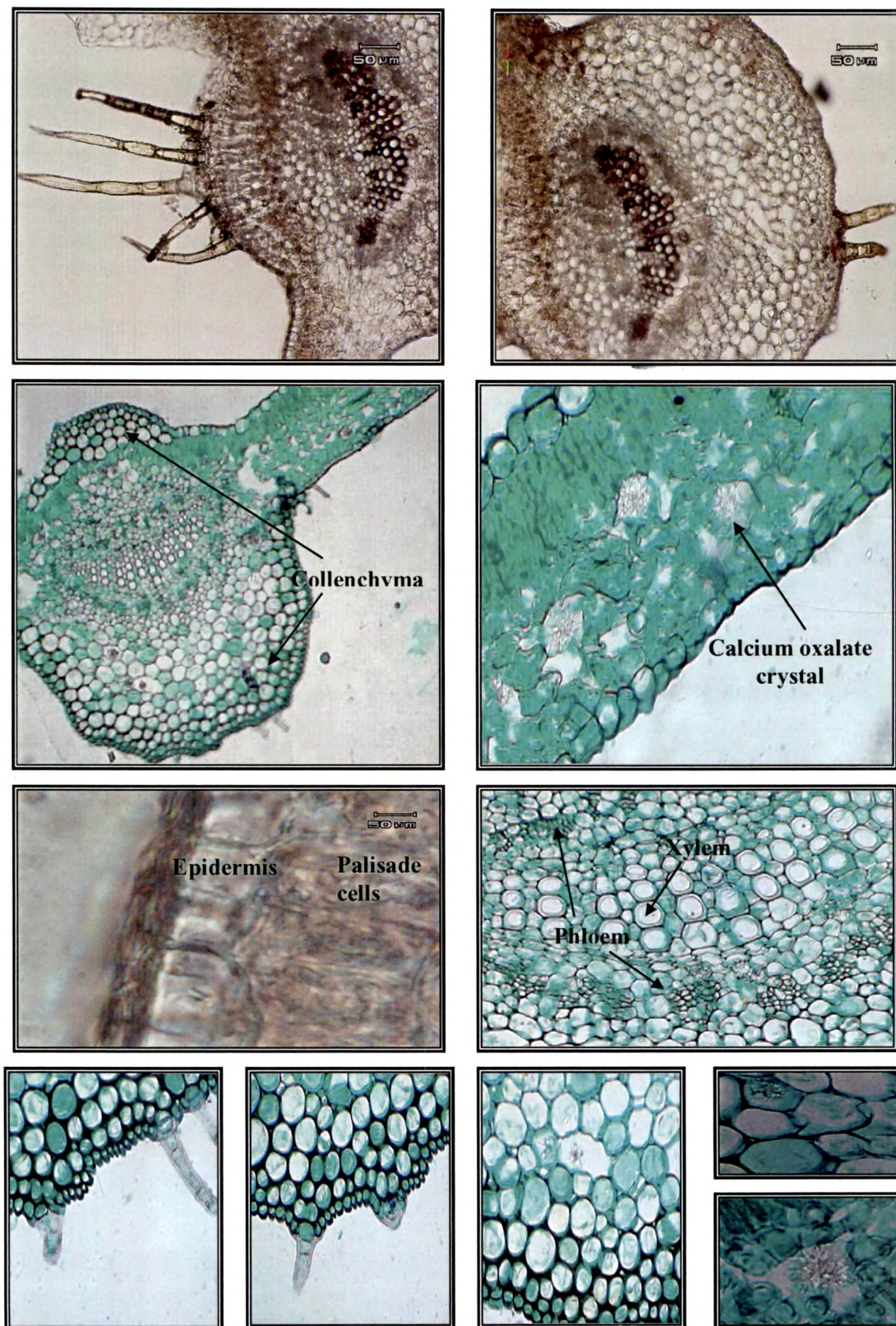


Figure 12 Microscopic characteristics of *G. sylvestre* leaf

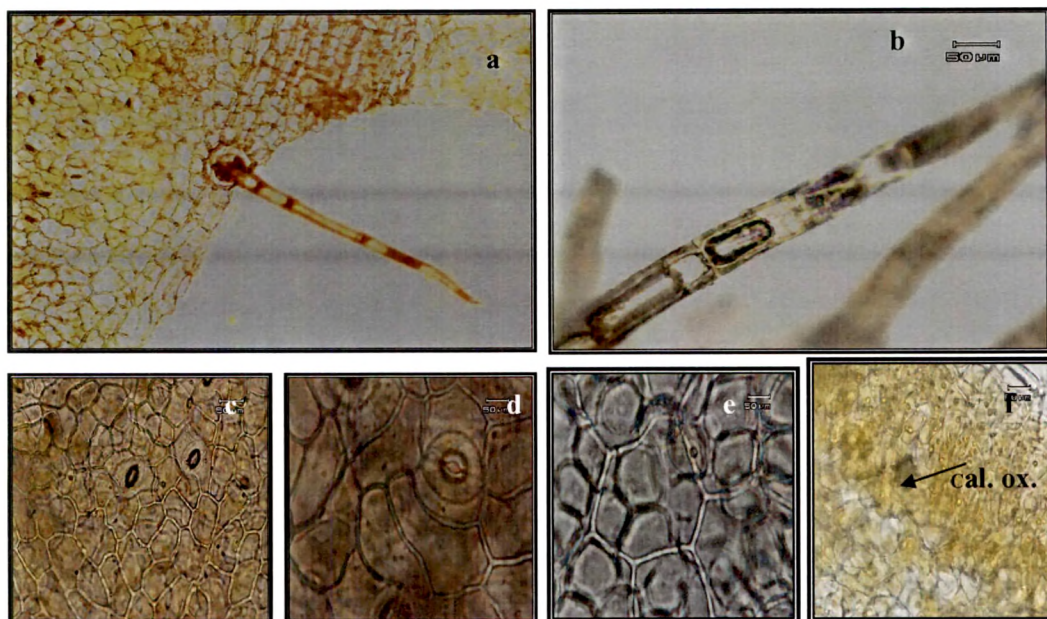


Figure 13 Surface preparation of *G. sylvestre* leaf (a) multicellular trichome (100X) (b) trochome (400X) (c) stomata (100X) (d) paracytic stomata (400X) (e) epidermis with palisade cells underneath (f) spheraphide of calcium oxalate crystal. photo micrograph of transverse section of stem is shown in figure 14.

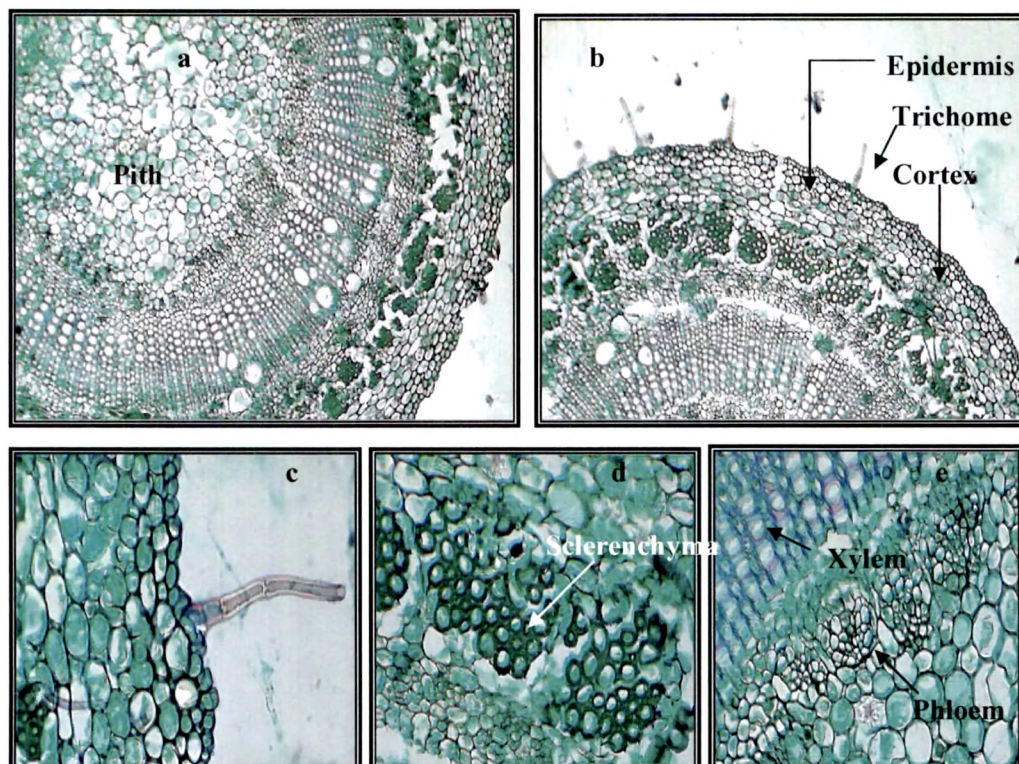


Figure 14 Microscopy of transverse section of (a) *G. sylvestre* stem (b) T.S. under 100X (c) stem hair, epidermis, hypodermis and cortex (d) sclerenchymatous pericycle (e) xylem vessels.

4.1.2.4 *Gymnema sylvestre* stem

Epidermis: It consists of single layer of epidermal cells with cuticle. Numerous covering trichomes which are uniseriate, multicellular unligified are seen. Apex of the trichomes is blunt in the nature.

Cortex: Outer cortex about 2-3 layers consists of collenchyma and inner cortex is many layered consists of large oval to irregular cortical parenchyma. There are small bunches of sclerenchymatous cells arranged in a ring (pericycle) are present above the phloem.

Phloem: It is present towards both side of xylem.

Xylem: It forms a continuous band appeared like a ring.

Pith: Centrally located, large and made up of thin walled unligified big polygonal to round parenchyma cells with intercellular spaces. Some of the pith cells show brownish matter. Photomicrograph of T.S. of *G. sylvestre* stem is shown in figure 14.

4.1.2.5 *Tinospora cordifolia* stem

Epidermis: It consists of single layer of epidermal cells. Cells have with thick wall with brownish pigments inside.

Cortex: Upper 3-4 layers of collenchymatous cells. Starch present. Major non-chlorophyllous region in upper part contains small, rounded parenchymatous cells and in lower part 5-7 layers of thin walled, bigger parenchymatous cells. Starch grains and calcium oxalate crystals are present.

Pericycle: 7-9 layers of lignified sclerenchymatous cells, forming a continuous circle of arches.

Vascular bundles: 16-20 open and collateral. It consist of:

Phloem: Appear like caps over the metaxylem. Calcium oxalate crystals present.

Cambium: Strip of thin walled cambium cell.

Xylem: Wedge shaped patches separated by multiseriate medullary rays. Large number of lignified pitted xylem vessels.

Medullary rays: Thin walled elongated parenchymatous cells. Packed with starch grains.

Pith: Small central parenchymatous portion, loaded with starch grains. Photomicrograph of transverse section of *T. cordifolia* stem are shown in figure 15.

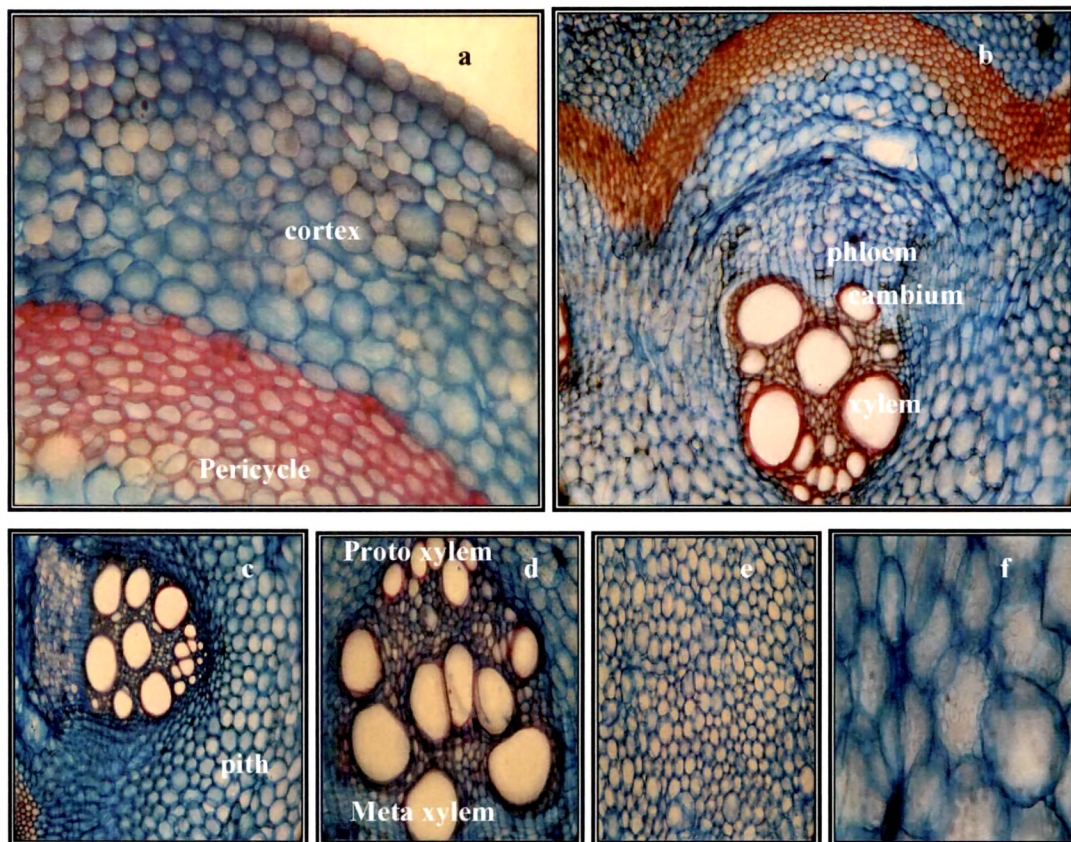


Figure 15 Microscopy of transverse section of *Tinospora cordifolia* stem (a) epidermis, cortex and cambium (b) vascular bundle 400X (c) pith cells (d) xylem vessels, protoxylem toward pith (e) and (f) central pith with starch (100X and 400X respectively).

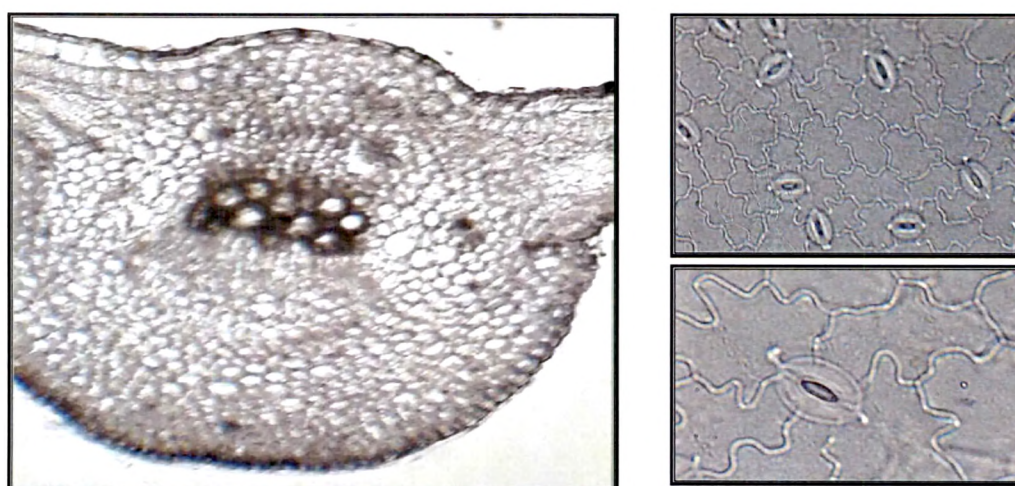


Figure 16 Transverse section of *T. cordifolia* leaf, anomocytic stomata on surface preparation.

4.1.2.6 *Tinospora cordifolia* leaf

It is dorsiventral leaf.

Epidermis: A single layer of thin walled, rectangular parenchyma with a thick cuticle layer.

In the *lamina* region round or polygonal parenchymatous cells are present. Below the upper epidermis are present a single layer of palisade cells which are narrow and elongated in nature. Below the palisade there is a presence of spongy parenchyma. Next appears lower epidermis which is similar to the upper epidermis. Both Upper and lower epidermis shows the presence of anomocytic stomata.

Midrib: Below the upper epidermis and above the lower epidermis (2-3 layers) are present layers of collenchyma. In the centre of the midrib there present well developed arch shaped bicollateral vascular bundle. The photo micrograph of transverse section of leaf is shown in figure 16.

4.1.2.7 *Eclipta alba* leaf

Eclipta alba consists of dorsiventral leaf.

Lamina: Single layer of upper epidermal cells covered with cuticle and the epidermal cells are rectangular in shape. Below the upper epidermis a single layer of palisade cells, narrow and elongated in nature are present. Below the palisade there is a presence of spongy parenchyma. Lower epidermis is similar to the upper epidermis.

Midrib: Upper and lower epidermis also extends into midrib region. Palisade cells are absent. Below the upper epidermis and above the lower epidermis (2-3 layers in case of upper epidermis, 1-2 layers in the case of lower epidermis) collenchymatous cells are present. In the centre of the midrib, an arc shaped, well developed bicollateral vascular bundle is present. Very few covering trichomes were present. The photo micrograph of T S of leaf is shown in figure 17.

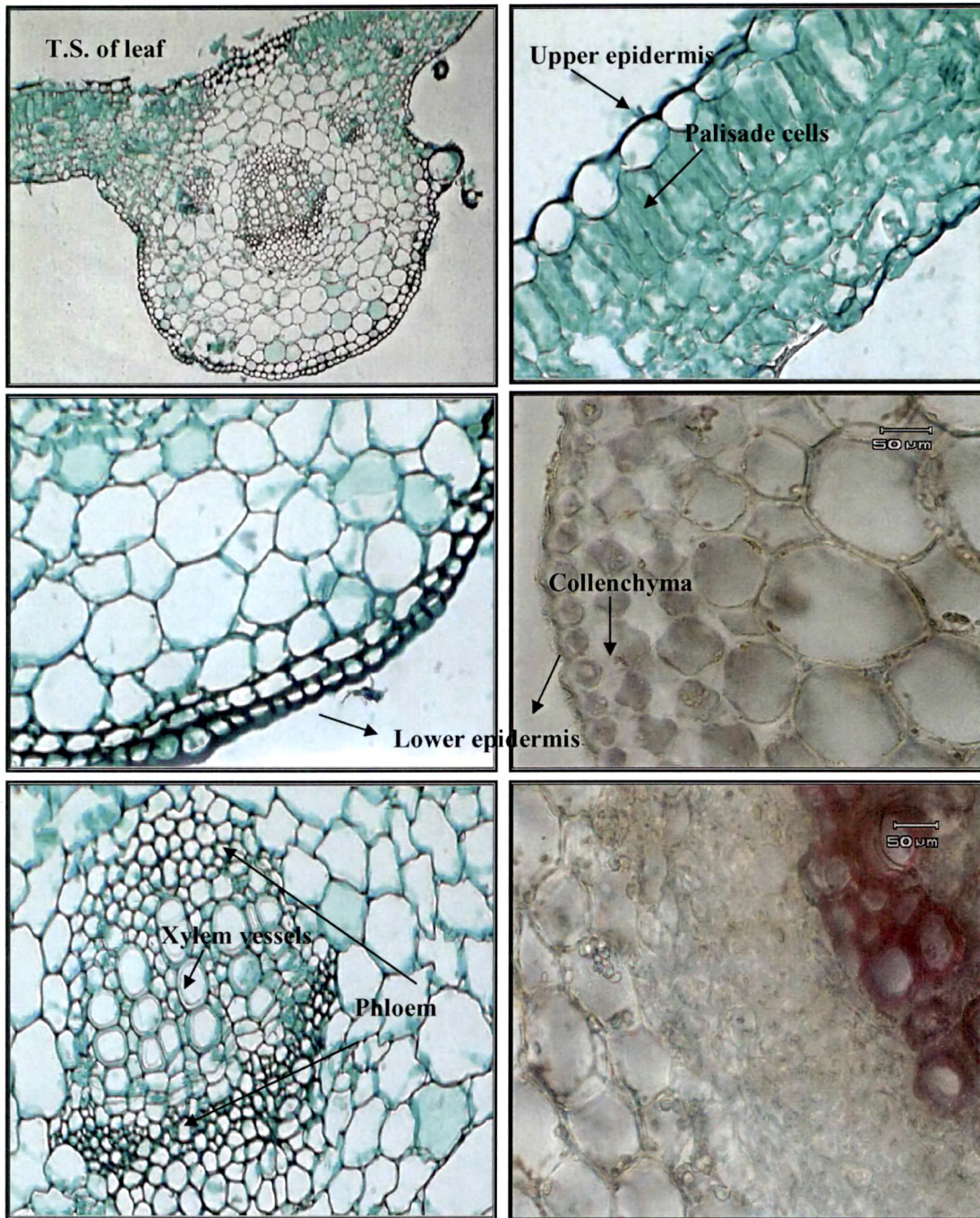


Figure 17 Microscopy of transverse section of *Eclipta alba* leaf

4.1.2.8 *Eclipta alba* stem

Epidermis: It consists of single layer of epidermal cells with cuticle. A covering trichomes which are uniseriate, multicellular unligified are seen.

Cortex: Outer cortex about 3-5 layers consists of collenchyma and inner cortex is many layered consists of oval or round cortical parenchyma. Inner cortex also consists of air sacs (aerenchyma) type of cavities in between which is larger in size towards epidermis and smaller at inner side.

Vascular bundles: They are 12-45 in numbers, arranged in a line towards periphery. Each vascular bundle is having a sclerenchymatous sheath looks like a cap of sclerenchyma. Immediately below this cap there is phloem present. Xylem consists of lignified vessels with metaxylem towards periphery and protoxylem towards centre.

Pith: A central region made up of thin walled, unligified, big polygonal to round parenchyma cells with intercellular spaces. A photo micrograph of transverse section of stem is shown in figure 18

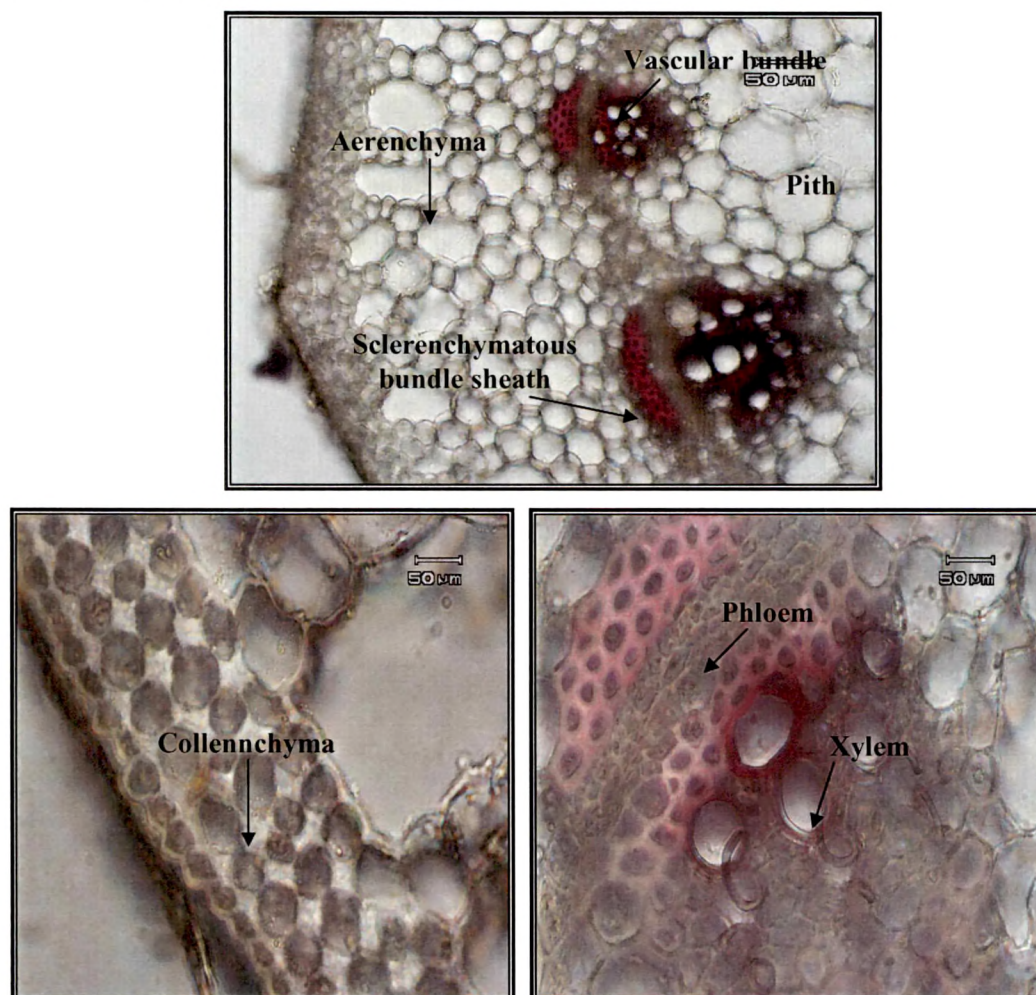


Figure 18 Microscopy of transverse section of *Eclipta alba* stem.

4.1.3 Proximate analysis

Proximate analysis helps to set up certain standards for the crude drugs in order to avoid batch to batch variations and also to judge their quality and purity. The results of proximate analysis are recorded in table 4.

Table 4 Proximate analysis of crude drugs.

	EH	GS	TC	EA
Foreign Organic matter	0.80	0.60	0.15	0.35
Loss on drying	7.8	5.3	6.2	8.5
Successive extraction:				
<i>Pet. Ether extractive (%w/w)</i>	6.38	2.75	0.67	1.25
<i>Benzene extractive (%w/w)</i>	2.15	1.12	0.53	0.68
<i>Chloroform extractive (%w/w)</i>	1.05	0.58	1.01	2.10
<i>Ethylacetate extractive (%w/w)</i>	3.34	2.31	1.24	5.78
<i>Acetone extractive (%w/w)</i>	4.56	1.28	1.63	6.23
<i>Methanol extractive (%w/w)</i>	31.12	10.02	2.35	12.26
Total alcohol extractive (%w/w)	37.25	14.13	11.38	23.34
Water soluble extractive (%w/w)	31.08	30.26	11.2	35.40
Total ash	11.61	15.10	7.53	24.09
Water soluble ash (%w/w)	2.12	1.83	1.60	4.65
Acid insoluble ash (%w/w)	0.83	0.96	0.51	1.15
Elements:				
<i>Sodium</i>	58.1 ppm	83.96 ppm	40.02 ppm	96.62 ppm
<i>Potassium</i>	46.63 ppm	79.52 ppm	32.71 ppm	88.25 ppm
<i>Magnesium</i>	33.15 ppm	10.20 ppm	16.51 ppm	15.63 ppm
<i>Manganese</i>	11.02 ppm	8.23 ppm	23.34 ppm	21.22 ppm
<i>Copper</i>	6.9 ppm	Nil	3.5 ppm	18.54 ppm
<i>Zinc</i>	88.46 ppm	65.25 ppm	43.31 ppm	98.14 ppm
<i>Mercury</i>	Nil	Nil	Nil	6.9 ppm
<i>Lead</i>	5.6 ppm	Nil	Nil	7.8 ppm
<i>Cadmium</i>	Nil	Nil	Nil	Nil
<i>Arsenic</i>	Nil	Nil	Nil	Nil

Values are mean of three determinations.

4.1.4 Phytochemical studies

The successive solvent extraction of the crude drug with solvent of increasing polarity generally results in separation of constituents according to their polarity. The non polar constituents are extracted in solvents like petroleum ether and benzene; semi-polar constituents are extracted in chloroform and acetone; while the polar and highly polar constituents are found in methanol and water. The values of successive solvent extraction provide an idea regarding the presence of various non-polar, semi-polar and polar constituents. In the present section, results obtained by various chemical tests performed on successive extracts are presented. Results indicated the presence of alkaloids, flavonoids, terpenoids, sterols, saponins, carbohydrates and amino acids in *E. hyssopifolium*; Phenolics, terpenoids, sterols, proteins and carbohydrates in *G. sylvestre*; alkaloids, phenolics, terpenoids, and amino acids in *T. cordifolia*; phenolics, terpenoids, sterols, saponins, aminoacids, carbohydrates, and fixed oil in *E. alba*. These results are depicted in table 5.

4.2 DNA Fingerprinting by RAPD

DNA isolated from fresh leaves of the plants collected from two different geographical conditions (Vadodara and Junagadh dist.), found to be free from protein, mRNA or other contaminations when purity was checked by gel electrophoresis (figure 19). Further the concentration of isolated DNA was estimated on Nano Drop ND-1000 spectrophotometer and found to be 459 ng/ μ l (EH1), 436 ng/ μ l (EH2), 521 ng/ μ l (GS1), 506 ng/ μ l, 213 ng/ μ l (TC1), 234 ng/ μ l (TC2), 498 ng/ μ l (EA1), 450 ng/ μ l (EA2).

Table 5 Qualitative evaluation of successive extracts

Constituents	<i>E. hyssopifolium</i>					<i>G. Sylvestre</i>					<i>T. Cordifolia</i>					<i>E. Alba</i>									
	P	B	C	E	A	M	P	B	C	E	A	M	P	B	C	E	A	M	P	B	C	E	A	M	
Alkaloids	-	-	-	-	-	+	-	-	-	-	-	-	-	-	-	-	-	-	-	-	-	-	-	-	-
Phenolic/ Flavonoids	-	-	-	+	+	+	-	-	-	-	-	+	-	-	-	-	-	-	-	-	-	+	+	+	+
Anthracene Glycoside	-	-	-	-	-	-	-	-	-	-	-	-	-	-	-	-	-	-	-	-	-	-	-	-	-
Terpenoids and sterols	+	+	+	-	-	-	+	+	+	-	-	+	+	+	+	-	-	-	-	-	+	+	-	-	-
Saponins	-	-	-	-	-	+	-	-	+	+	+	+	+	+	-	-	-	-	-	-	-	-	-	-	+
Aminoacids/ Proteins	-	-	-	-	-	+	-	-	-	-	-	+	+	+	-	-	-	-	-	-	-	-	-	-	+
Carbohydrates	-	-	-	-	-	+	-	-	-	-	-	+	+	+	-	-	-	-	-	-	-	-	-	-	+
Fixed oils	-	-	-	-	-	-	-	-	-	-	-	-	-	-	-	-	-	-	-	-	-	-	-	-	-
Volatile oils	-	-	-	-	-	-	-	-	-	-	-	-	-	-	-	-	-	-	-	-	-	-	-	-	-

P: Petroleum ether; B: Benzene; C: Chloroform; E: Ethylacetate; A: Acetone; M: Methanol; -: Absent; +: Present.

TLC study of these extracts confirms the presence of secondary metabolites that were found to be present during qualitative evaluation.

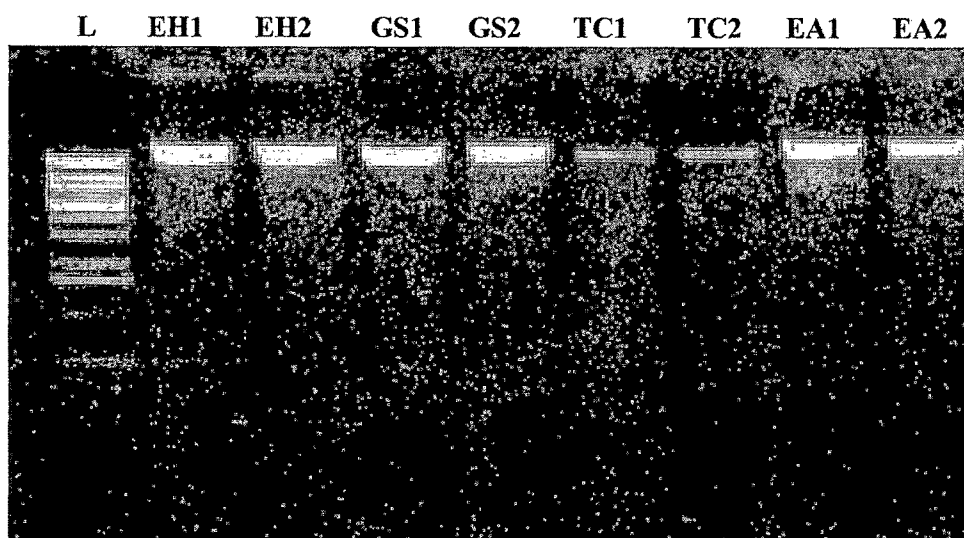


Figure 19 Gel electrophoresis of isolated DNA from plant leaves. EH1 and EH2: *Enicostemma hyssopifolium* collected from Vadodara and Junagadh district respectively, GS and GS: *Gymnema sylvestre* collected from Vadodara and Junagadh district respectively, TC1 and TC2: *Tinospora cordifolia* collected from Vadodara and Junagadh district respectively, EA1 and EA2: *Eclipta alba* collected from Vadodara and Junagadh district respectively. L: 100 bp ladder.

A set of 10 primers were checked individually on each isolated genomic DNA. Out of these 10 oligomers, only 2 primers i.e., 5'-GGTGCGGGAA-3' and 5'-GTGACATGCC-3' gave positive result after amplification in thermocycler. A gelchromarogram is shown in fig. and

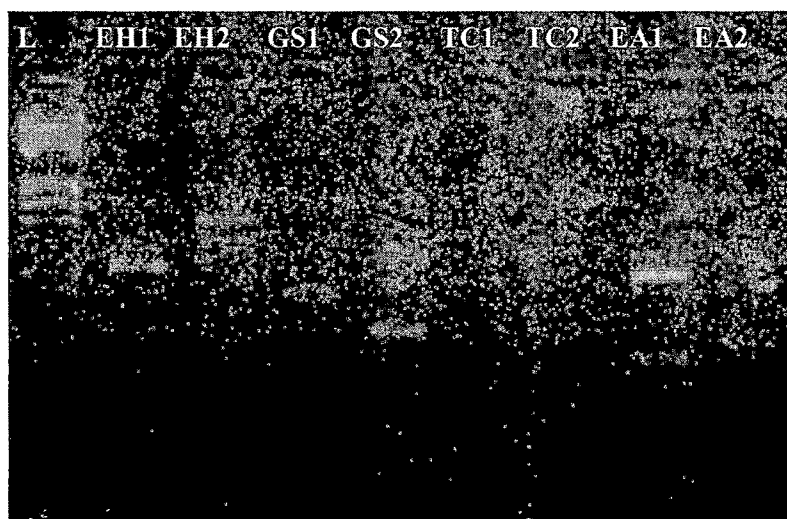


Figure 20 Representative gel fractionation of RAPD-PCR amplification products of plant genomic DNA using the primer (5'-GGTGCGGGAA-3').



Figure 21 Representative gel fractionation of RAPD-PCR amplification products of plant genomic DNA using the primer (5'-GTGACATGCC-3')

A few common bands of identical base pair were observed after amplification with specific primer in plant DNA isolated from different locations. Even though some bands are also observed which are not common. DNA of *T. cordifolia* leaf was not amplified with 5'-GGTGCGGGAA-3' oligomer.

4.3 Plant Extraction, Fractionation and Isolation

4.3.1 *Enicostemma hyssopifolium*

Coarsely powdered plant material of *E. hyssopifolium* was extracted with methanol and the extract was subjected to fractionation. Since the plant is very bitter in taste and bitters are reported to be present in high quantity, a fraction rich in these bitter constituents was prepared. Similarly, there are many flavonoids reported which are not much common in all other plants. A flavonoid fraction of *E. hyssopifolium* was prepared as described in chapter 3. As shown in figure 22, methanol extract (track 4 and 5) contain two constituents in very high quantity. They were identified and isolated as described in materials and methods chapter.

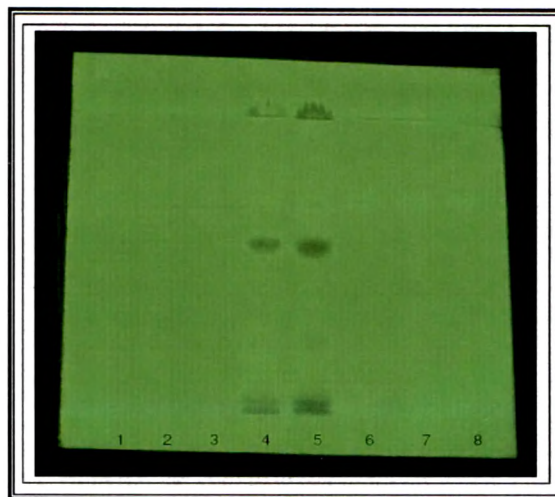


Figure 22 Co-TLC Track : 1, 2 and 3 = EH002; 4 and 5 = EH methanol extract; 6, 7 and 8 = EH001.

4.3.2 *Tinospora cordifolia*

Stem of *T. cordifolia* found to contain very high amount of alkaloids. A fraction rich in these alkaloids was prepared. A TLC photograph of plate developed in mobile phase ethyl acetate : formic acid : acetic acid : water (100 : 11 : 11 : 32) is shown in figure 23.

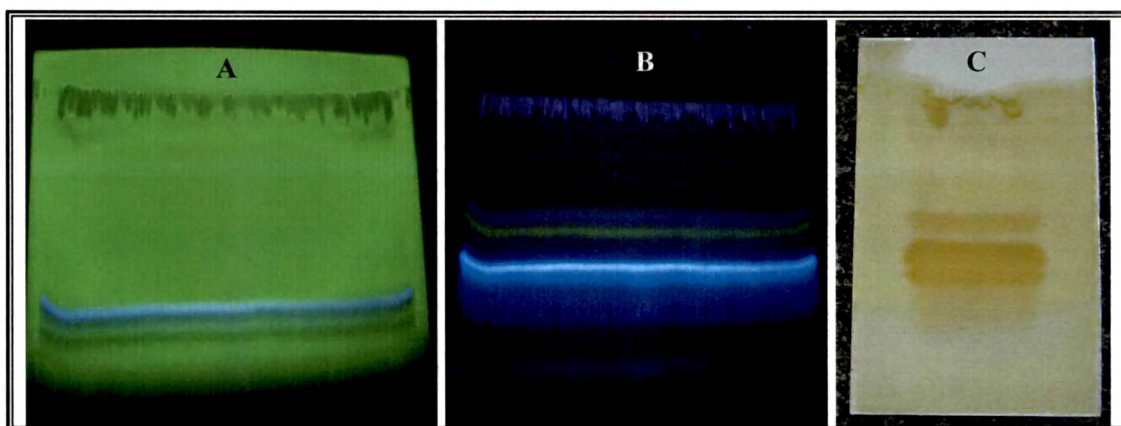


Figure 23 TLC pattern of alkaloid fraction isolated from *T. cordifolia* stem.
TLC plate under (A) U V 254 nm (B) 366 nm (C) derivatized with dragendroff's reagent

Apart from alkaloids, a clerodane furano-diterpene, tinosporaside was identified in methanol and aqueous extract of *T. cordifolia* by TLC. Tinosporaside was used to standardize the extract. Developed TLC plate for detection of tinosporaside is shown as figure 24.

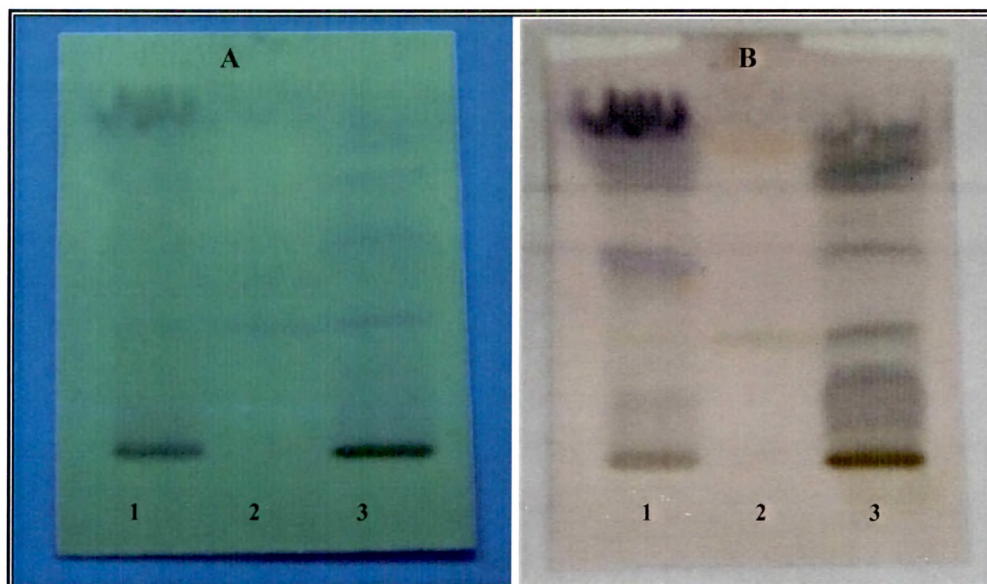


Figure 24 TLC plate; Track 1: TC aqueous extract, 2: Tinosporaside, 3: TC methanol extract.

A: TLC plate observed under UV 254 nm.

B: TLC plate observed after treatment with anisaldehyde sulphuric acid reagent and heated at 110 °C for 5 min.

4.3.3 *Gymnema sylvestre*

Crude gymnemic acid and its genin moiety gymenamgenin were isolated. A TLC chromatogram developed in chloroform : methanol (1 : 1) mixture is shown in figure 25.

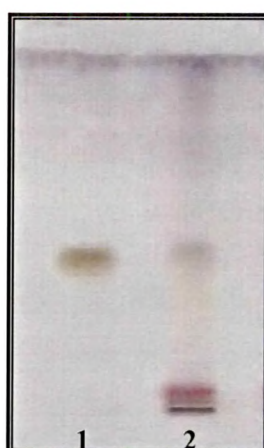


Figure 25 TLC plate; Track 1: Isolated gymnamgenin, 2: crude gymnemic acid (plate derivetized with anisaldehyde sulphuric acid reagent).

4.3.4 *Eclipta alba*

Methanol extract was utilized to prepare two fractions, one being rich in phenolics and another in sterol constituents. Phenolic fraction was used for isolation of wedelolactone, a major coumestan derivative present in *E. alba* aerial part. TLC pattern in toluene : acetone : formic acid (11 : 6 : 1 v/v/v) is shown in figure 26. A sterol fraction found to contain a new sesquiterpene derivative which was then isolated from chloroform extract of *E. alba*. TLC pattern of sterol fraction and isolated EA002 in mobile phase toluene:ethyl acetate (4:1 v/v) is shown in figure 27.

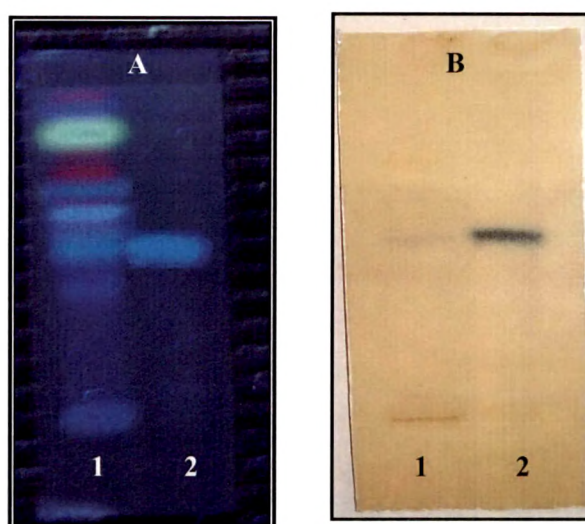


Figure 26 TLC plate (A) under 366 nm (B) after derivatization with ferric chloride. Track 1: EA methanol extract, 2: Isolated wedelolactone.

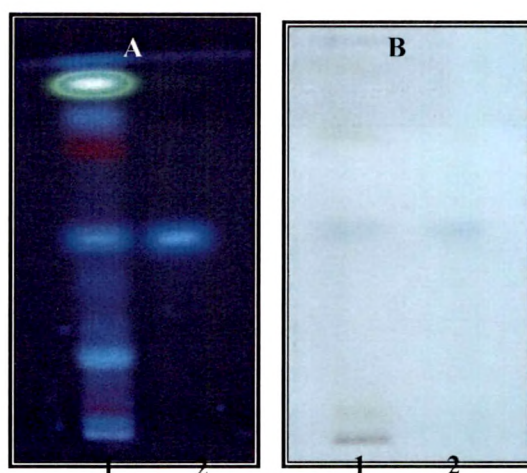


Figure 27 TLC plate (A) under 366 nm (B) after derivatization with antimony trichloride. Track 1: EA sterol fraction, Track 2: Isolated EA002.

4.4 Fingerprinting of extracts, fractions and formulations

4.4.1 High Performance Thin Layer Chromatography (HPTLC)

Fingerprint of the ethanol extracts in three different solvent systems were obtained. Developed plates were scanned and their chromatograms were recorded. TLC photographs with their HPTLC chromatograms are presented in figures 28-38. HPTLC fingerprints of fractions were developed using suitable solvent system which were optimized to resolve the major constituents present in particular fraction. Ethanol extract of the studied formulation was chromatographed on three different solvent systems as mentioned in chapter 3. Chromatograms are presented in figure 44-46.

4.4.1.1 Fingerprinting of extracts

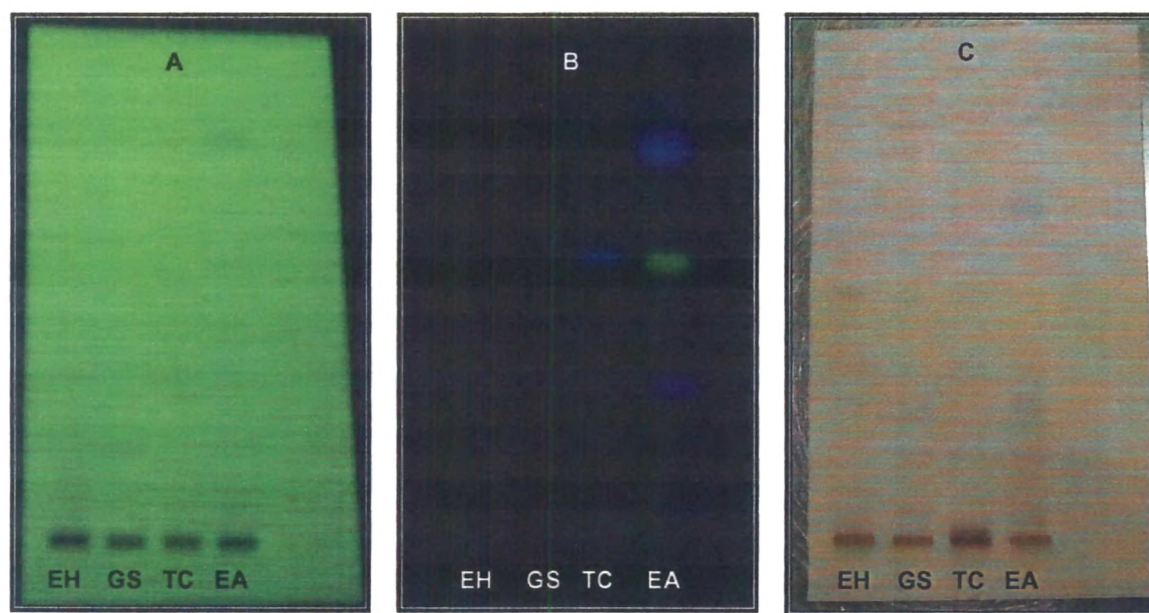


Figure 28 Finger printing of extracts in hexane : ethylacetate (4 : 1) mobile phase. (A) under 254 nm (B) under 366 nm (C) after derivatization with anisaldehyde sulphuric acid reagent.

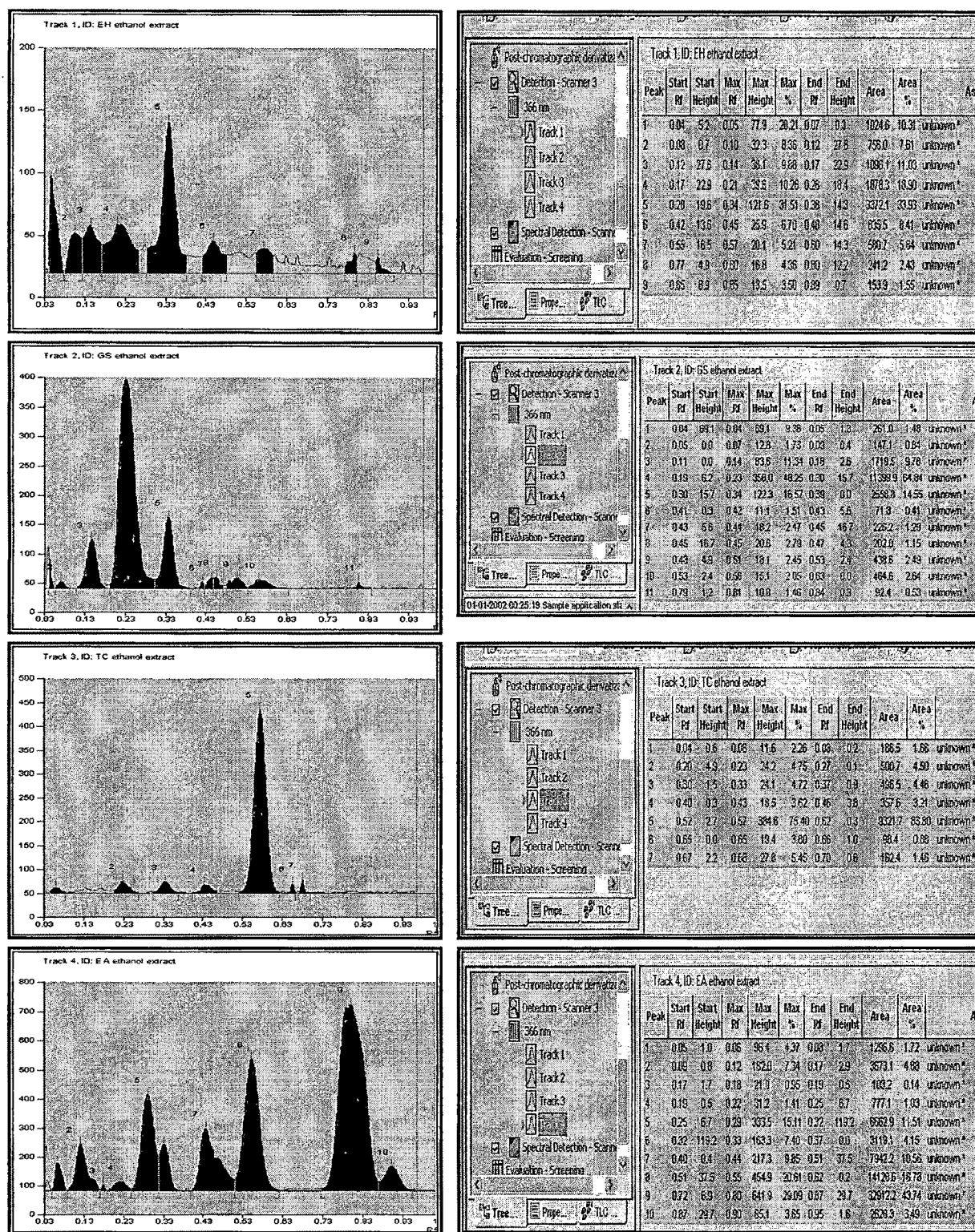


Figure 29 HPTLC chromatogram of ethanol extracts developed in hexane : ethylacetate (4 : 1) mobile phase, scanned @ 366 nm.

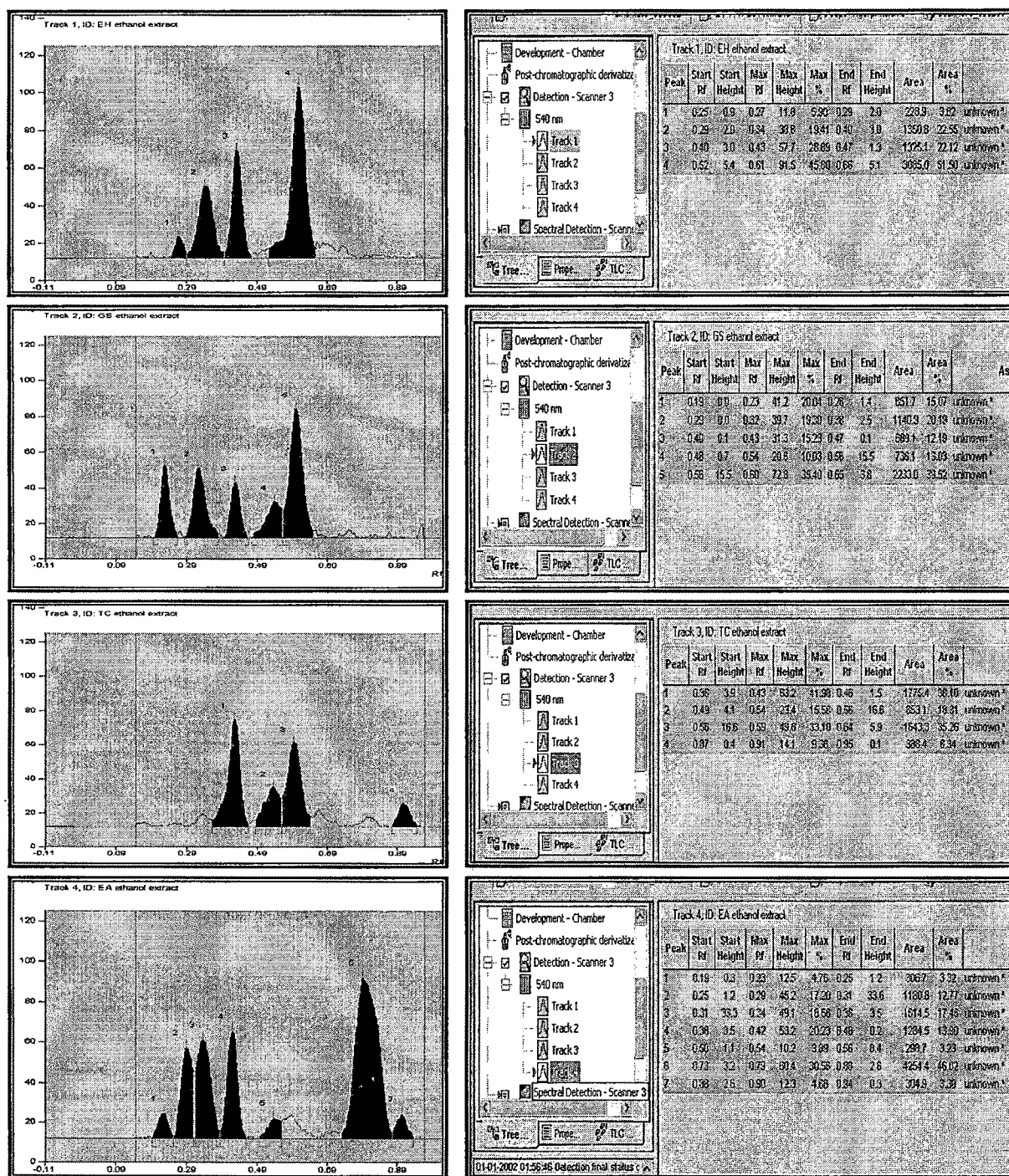


Figure 30 Fingerprinting data of extract (track developed in hexane : ethylacetate (4 : 1), scanned @ 540 nm.

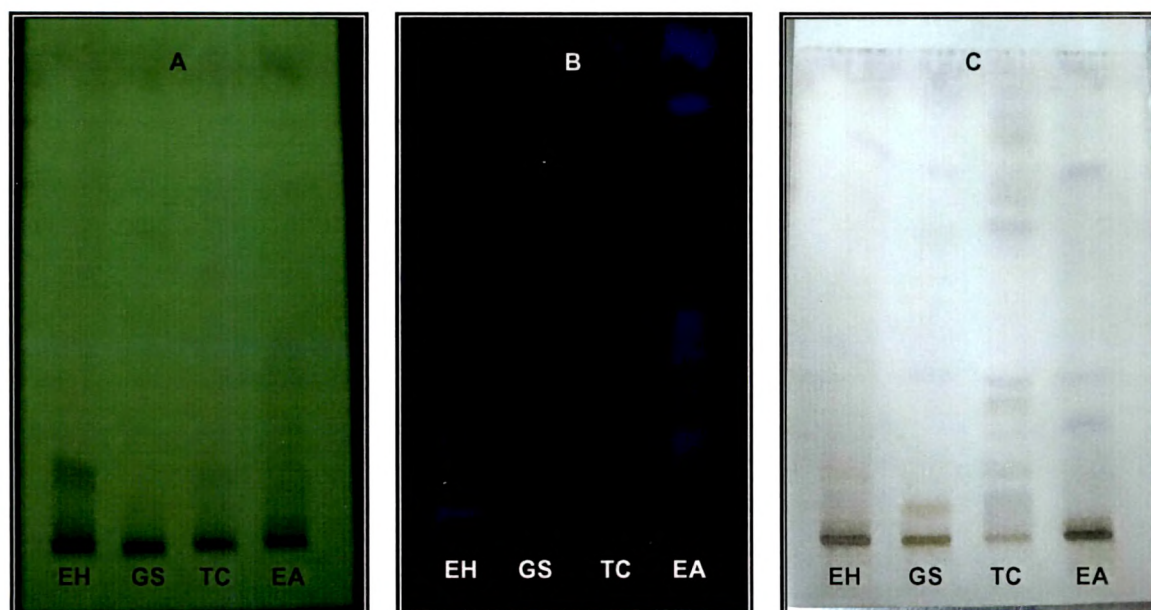


Figure 31 Finger printing of extracts in chloroform : methanol (4.5 : 0.5) mobile phase. (A) under 254 nm (B) under 366 nm (C) after derivatization with anisaldehyde sulphuric acid reagent.

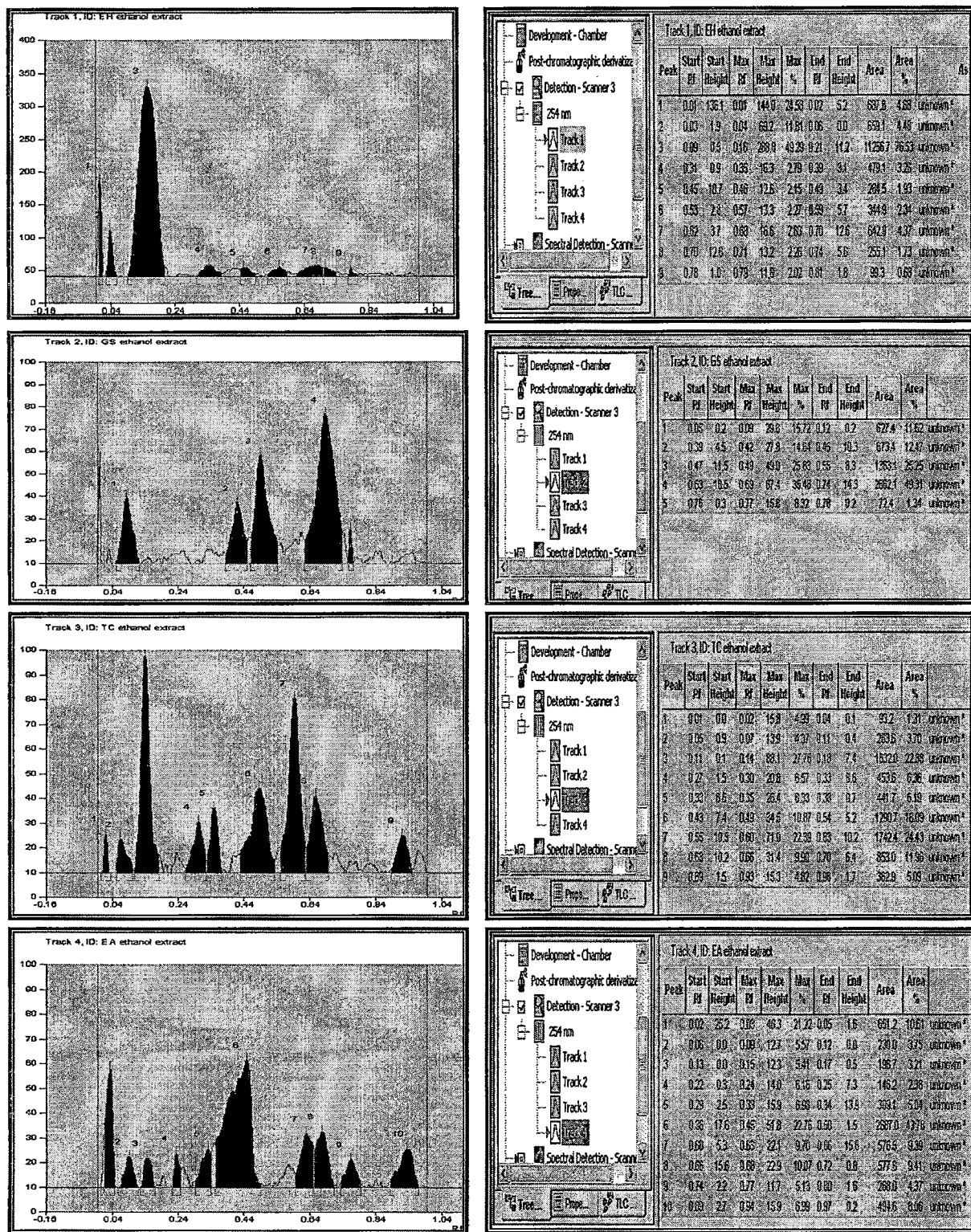


Figure 32 HPTLC chromatogram of ethanol extracts developed in chloroform : methanol (4.5 : 0.5) mobile phase, scanned @ 254 nm.

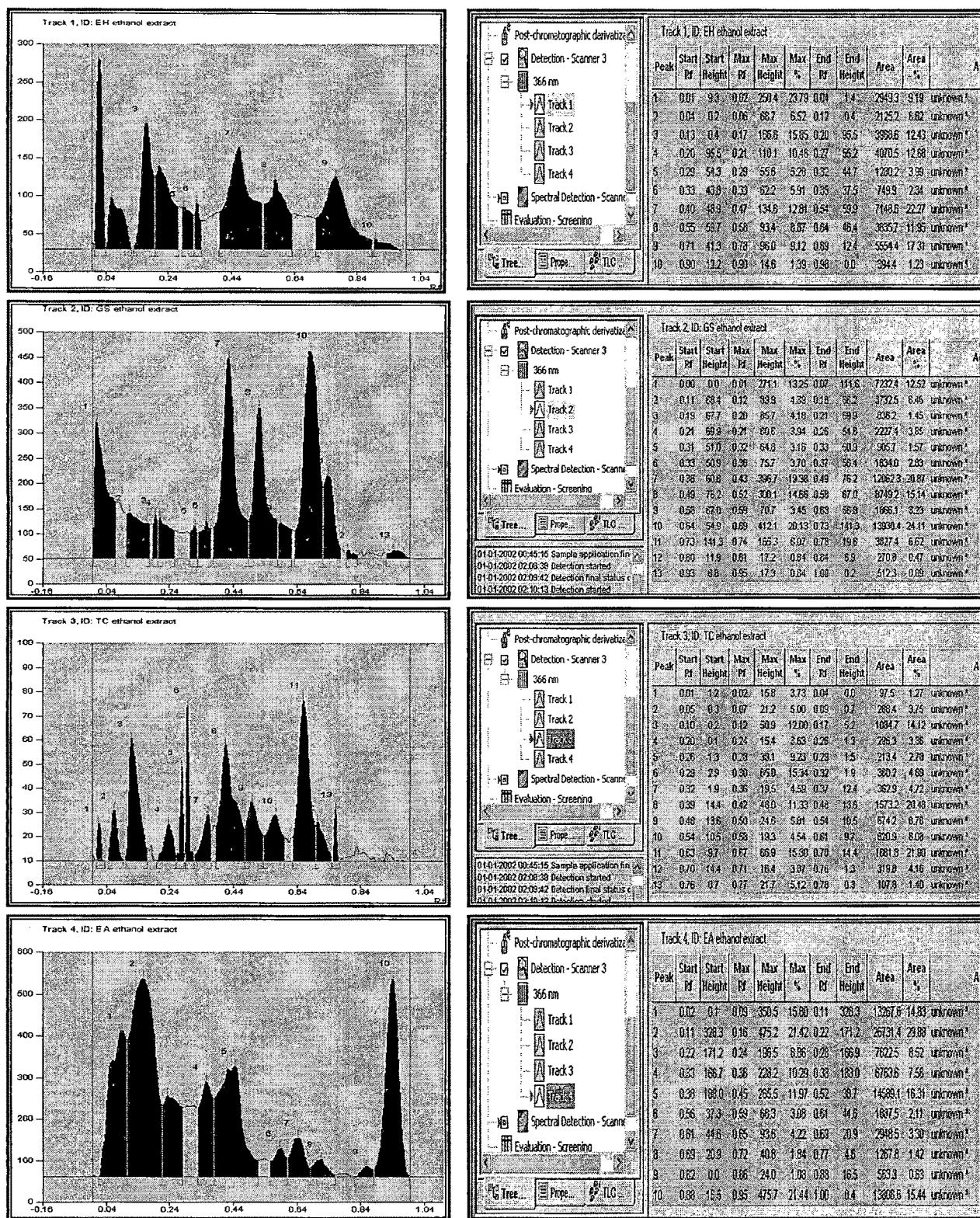


Figure 33 HPTLC chromatogram of ethanol extracts developed in chloroform : methanol (4.5 : 0.5) mobile phase, scanned @ 366 nm.

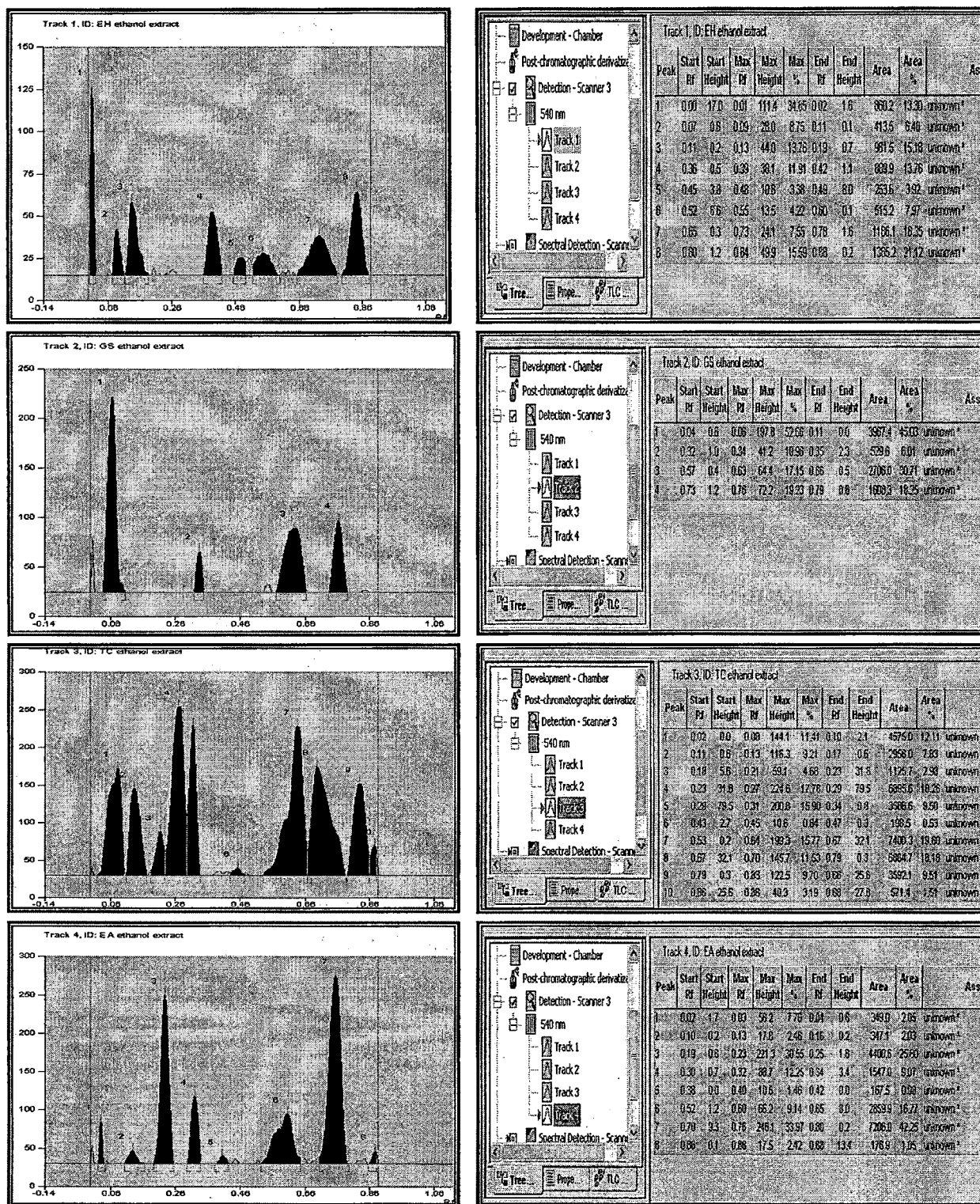


Figure 34 HPTLC chromatogram of ethanol extracts developed in chloroform : methanol (4.5 : 0.5) mobile phase, scanned @ 540 nm.

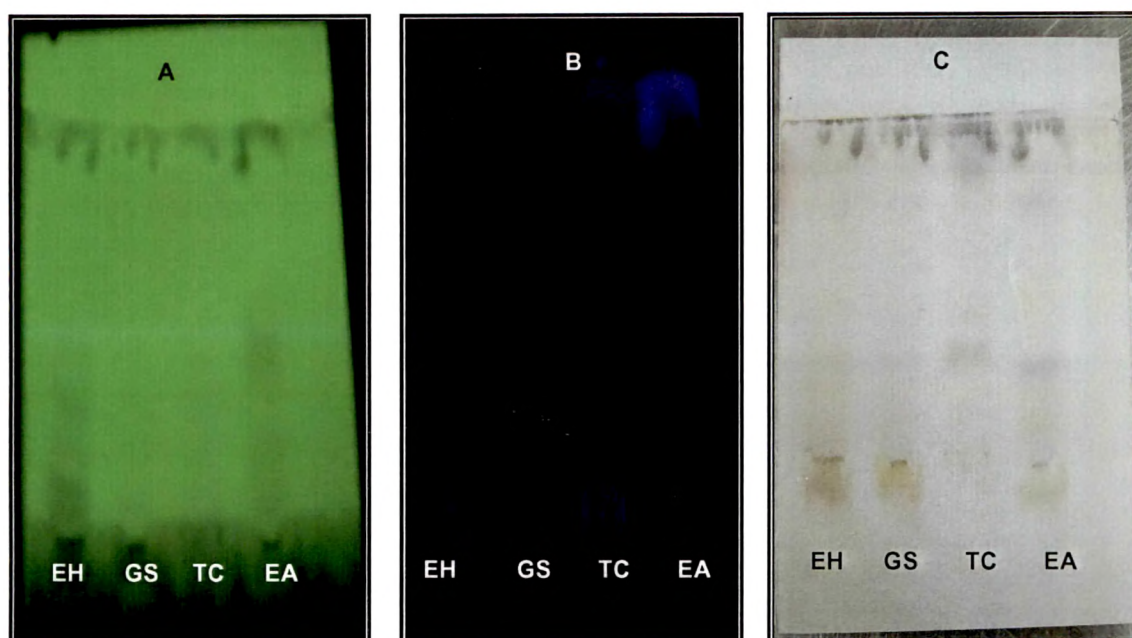


Figure 35 Finger printing of extracts in ethyl acetate : acetic acid : formic acid : water (55 : 2.75 : 2.75 : 6.5) mobile phase. (A) under 254 nm (B) under 366 nm (C) after derivatization with anisaldehyde sulphuric acid reagent.

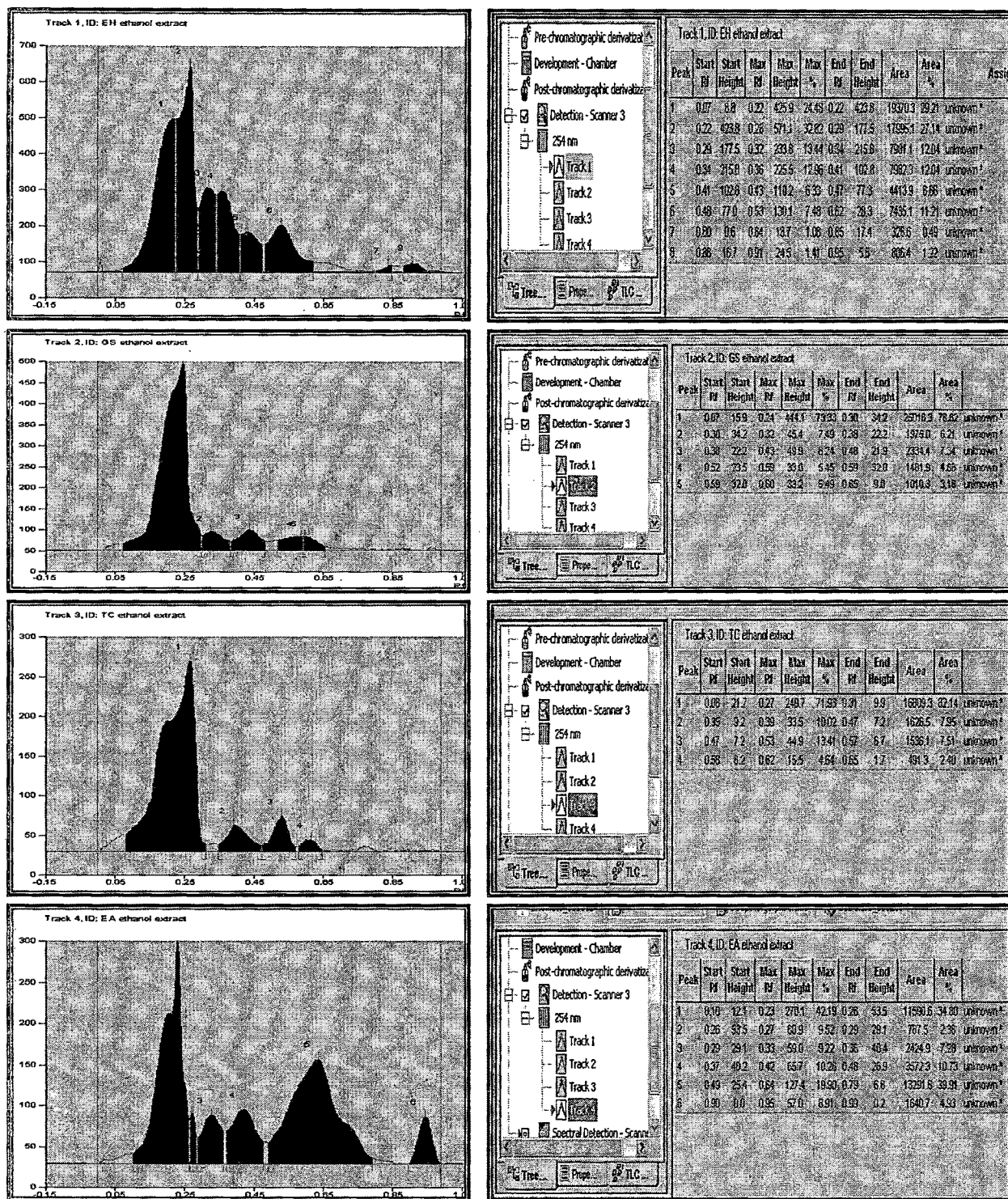


Figure 36 HPTLC chromatogram of ethanol extracts developed in ethyl acetate : acetic acid : formic acid : water (55 : 2.75 : 2.75 : 6.5) mobile phase, scanned @ 254 nm.

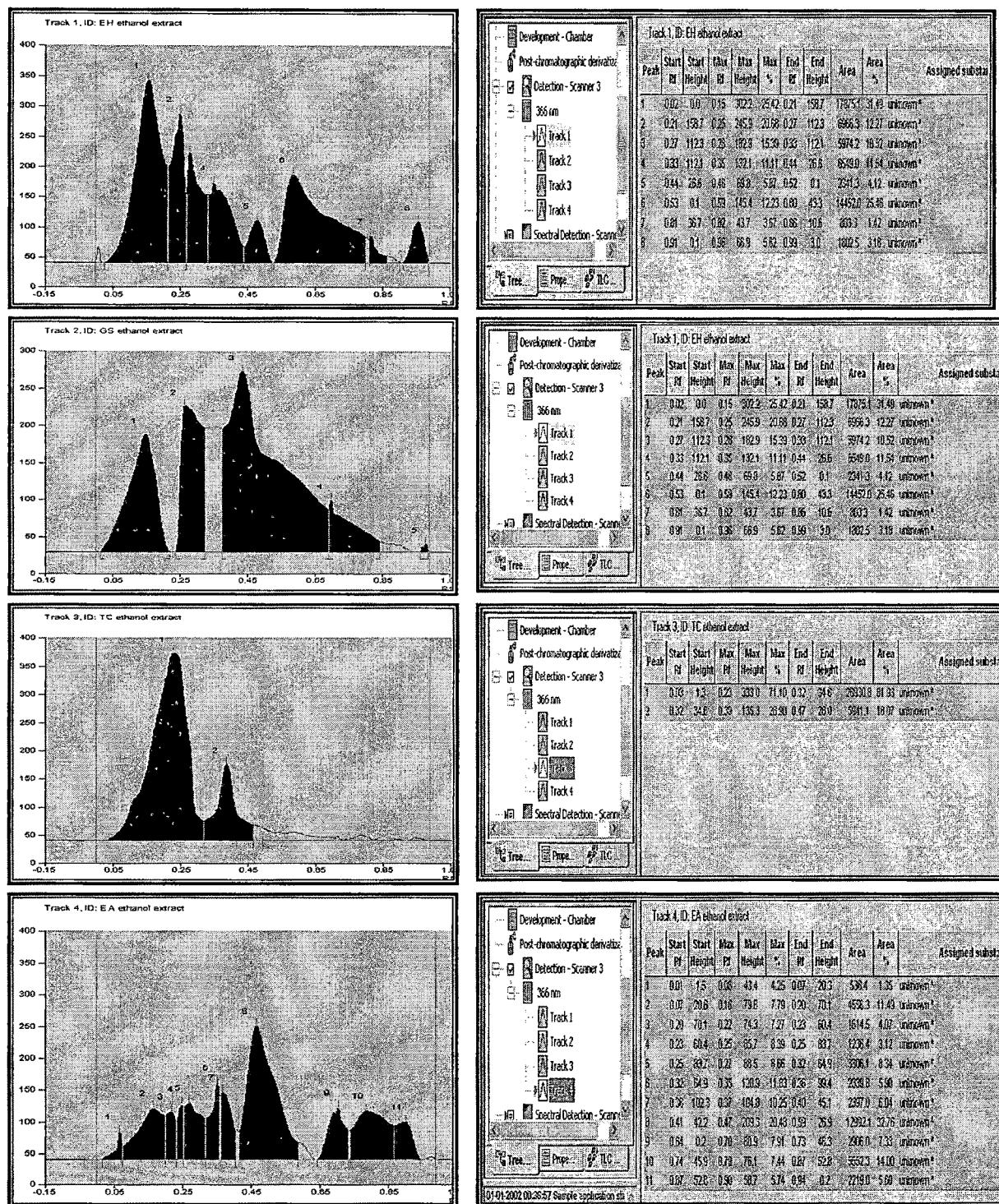


Figure 37 HPTLC chromatogram of ethanol extracts developed in ethyl acetate : acetic acid : formic acid : water (55 : 2.75 : 2.75 : 6.5) mobile phase, scanned @ 366 nm.

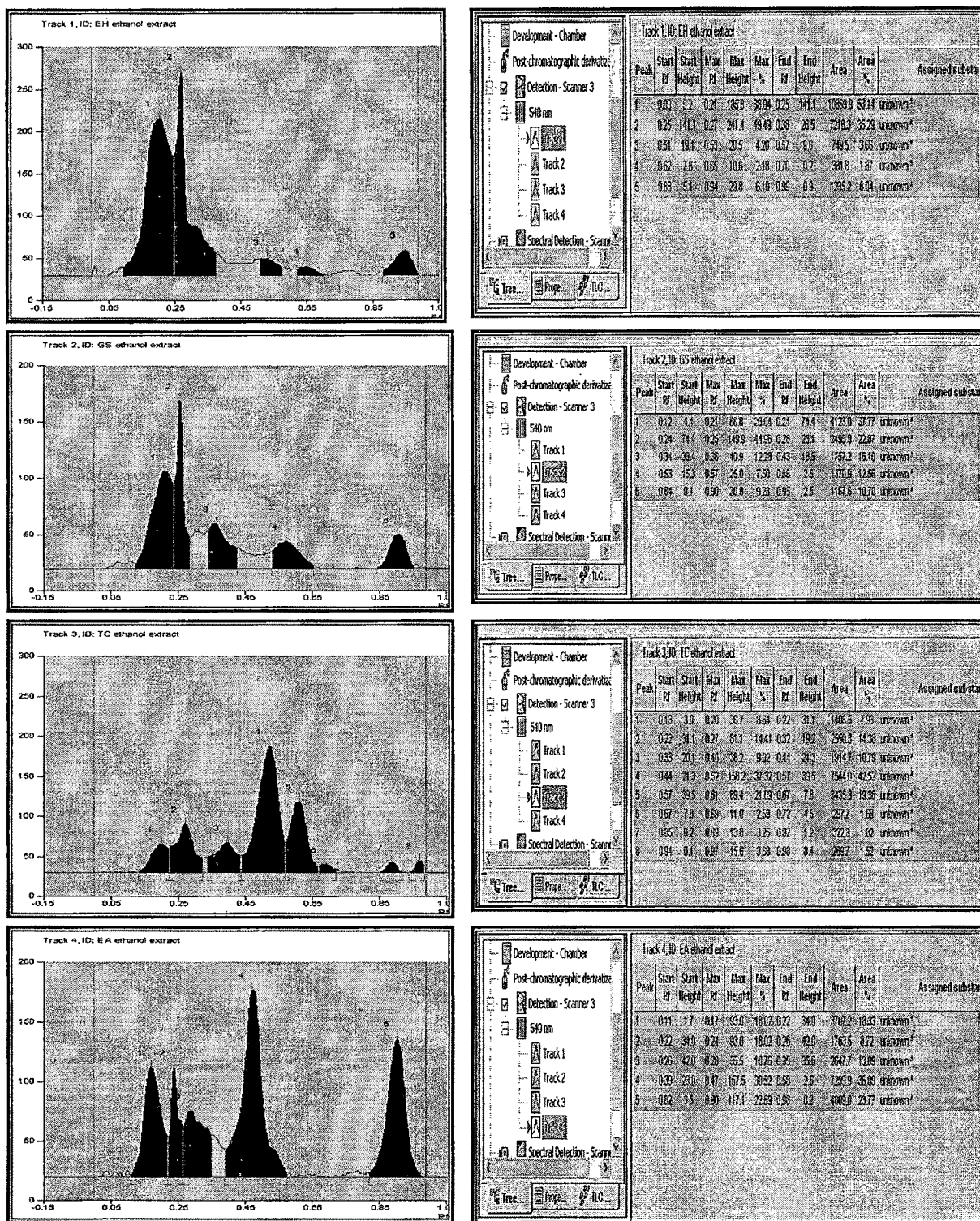


Figure 38 HPTLC chromatogram of ethanol extracts developed in ethyl acetate : acetic acid : formic acid : water (55 : 2.75 : 2.75 : 6.5) mobile phase, scanned @ 540 nm.

4.4.1.2 Fingerprinting of fractions and formulations

HPTLC fingerprinting of all fractions prepared were performed. Bitter fraction and flavonoid fraction of *E. hyssopifolium* were chromatographed in ethyl acetate : methanol : water (77 : 15 : 8), alkaloids fraction of *T. cordifolia* were separated over TLC plate in ethyl acetate : acetic acid : formic acid : water (100 : 11 : 11 : 32), chromatogram of crude gymnemic acid was obtained in chloroform : methanol : acetic acid (5 : 1 : 1) and in isopropylalcohol : chloroform : methanol : acetic acid (5 : 3 : 1 : 0.5), whereas phenol fraction and sterol fraction from *E. alba* were chromatographed in toluene : acetone : formic acid (11 : 6 : 1) and pet. ether : ethyl acetate (4 : 1) respectively.

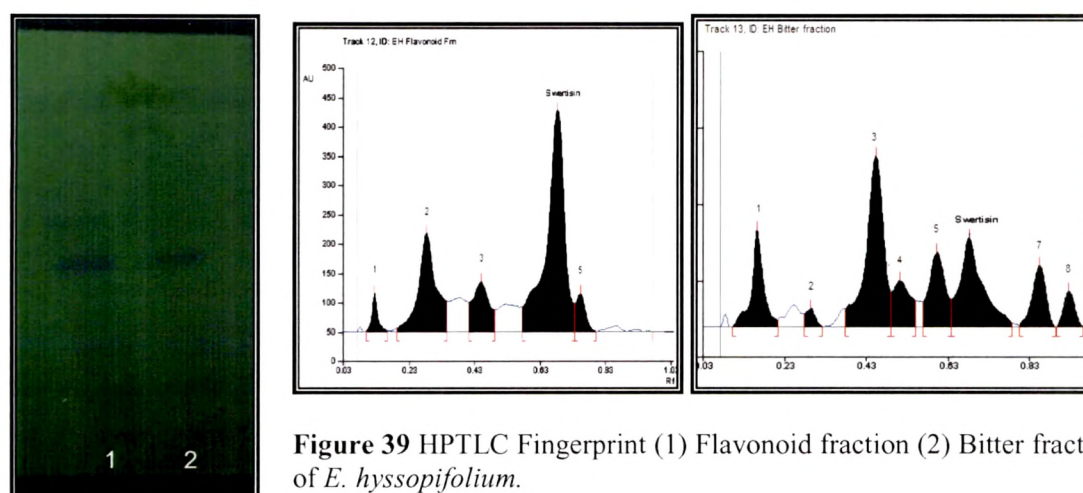


Figure 39 HPTLC Fingerprint (1) Flavonoid fraction (2) Bitter fraction of *E. hyssopifolium*.

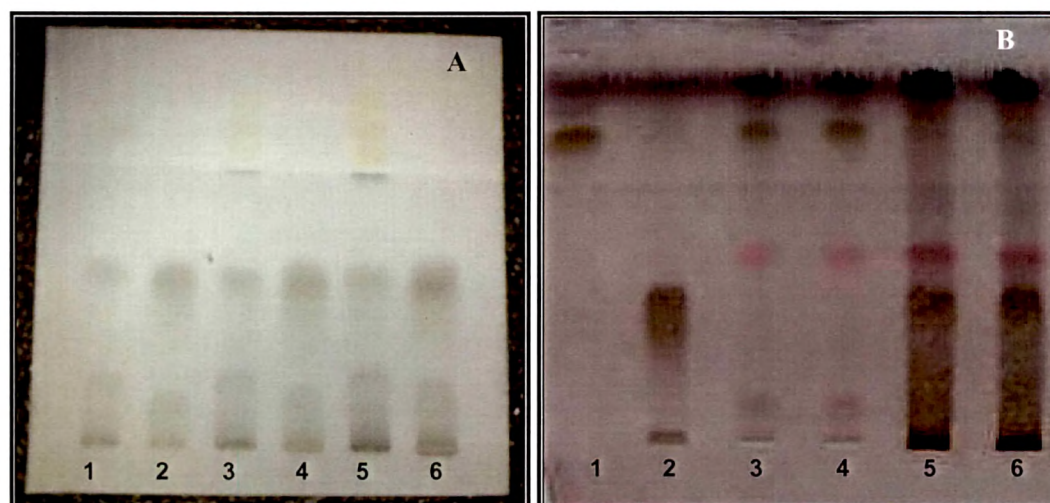


Figure 40 HPTLC plate for finger printing of *Gymnema sylvestri*; (A) mobile phase - chloroform : methanol : acetic acid (5 : 1 : 1); Track 1, 3 and 5 – GS methanol extract and Track 2, 4, and 6 – GS aqueous extract (methanol soluble fraction). (B) mobile phase - isopropylalcohol : chloroform : methanol : acetic acid (5 : 3 : 1 : 0.5); Track 1-gymnemagenin, 2-gymnemic acid, 3 and 4-methanol extract after hydrolysis, 5 and 6-methanol extract before hydrolysis.

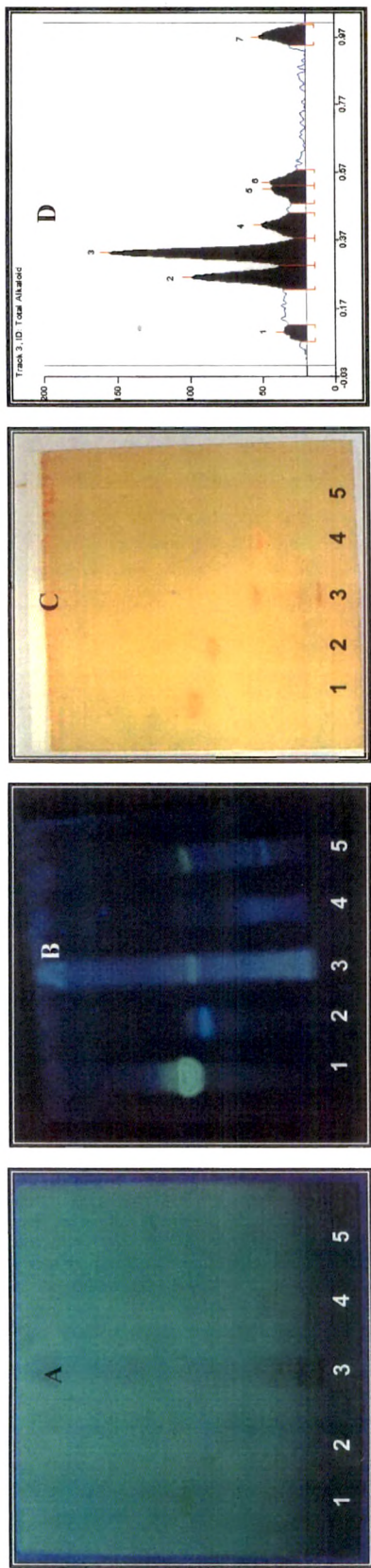


Figure 41 HPTLC fingerprint of *Tinospora cordifolia* alkaloid fraction (A) TLC plate at 254 nm (B) after Dragendroff spray (C) Chromatogram of Track 3 at 254 nm. (Track 1 - TCY, 2 - TCB, 3 - TC alkaloid fraction, 4 - TCA, 5 - TC methanol extract).

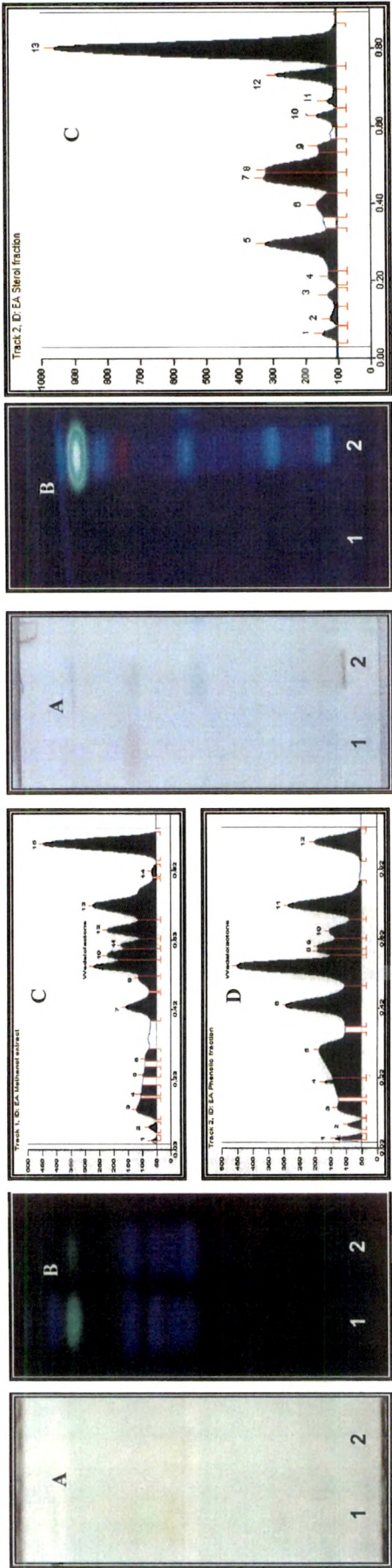


Figure 42 Fingerprinting of *Eclipta alba* (A) TLC plate, Visible (B) TLC plate, under UV 366 nm, Track 1 - EA methanol extract, Track 2 - EA phenolic fraction (C) HPTLC chromatogram of EA methanol extract (D) EA phenolic fraction.

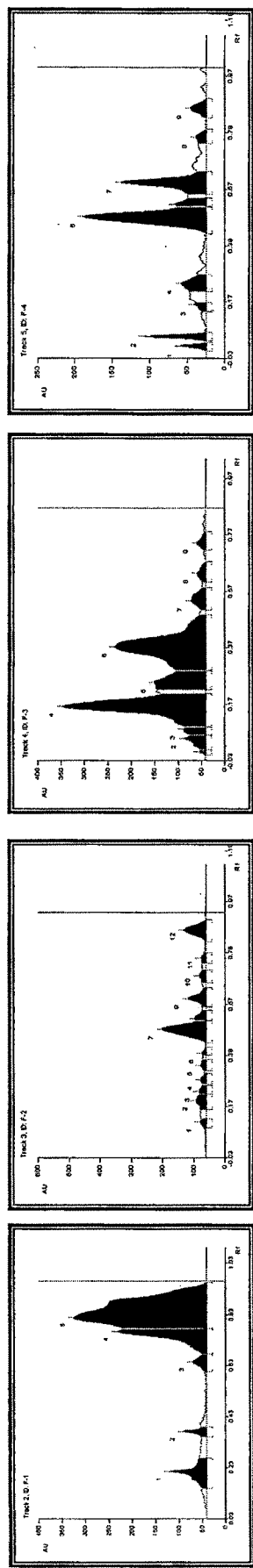


Figure 44 HPTLC chromatograms of formulations (fingerprinting) in hexane : ethyl acetate (4 : 1).

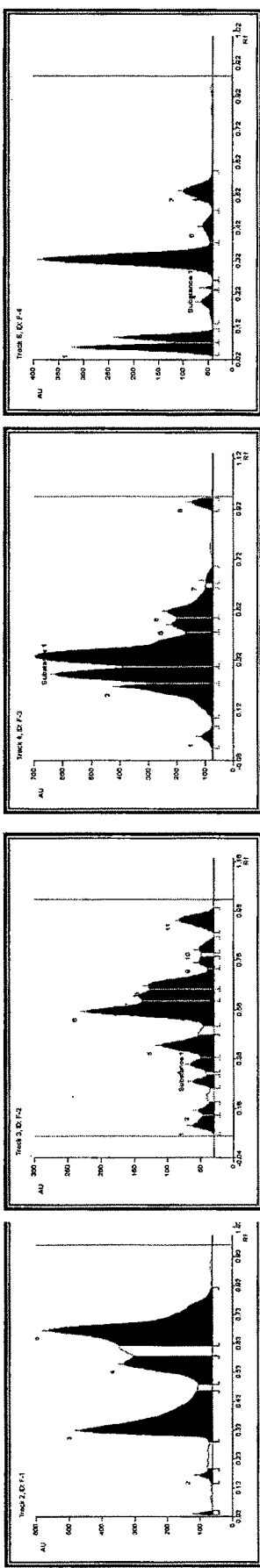


Figure 45 HPTLC chromatograms of formulations (fingerprinting) in ethylacetate : acetic acid : water (25 : 2.75 : 2.75 : 6.5).

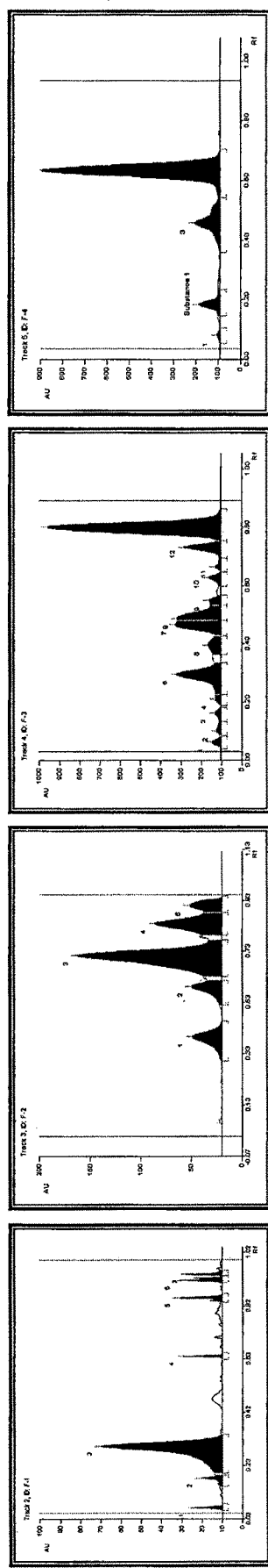


Figure 46 HPTLC chromatograms of formulations (fingerprinting) in chloroform : methanol (4.5 : 0.5).

4.4.2 High Performance Liquid Chromatography (HPLC)

4.4.2.1 *Enicostemma hyssopifolium*

HPLC finger printing of bitter fraction and flavonoid fraction were performed by preparing their stock solution in methanol (1 mg/ml) and dilutions were made with the mobile phase i.e., acetonitrile : water (25 : 75). Flow rate was kept at 0.8 ml/min. and detection was carried out by using UV detector at 238 and 342 nm. HPLC chromatograms are shown in figure 47.

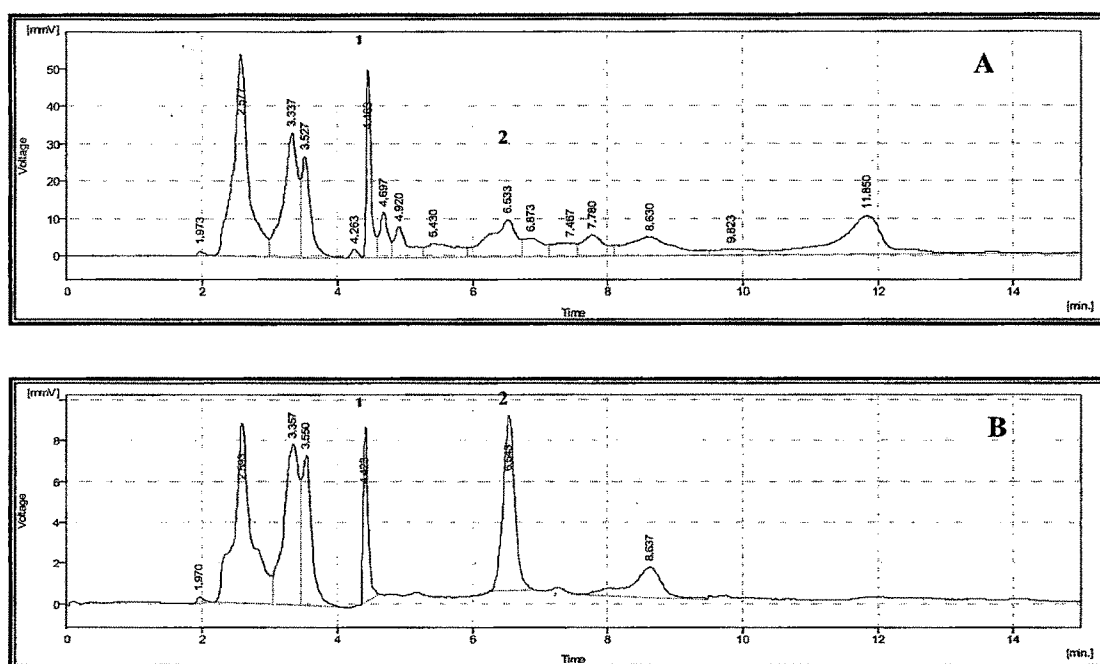


Figure 47 HPLC fingerprint of *E. hyssopifolium* (A) bitter fraction scanned at 238 nm (B) flavonoid fraction scanned at 342 nm. Peak 1 – EH002 and peak 2 – EH001.

4.4.2.2 *Tinospora cordifolia*

HPLC fingerprint of alkaloid fraction was obtained by injecting 20 μ l of solution (0.5 mg/ml) prepared in mobile phase, acetonitrile : Britton Robinson buffer (245 : 5, pH 3). Flow rate was adjusted to 1 ml/min, UV detection was performed at 345 nm. Isolated alkaloid, TCA was detected in aqueous extract by using methanol : acetic acid : triethanolamine : water (30 : 1 : 0.5 : 68.5) as mobile phase. Detection was performed at 270 nm. HPLC chromatograms are shown in figure 48.

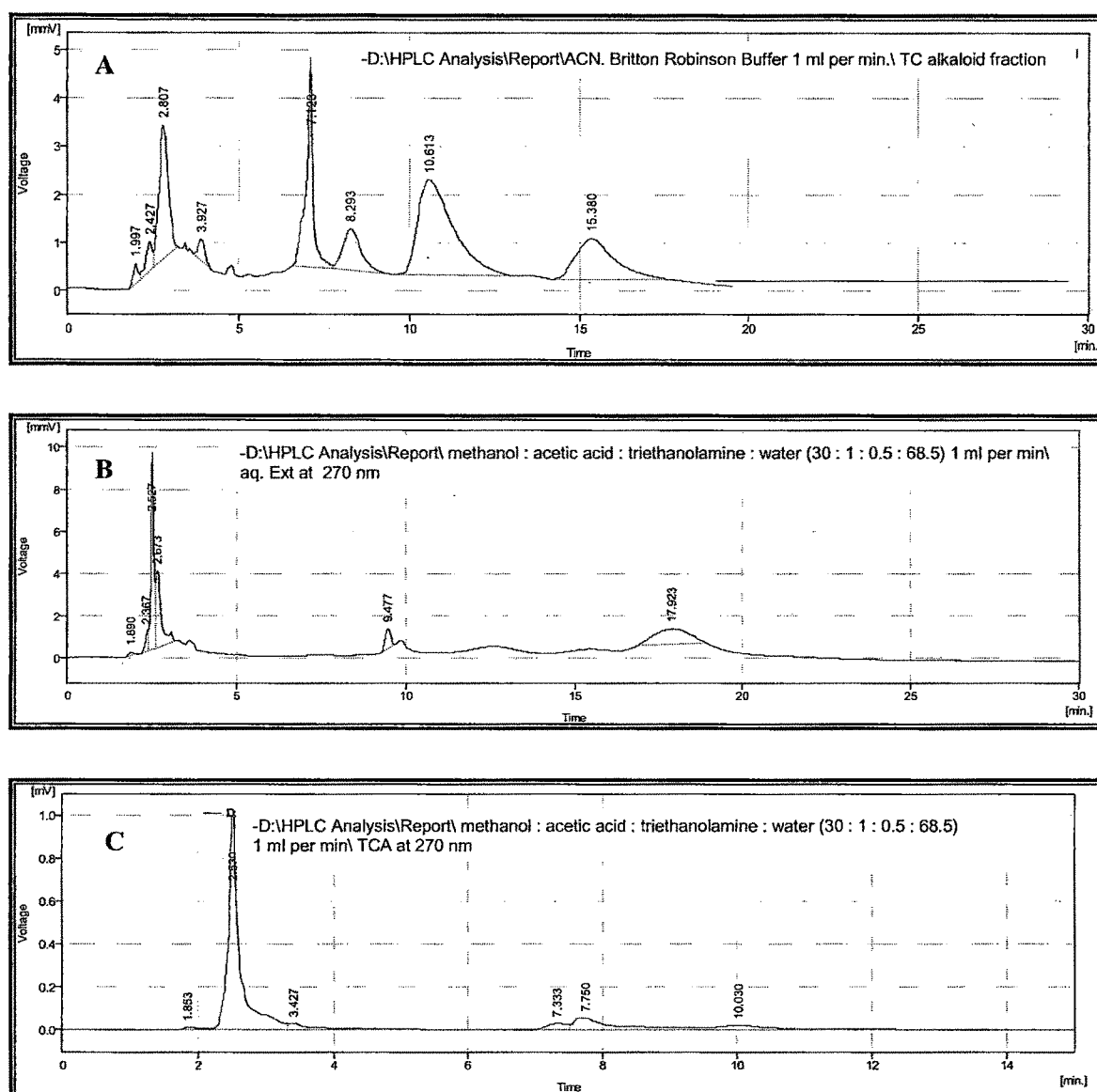


Figure 48 HPLC fingerprint of *T. cordifolia* (A) Alkaloid fraction scanned at 345 nm (B) Aq. Extract 270 nm (C) Alkaloid TCA at 270 nm.

4.4.2.3 *Gymnema sylvestre*

Methanol extract was subjected to HPLC fingerprinting. Mobile phase was optimized as acetonitrile : 0.1% KH_2PO_4 (40 : 60) at the flow rate of 0.8 ml/min. Detection was performed at 210 nm. A chromatogram representing the fingerprint is shown in figure 49.

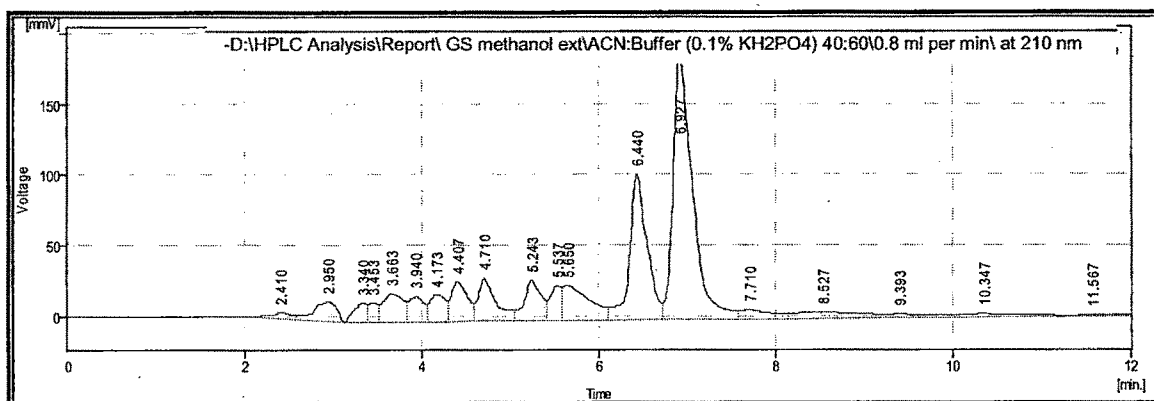


Figure 49 HPLC fingerprint of *Gymnema sylvestre* methanol extract.

4.4.2.4 *Eclipta alba*

HPLC fingerprinting of phenolic fraction (0.1 mg/ml) was done using mobile phase acetonitrile : methanol : acetic acid (0.5%), 10 : 45 : 45. Flow rate was kept at 1 ml/min and detection was performed at 351 nm using UV detector. Finger print of phenolic fraction was also obtained using pure acetonitrile as mobile phase at flow rate of 0.8 ml/min (@ 360nm). Fingerprint of sterol fraction (0.5 mg/ml) was obtained by using pure acetonitrile as mobile phase at flow rate of 0.8 ml/min. Detection was performed at 360 nm using UV detector.

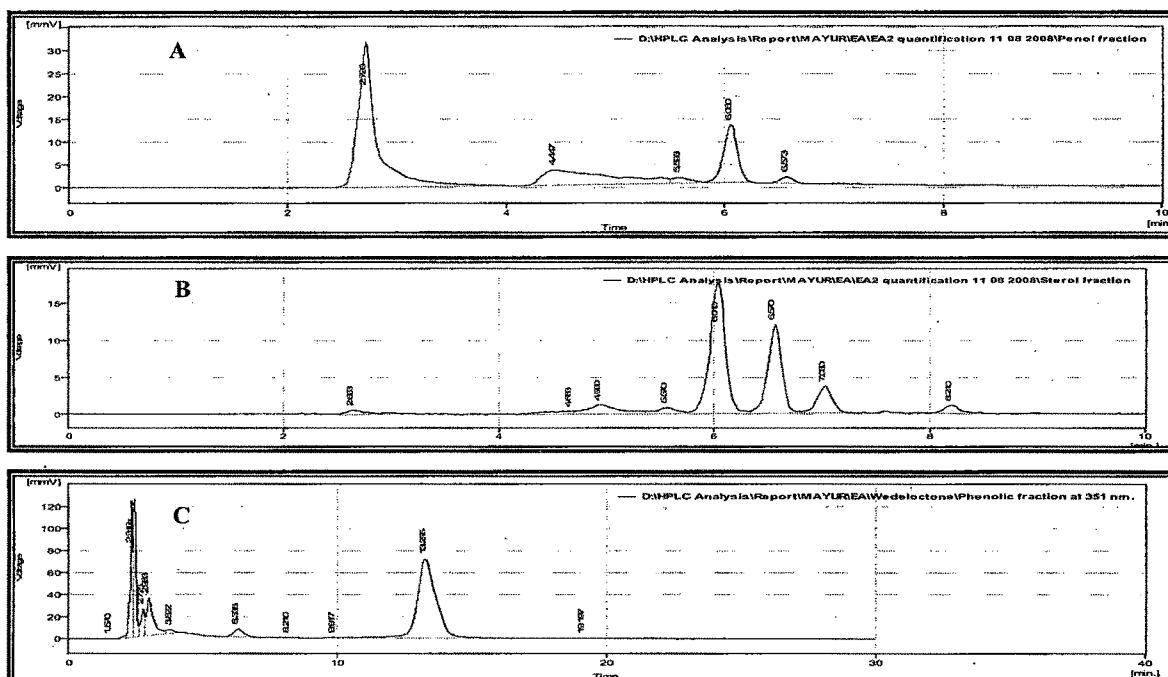


Figure 50 HPLC fingerprint of *E. alba* (A) phenolic fraction (B) sterol fraction; mobile phase ACN, detection @360 nm. (C) phenolic fraction; mobile phase acetonitrile : methanol : acetic acid (0.5%), 10 : 45 : 45, detection @ 351 nm.

4.5 Estimation of markers

4.5.1 Estimation of markers in *Enicostemma hyssopifolium*

Markers EH001 and EH002 were identified as swertisin and swertiamarin respectively. HPTLC quantitation of markers, swertiamarin and swertisin was performed to standardize the extract. Representative HPTLC plates developed for estimation of swertiamarin and swertisin are shown in figure 51 and 52 respectively. Their chromatograms are presented in figure 53 and 54 respectively.

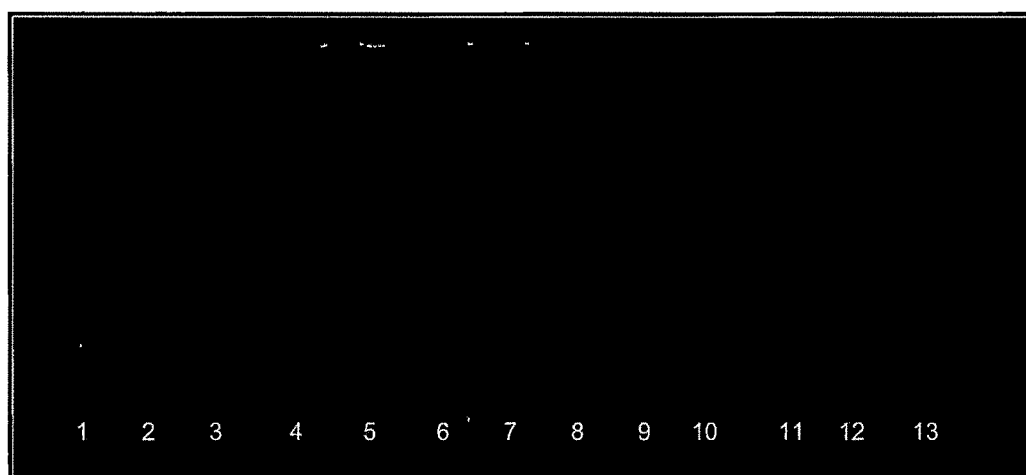


Figure 51 Quantification of swertiamarin. Track : 1 - 9 swertiamarin, 10 – E H methanol extract, 11 – polyherbal formulation, 12 – E H Flavonoid fraction, 13 – E H Bitter fraction.



Figure 52 Quantification of swertisin Track : 1 - 7 swertisin, 8 – EH methanol extract (leaf), 9 – EH methanol extract (stem) , 10 - EH methanol extract (root), 11 – polyherbal formulation, 12 – EH Flavonoid fraction, 13 – EH Bitter fraction.

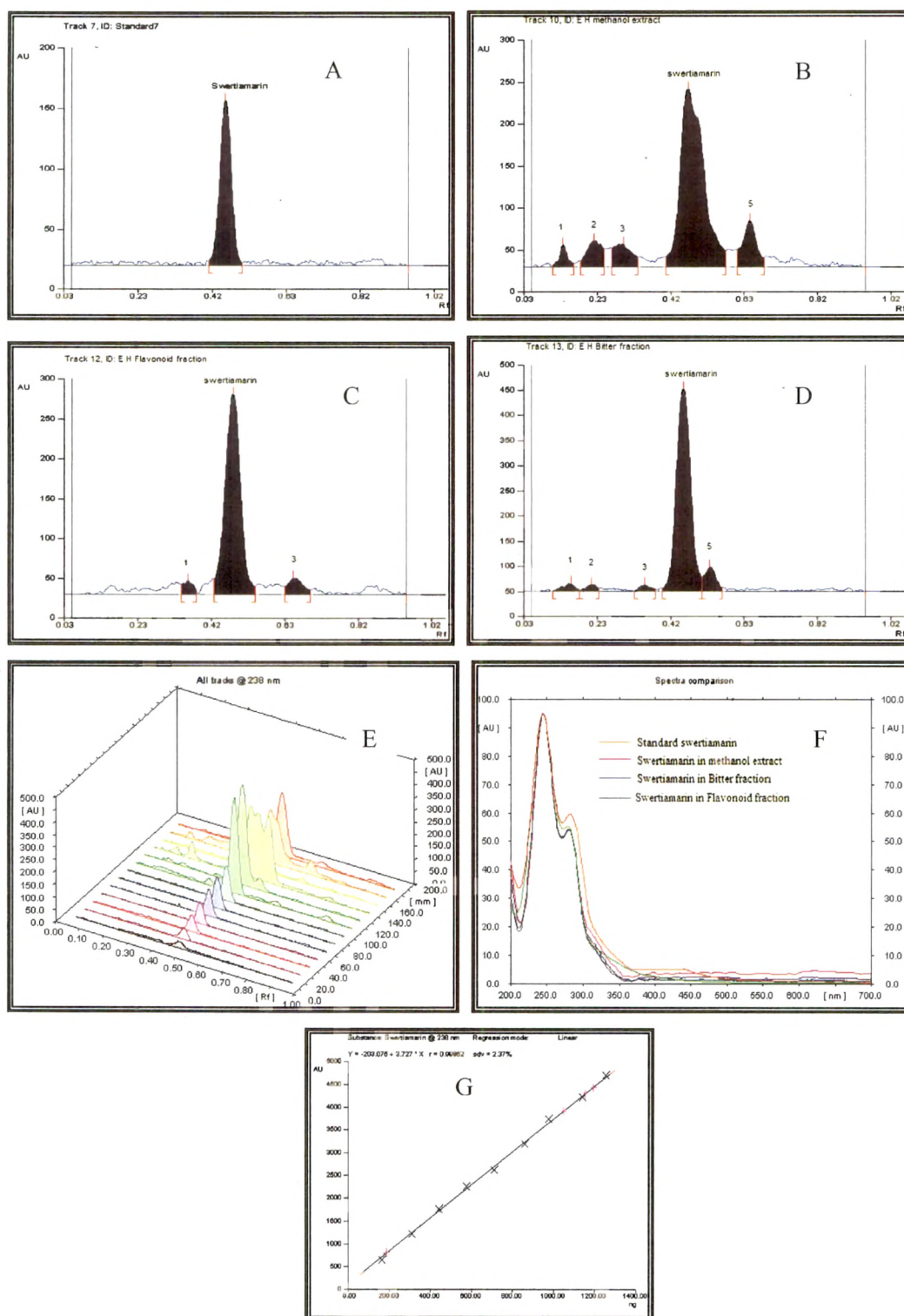


Figure 53 HPTLC quantification of swertiamarin. HPTLC chromatogram of (A) swertiamarin standard (B) EH methanol extract (C) EH Flavonoid fraction (D) EH Bitter fraction (E) spectral comparison (F) overlain spectrum of swertiamarin and (G) calibration curve of swertiamarin.

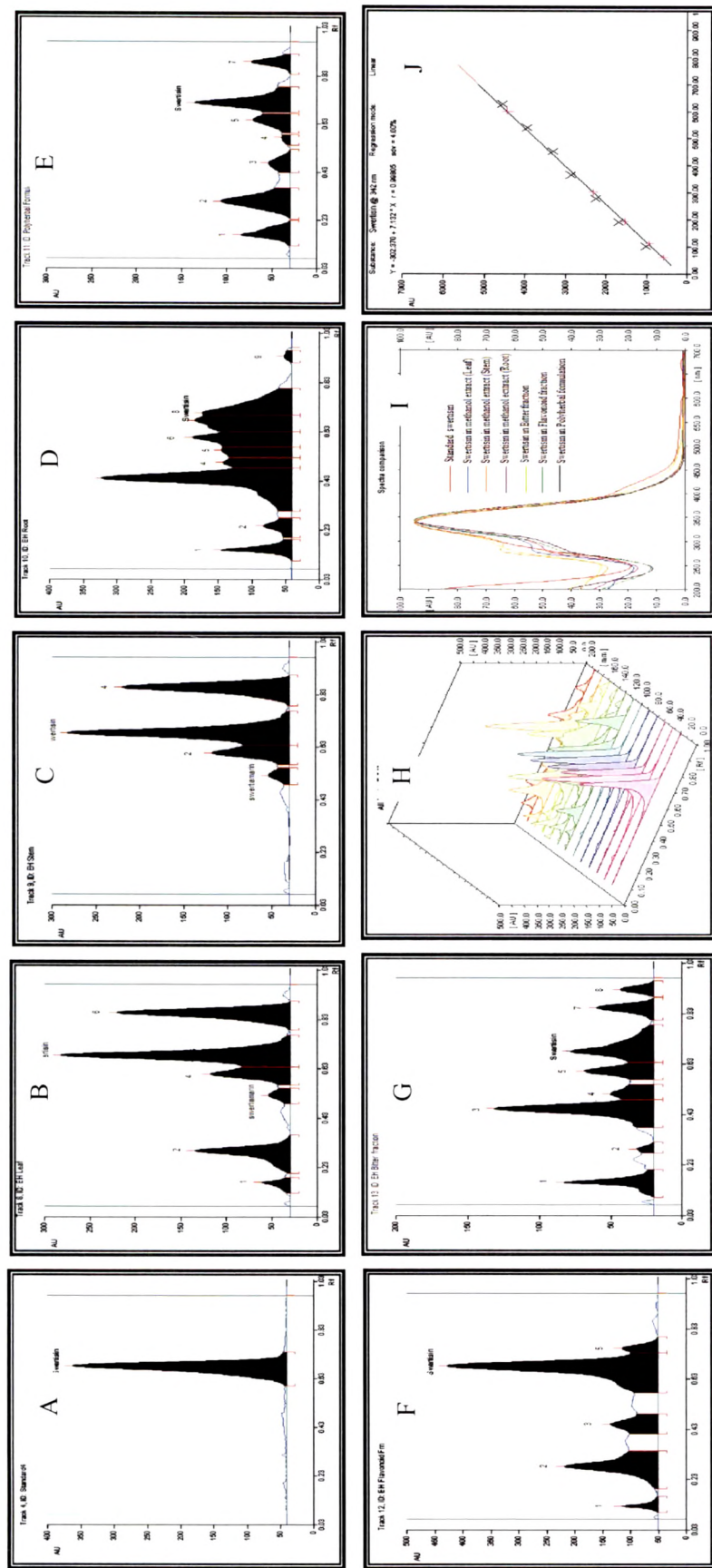


Figure 54 HPTLC quantification of swertisin. HPTLC chromatogram of (A) swertisin standard (B) EH methanol extract of leaf (C) EH methanol extract of stem (D) EH methanol extract of root (E) Polyherbal formulation (F) EH Flavonoid fraction (G) EH Bitter fraction (H) spectral comparison (I) overlain spectrum of swertisin and (J) calibration curve of swertisin.

Developed HPTLC method was validated and parameters are depicted in table 4.

Table 4 Validation parameters for swertiamarin and swertisin quantitation by HPTLC.

Parameters	Values	
	Swertiamarin	Swertisin
Detection wavelength	238 nm	342 nm
Linearity range (ng/spot)	375 - 1250	100 – 700
Limit of detection (LOD)	75 ng	30 ng
Limit of Quantification (LOQ)	150 ng	100 ng
Regression equation ($y = mx + c$)	$Y = 3.727 X - 203.075$	$Y = 7.132 X - 302.370$
Correlation coefficient	0.99852	0.99805
Recovery study		
80% level	$98.11 \pm 0.08^{\#}$	$99.94 \pm 0.11^{\#}$
100% level	$99.63 \pm 0.12^{\#}$	$101.3 \pm 0.26^{\#}$
120% level	$100.35 \pm 0.17^{\#}$	$102.01 \pm 0.26^{\#}$
Precision (%RSD)		
Intra-day (n=5)	0.63	0.40
Inter-day (n=5)	0.36	0.38

Each value is mean \pm standard deviation of three determinations.

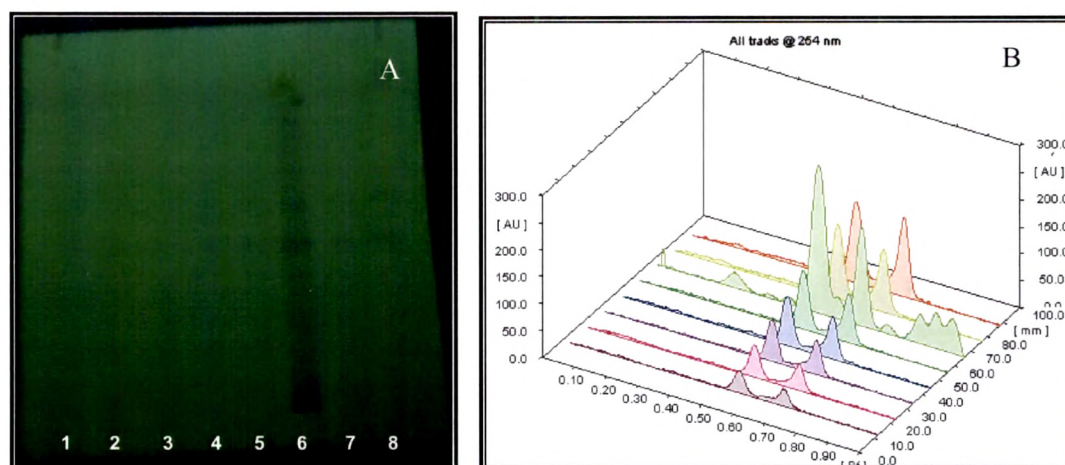


Figure 55 Simultaneous estimation of swertiamarin and swertisin in methanol extract of *E. hyssopifolium*. (A) HPTLC plate, Track 1-5 and 7, 8 – standard mixture, Track 6- EH methanol extract (B) spectral comparison.

As shown in figure 56 is a representative chromatogram for simultaneous estimation of two markers; swertiamarin and swertisin by HPTLC. Validation parameter for it is presented in table 5.

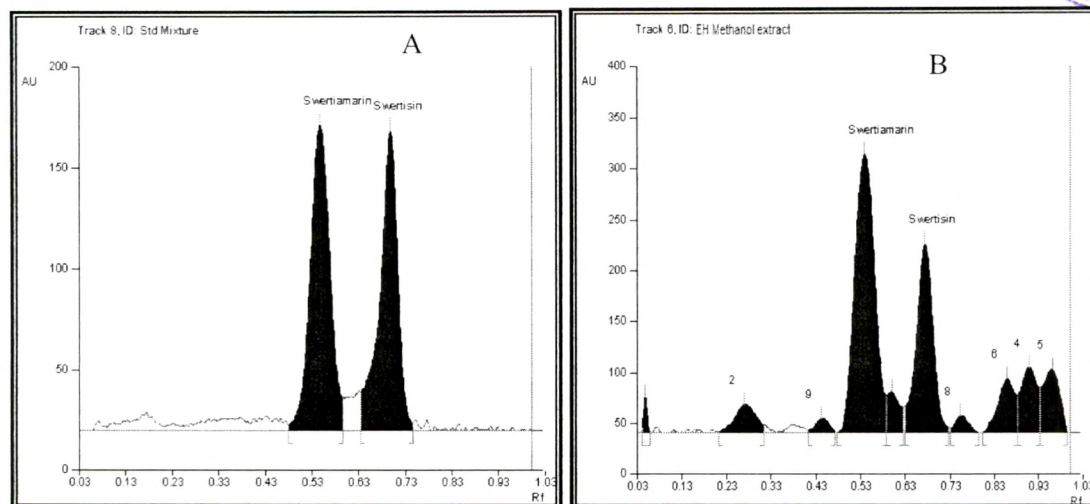


Figure 56 HPTLC chromatogram of (A) swertiamarin-swertisin standard mixture and (B) EH methanol extract.

Table 5 Validation parameters for simultaneous estimation of swertiamarin and swertisin by HPTLC.

Parameters	Values	
	Swertiamarin	Swertisin
Detection wavelength	254 nm	
Linearity range (ng/spot)	500 - 1250	350 - 875
Regression equation ($y = mx + c$)	$Y = 3.2477 X + 139.54$	$Y = 4.7029 X - 519.36$
Correlation coefficient	0.9956	0.9979
Recovery study		
80% level	95.36 ± 0.18	89.94 ± 0.21
100% level	103.63 ± 0.23	94.33 ± 0.19
120% level	92.35 ± 0.35	93.18 ± 0.43
Precision (%RSD)		
Intra-day (n=5)	1.02	0.94
Inter-day (n=5)	0.63	0.73

Results for the marker estimation individually and simultaneously in various samples are presented in table 6. Simultaneous estimation also gave results comparable to that measured individually. Amongst studied formulation only F-2 showed the presence of swertisin and no peak for swertiamarin was obtained.

Table 6 HPTLC estimation of swertiamarin and swertisin in different samples.

Sample	Individual estimation		Simultaneous estimation	
	Swertiamarin @ 238 nm (% w/w)	Swertisin @ 342 nm (% w/w)	Swertiamarin @ 254 nm (% w/w)	Swertisin @ 254 nm (% w/w)
	EH Root	0.230	0.660	
EH Stem	0.521	0.730		
EH leaf	0.556	0.820		
Methanol extract (Aerial parts)	1.404	2.100	1.340	2.170
EH Bitter Fraction	18.65	12.37	(0.499 % w/w in aerial part)	(0.808% w/w in aerial part)
EH Flavonoid Fraction	19.54	25.82		
Polyherbal Formulation (F2)	-	0.0095		

HPLC quantitation of markers, swertiamarin and swertisin in both the fractions were also carried out at 238 and 342 nm wavelength respectively at the flow rate of 1 ml/min. Method for the estimation of marker compound in plant fraction was also been validated. HPLC chromatograms are presented in figure 57 and 58.

Table 7 Validation parameters for swertiamarin and swertisin quantitation by HPLC.

Parameters	Values	
	Swertiamarin	Swertisin
Detection wavelength	238 nm	342 nm
Linearity range ($\mu\text{g/ml}$)	10-100	20-200
Limit of detection (LOD)	2.5 $\mu\text{g/ml}$	12.5 $\mu\text{g/ml}$
Limit of Quantification (LOQ)	10 $\mu\text{g/ml}$	20 $\mu\text{g/ml}$
Regression equation ($y = mx + c$)	$Y = 11.205X + 2.264$	$Y = 3.996X + 0.8254$
Correlation coefficient	0.9990	0.9966
Recovery study		
80% level	$96.45 \pm 0.12^{\#}$	$98.33 \pm 0.13^{\#}$
100% level	$97.34 \pm 0.06^{\#}$	$96.61 \pm 0.08^{\#}$
120% level	$99.62 \pm 0.09^{\#}$	$100.51 \pm 0.18^{\#}$
Precision (%RSD)		
Intra-day (n=5)	0.52	0.68
Inter-day (n=5)	0.66	0.93

value is mean \pm standard deviation of three determinations.

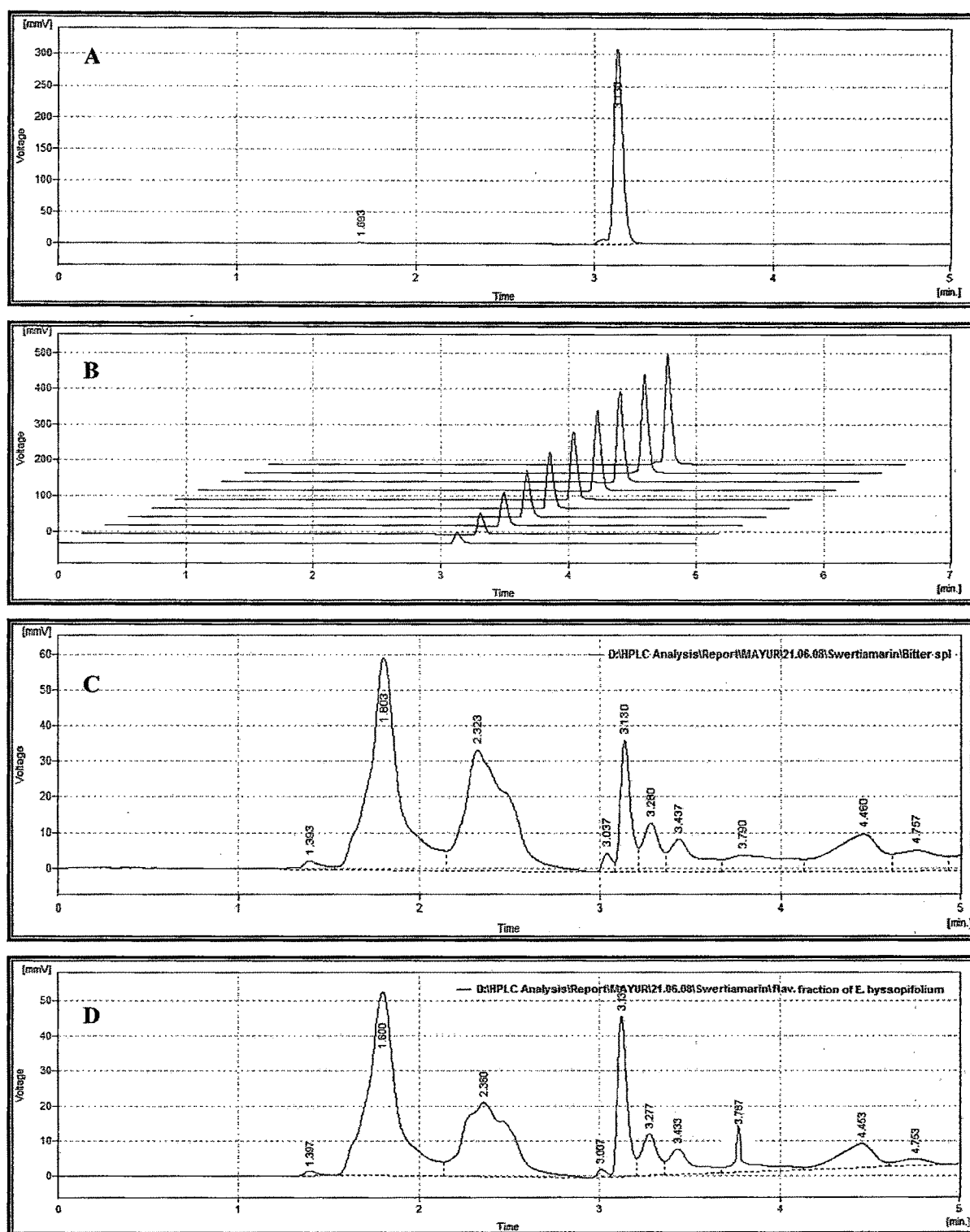


Figure 57 HPLC quantification of swertiamarin. (A) HPLC chromatogram of swertiamarin standard (B) stacked chromatogram of calibration (C) EH Bitter fraction (D) EH Flavonoid fraction.

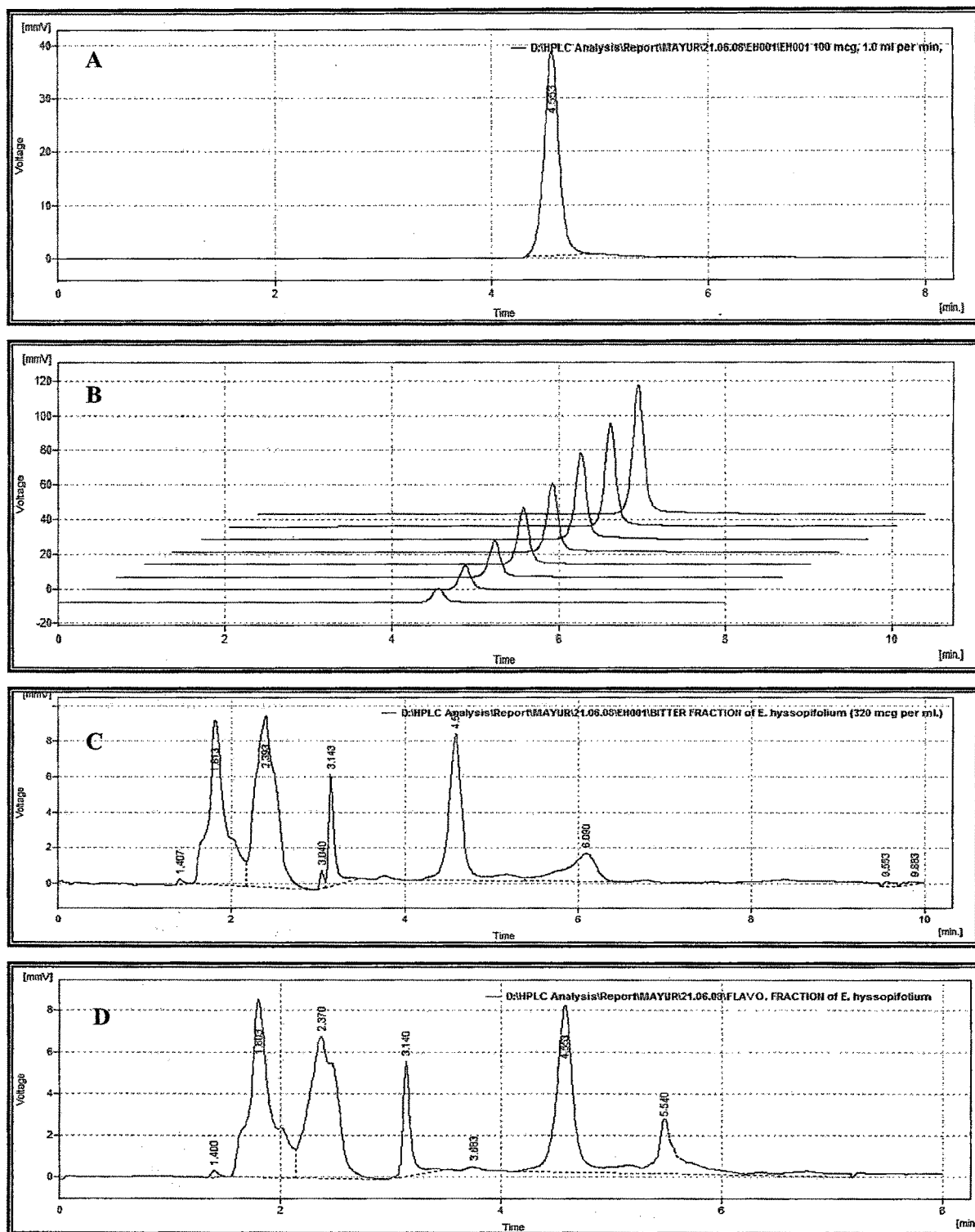


Figure 58 HPLC quantification of swertisin. (A) HPLC chromatogram of swertisin standard (B) stacked chromatogram of calibration (C) EH Bitter fraction (D) EH Flavonoid fraction.

Retention time (R_t) for swertiamarin and swertisin was found to be 3.13 and 4.55 min respectively. In the optimized condition for HPLC satisfactory resolution was obtained. Content of marker estimated by HPLC are shown in table 8. The results are comparable to that of HPTLC results.

Table 8 HPLC quantitation of markers in *E. hyssopifolium*.

Sample	Marker content (% w/w)
EH aerial parts	Swertiamarin - 0.46
EH aerial parts	Swertisin - 0.73

4.5.2 Estimation of markers in *Tinospora cordifolia*

Quantitation of marker compound, tinosporaside in plant extracts was performed using the mobile phase chloroform : methanol (4 : 1). Scanning was done at 255 nm in absorption mode. Validation parameters are depicted in table 9.

Table 9 Validation parameters for estimation of Tinosporaside by HPTLC.

Parameters	Values
Detection wavelength	254 nm
Linearity range (ng/spot)	225 – 1125
Regression equation ($y = mx + c$)	$Y = 0.198 X - 38.570$
Correlation coefficient	0.99722
Recovery study	
80% level	96.93 ± 0.56
100% level	100.42 ± 0.41
120% level	98.58 ± 0.64
Precision (%RSD)	
Intra-day (n=5)	0.89
Inter-day (n=5)	0.95

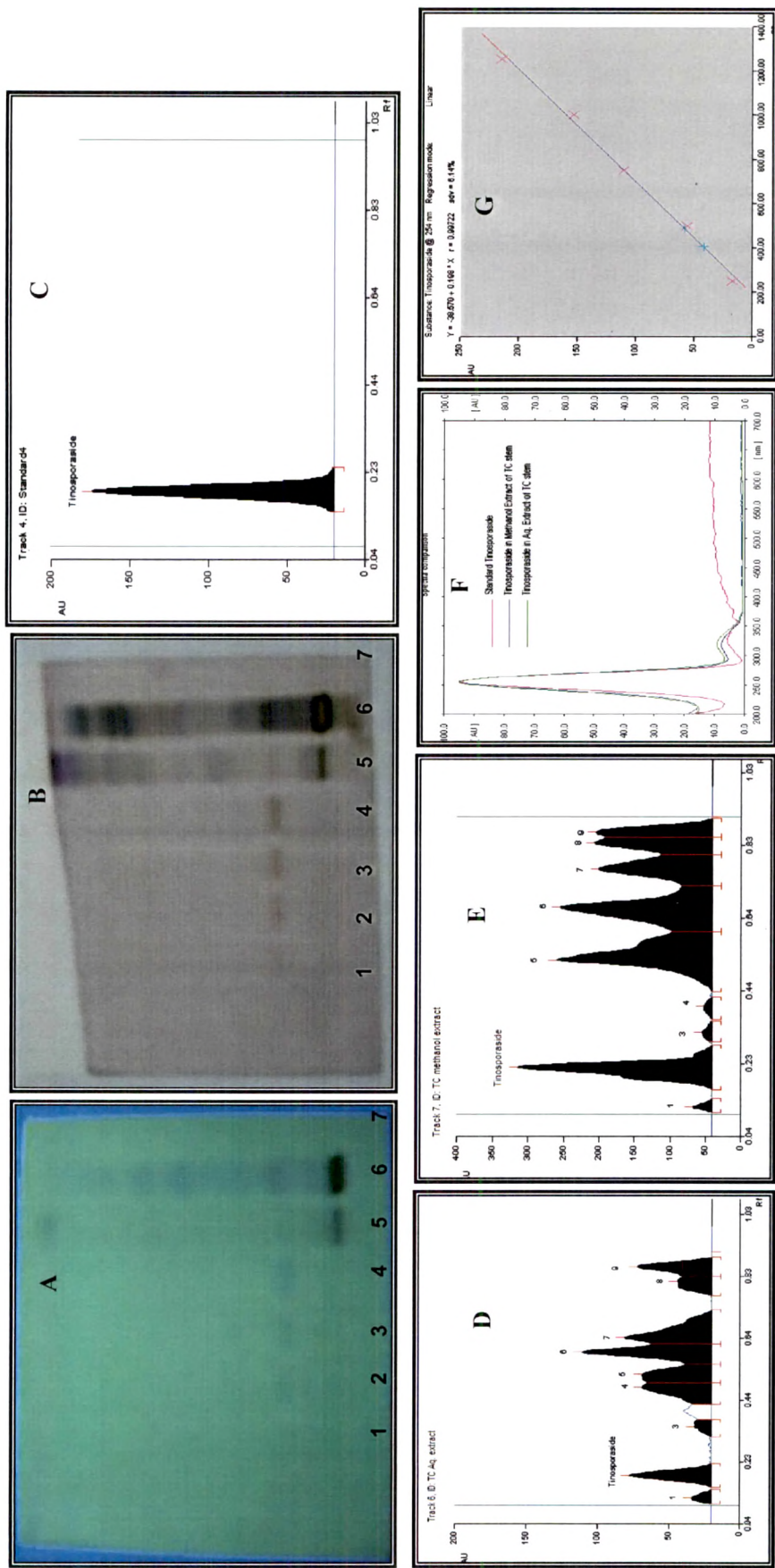


Figure 59 HPTLC quantification of Tinosporaside. (A) HPTLC plate under 254 nm; Track 1-5: Standard tinosporaside, 6: TC aqueous extract, 7: TC methanol extract. (B) HPTLC plate after AS spray and heat for 5 min. at 110 °C (C) HPTLC chromatogram of tinosporaside standard (D) TC methanol extract of stem (E) TC aqueous extract of stem (F) Spectral comparison, Overlain spectrum of tinosporaside and (G) Calibration curve of tinosporaside.

Validation parameters found to be in great agreement to adopt the method for routine analysis of *T. cordifolia* extract by HPTLC. Content of tinosporaside in different sample are presented in table 10. Three herbal formulations F-2, F-3 and F-4 found to contain tinosporaside 0.003%, 0.006% and 0.004% w/w tinosporaside respectively.

Table 10 HPTLC estimation of tinosporaside in extracts and formulation.

Sample	Tinosporaside @ 254 nm (% w/w)
TC Stem	0.001
TC methanol extract	0.085
TC aqueous extract	0.032
Polyherbal formulation (F2)	0.003
Polyherbal formulation (F3)	0.006
Polyherbal formulation (F4)	0.004

4.5.3 Estimation of markers in *Gymnema sylvestre*

The total saponin fraction, referred to as gymnemic acids, of the leaves of *Gymnema sylvestre* has been identified and the quality of *Gymnema sylvestre* extracts and formulations were assessed by the content of gymnemagenin. Direct estimation of gymnemic acids is very difficult because they are a complex mixture of several closely related compounds. Figure 60 shows HPTLC chromatograms of gymnemagenin (R_f 0.67) and of a *Gymnema sylvestre* leaf extract, hydrolysed according to the method described.

Table 11 Validation parameters for estimation of gymnemagenin by HPTLC.

Parameters	Values
Detection wavelength	450 nm
Linearity range ($\mu\text{g}/\text{spot}$)	50 - 400
Regression equation ($y = mx + c$)	$Y = 6.697 X + 677.618$
Correlation coefficient	0.98537
Recovery study	
80% level	90.11 ± 1.38
100% level	93.52 ± 2.41
120% level	95.63 ± 1.06
Precision (%RSD)	
Intra-day (n=5)	1.23
Inter-day (n=5)	0.95

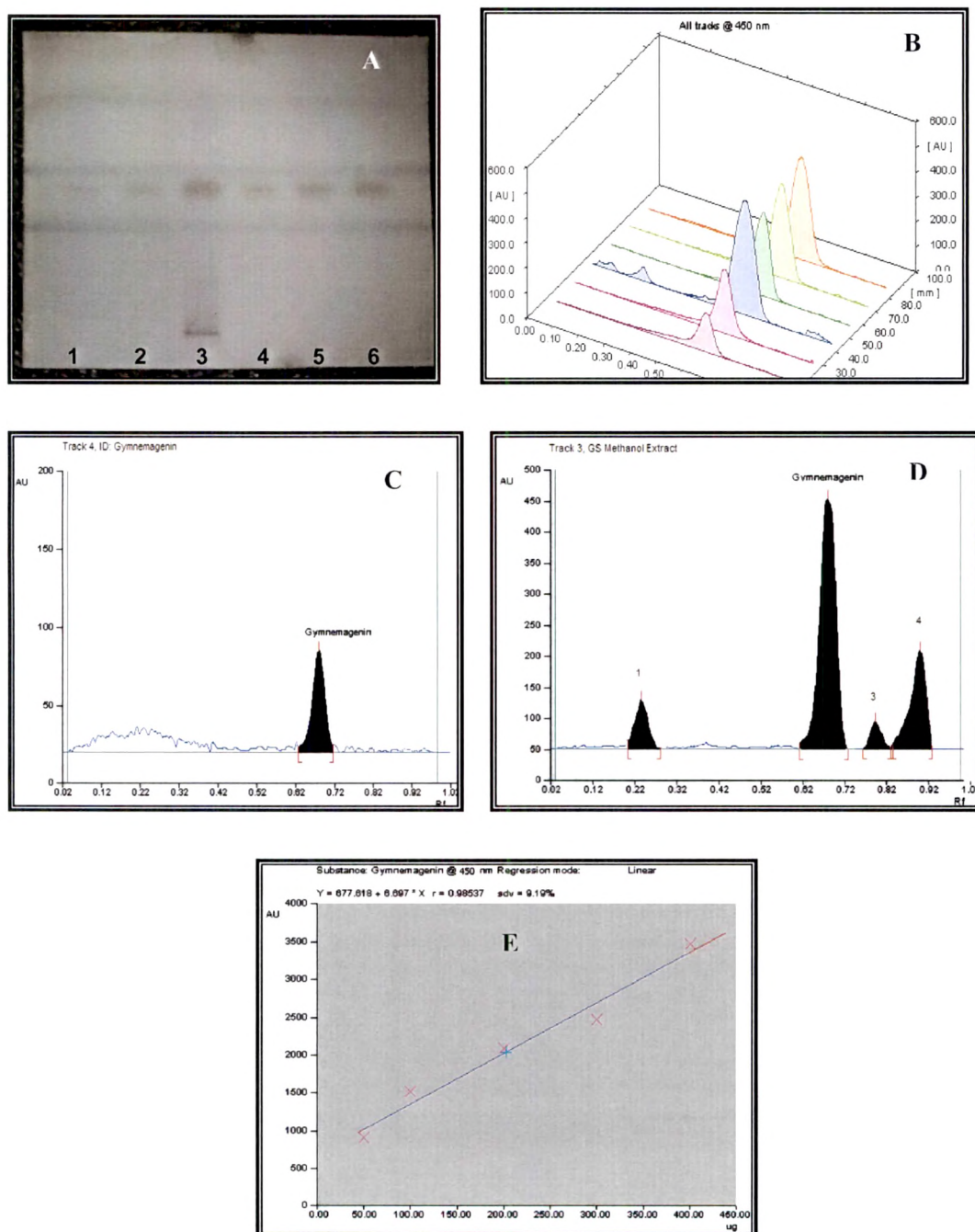


Figure 60 HPTLC quantification of Gymnemagenin. (A) HPTLC plate after AS spray and heat for 5 min. at 110 °C (B) spectral comparison (C) HPTLC chromatogram of isolated gymnemagenin (D) GS methanol extract (E) calibration curve at 450 nm.

Gymnemagenin content in various samples are shown in table 12. Formulation F-1 found to have 0.008% w/w gymnemagenin, none of the other formulations found to contain gymnemagenin in quantifiable amount.

Table 12 HPTLC estimation of gymnemagenin in extracts and formulation.

Sample	Gymnemagenin @ 450 nm (% w/w)
GS leaves	1.69
GS methanol extract	5.62
GS aqueous extract	2.81
Polyherbal formulation (F1)	0.008

4.5.4 Estimation of markers in *Eclipta alba*

A major coumestan, wedelolactone was quantified in *E. alba* extracts and fraction by HPTLC method. Data for analytical methods are shown in figure 61 and in table 13 and 14.

Table 13 Parameters for estimation of wedelolactone by HPTLC.

Parameters	Values
Detection wavelength	351 nm (Fluorescent mode)
Linearity range (ng/spot)	100 – 500
Regression equation (y = mx + c)	Y = 17.573 X – 408.902
Correlation coefficient	0.98869
Recovery study	
80% level	100.23 ± 1.05
100% level	99.36 ± 0.82
120% level	97.65 ± 0.51
Precision (%RSD)	
Intra-day (n=5)	0.58
Inter-day (n=5)	1.23

HPTLC quantitation of wedelolactone in different samples of *E. alba* gave following results.

Table 14 HPTLC estimation of wedelolactone in extracts and fraction.

Sample	Wedelolactone @ 351 nm (% w/w)
EA aerial parts	1.879
EA methanol extract	5.310
<i>EA phenolic fraction</i>	19.69

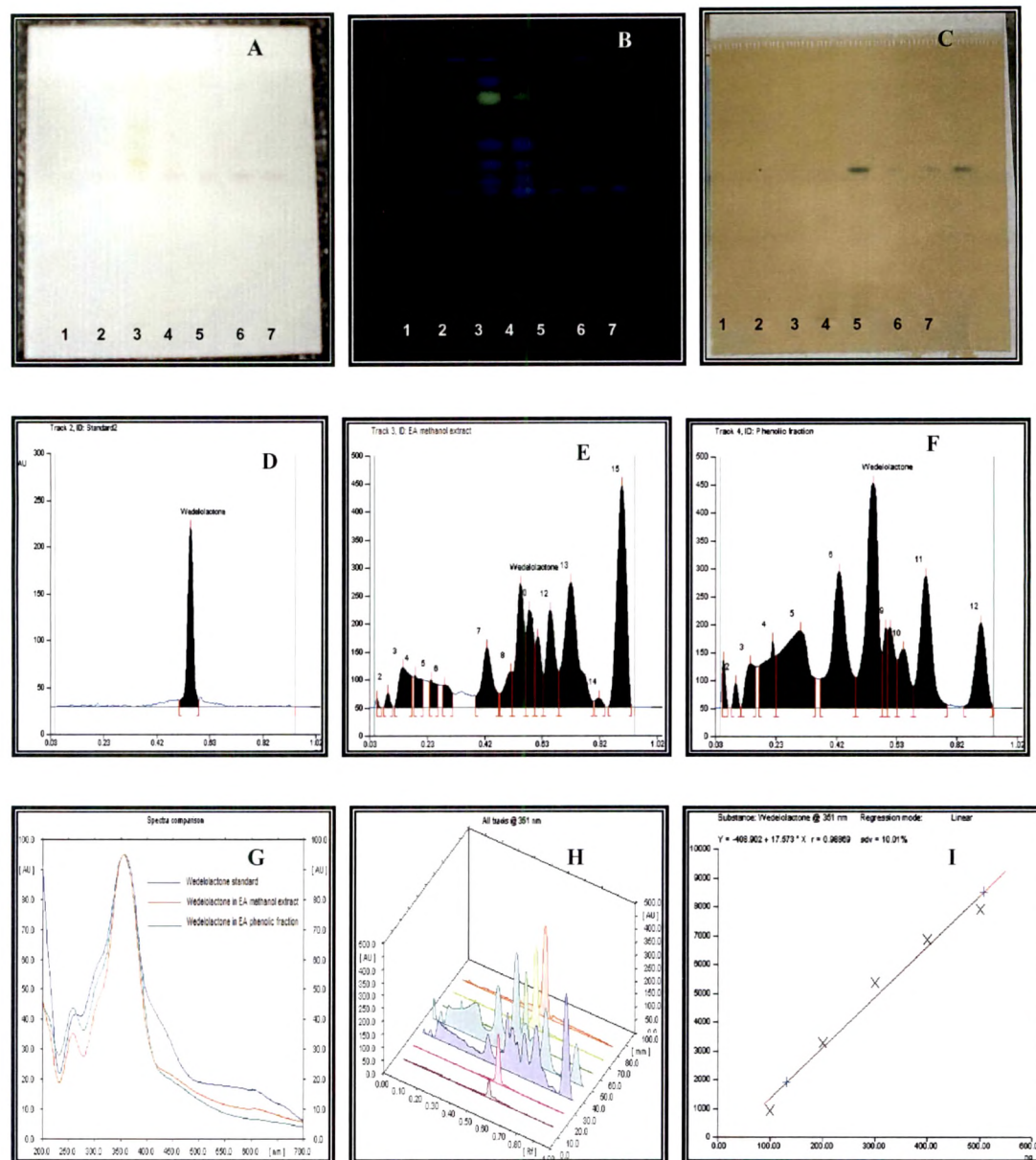


Figure 61 HPTLC quantification of wedelolactone. (A) HPTLC plate in visible light (B) under UV 366 nm (C) after spray with ferric chloride; Track 1, 2, 5, 6, 7 – standard wedelolactone; Track 3 - EA methanol extract; Track 4 – EA phenolic fraction (D) HPTLC chromatogram of wedelolactone standard (E) EA methanol extract (F) EA phenolic fraction (G) overlain spectrum of wedelolactone (H) spectral comparison and (I) calibration curve of wedelolactone.

The same marker was also been estimated by HPLC method. Data are shown in figure 62 and table 15 and 16. A sterol fraction of *E. alba* was quantified for its EA002 content by HPLC. Results are depicted in form of HPLC chromatogram (figure 63).

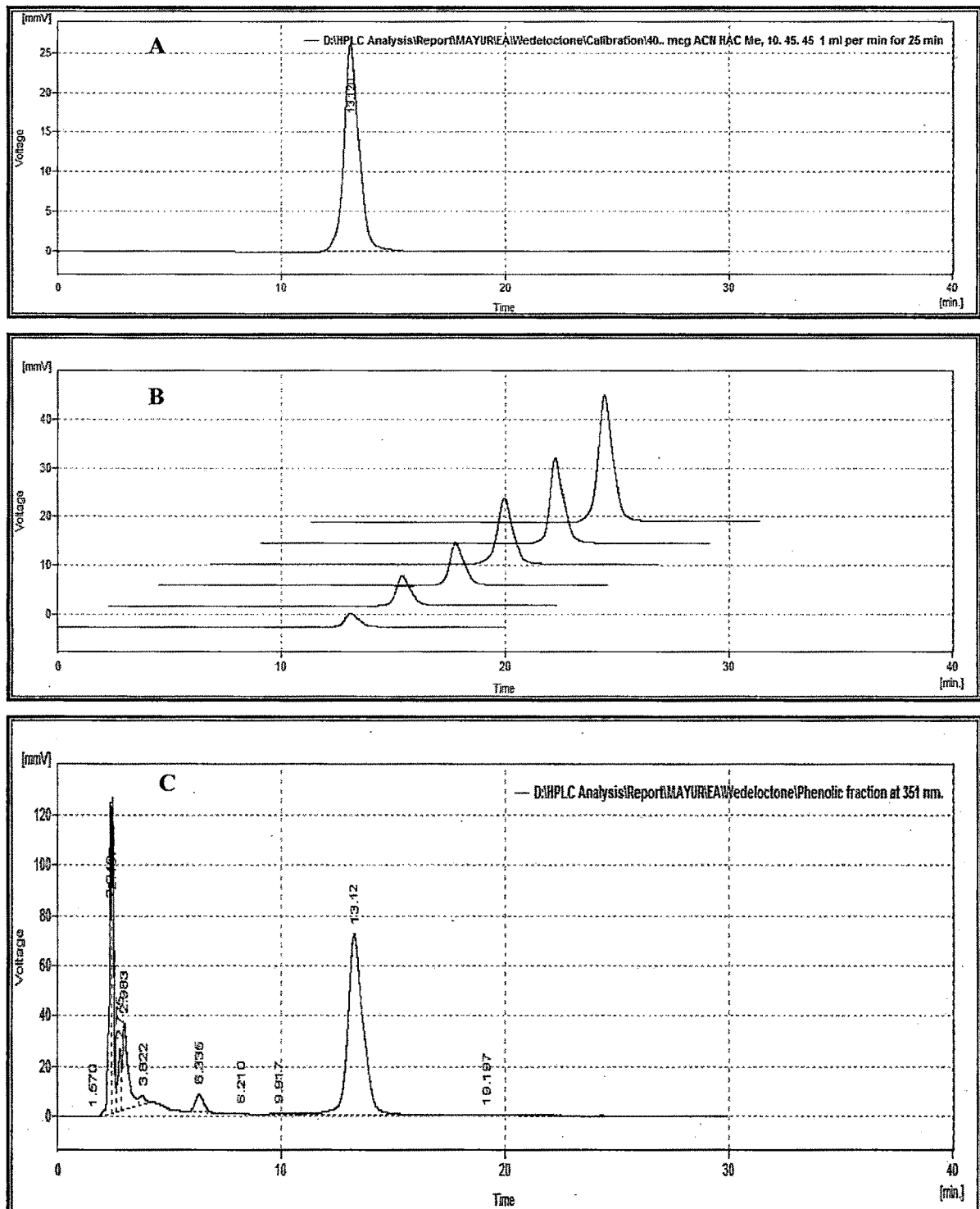


Figure 62 HPLC quantification of wedelolactone (A) HPLC chromatogram of wedelolactone standard (Rt 13.12 min) (B) stacked chromatogram of calibration (C) EA phenolic fraction.

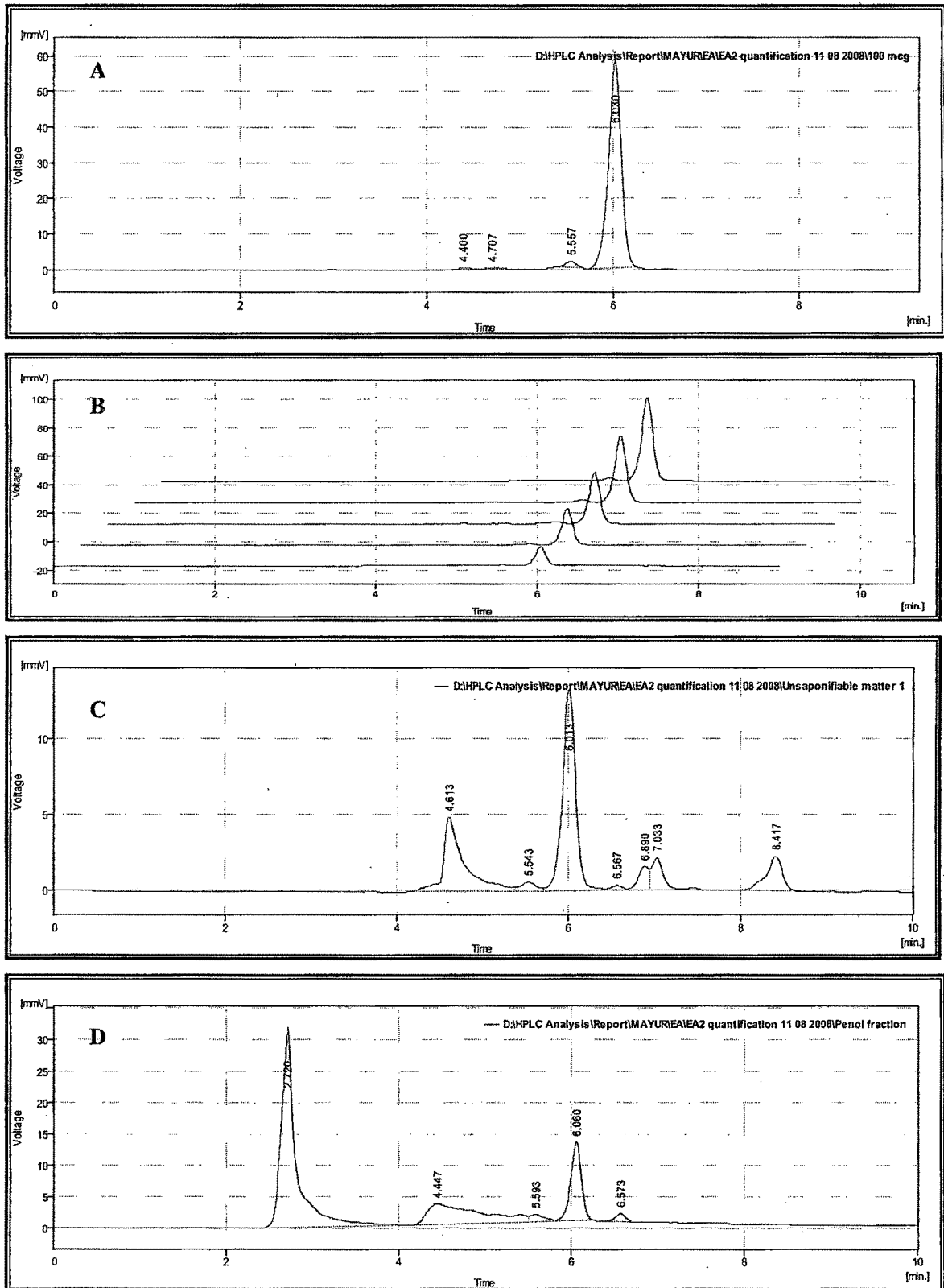


Figure 63 HPLC quantification of EA002 (A) HPLC chromatogram of EA002 (R_t 6.03 min) (B) stacked chromatogram of calibration (C) EA Sterol fraction (D) EA Phenolic fraction.

Table 15 Validation parameters for wedelolactone and EA002 quantitation by HPLC.

Parameters	Values	
	Wedelolactone	EA002
Detection wavelength	351 nm	361 nm
Linearity range ($\mu\text{g/ml}$)	4-40	10 – 50
Limit of detection (LOD)	800 ng/ml	3.0 μg
Limit of Quantification (LOQ)	2.5 $\mu\text{g/ml}$	10.0 μg
Regression equation ($y = mx + c$)	$Y = 37.511X - 95.69$	$Y = 7.132 X - 302.370$
Correlation coefficient	0.9956	0.99805
Recovery study		
80% level	$95.53 \pm 0.89^{\#}$	$99.94 \pm 0.11^{\#}$
100% level	$100.21 \pm 0.08^{\#}$	$101.3 \pm 0.26^{\#}$
120% level	$98.50 \pm 0.53^{\#}$	$102.01 \pm 0.26^{\#}$
Precision (%RSD)		
Intra-day (n=5)	0.68	0.40
Inter-day (n=5)	0.94	0.38

[#] value is mean \pm standard deviation of three determinations.

Content of marker constituents estimated in *E. alba* samples by HPLC method are presented in table 16.

Table 16 HPLC quantitation markers in *E. alba*

Sample	Marker content (% w/w)	
	Wedelolactone	EA002
EA aerial parts	1.52	0.05
EA phenolic fraction	20.02	1.63
EA sterol fraction	11.53	5.26

[#] value is mean of three determinations.

4.6 Biological Studies

4.6.1 Glucose uptake study on rat everted gut sac

The most challenging goal in the management of patients with DM is to achieve blood glucose level as close to normal as possible. Unfortunately, postprandial hyperglycaemia (PPHG) or hyperinsulinaemia are independent risk factors for the development of vascular complications in DM patients (Tiwari and Madhusudana, 2002). Mechanisms playing role in release and transport of glucose across the intestinal brush border membrane down to the blood stream have attracted much attention recently as potential targets to control PPHG. In this category, majority of recent studies reported the potential use of antidiabetic medicinal plants on inhibition of glucose transport. Drugs that reduce PPHG by suppressing the absorption of carbohydrate are effective in prevention and treatment of non-insulin dependent DM. Findings of this experiment would tend to indicate that glucose transport was significantly decreased in the presence of the aqueous extract of TC stem, GS leaf, and EA aerial parts which caused a decrease in the V_{max} . Biochemical parameters of D (+)-glucose transport across rat everted small intestines *in vitro* are shown in tabular and graphical forms in table 17 and figure 64. The K_m and V_{max} were calculated in the absence as well as in the presence of plant extracts in the mucosal solution and are shown in Table 57. Data analysis revealed that V_{max} for glucose uptake decreased by 28.67, 83.67, and 50.75 $\mu\text{M hr}^{-1}$ in the presence of the aqueous TC stem extract, GS leaf and EA aerial parts, respectively. The apparent K_m remained unaltered in the all case of the studied plant extracts. Only the aqueous extract of aerial parts of EH did not decreased the glucose absorption *in vitro* rather it increases the V_{max} . Since the aqueous extract of aerial parts of EH found to contain high amount of reducing sugars in free form it may presume that it could cause enhancement of glucose uptake *in vitro*. However, the K_m remained unaltered in the presence as well in the absence of these extracts. This indicates that these extracts act by bringing a non-competitive type of inhibition of glucose at the level of the small intestine.

Table 17 Effects of plant extracts on the uptake of varying concentration of substrate (D (+) Glucose) by everted intestinal sacs of rats.

	Substrate conc. in the medium (mM)	Uptake	Uptake
		($\mu\text{mol/g}$ tissue wet wt/h) Control without the plant extract (n=5)	($\mu\text{mol/g}$ tissue wet wt/h) In presence of plant extracts (n=5)
EH	5	28.0 \pm 0.23	29.1 \pm 0.21
	10	41.2 \pm 0.62	42.3 \pm 0.32
	15	51.2 \pm 0.20	54.1 \pm 0.54
	20	58.2 \pm 0.61	60.1 \pm 0.14
TC	5	29.2 \pm 0.15	19.5 \pm 0.66
	10	40.4 \pm 0.23	25.6 \pm 0.51
	15	52.8 \pm 0.55	32.6 \pm 0.21
	20	56.6 \pm 0.26	38.9 \pm 0.25
GS	5	25.6 \pm 0.11	18.8 \pm 0.61
	10	40.2 \pm 0.38	25.3 \pm 0.57
	15	51.3 \pm 0.61	31.1 \pm 0.52
	20	58.3 \pm 0.24	35.1 \pm 0.14
EA	5	33.1 \pm 0.51	25.6 \pm 0.12
	10	41.5 \pm 0.18	36.2 \pm 0.36
	15	56.1 \pm 0.14	47.8 \pm 0.32
	20	66.1 \pm 0.26	53.3 \pm 0.61

n= number of sacs used. The everted gut sacs were incubated in Krebs- Henseleit buffer (pH= 7.4) at 37°C.

Table 18 Biochemical parameters obtained for the effect of plant extracts on the transport of D (+)-glucose at different concentrations (5-20 mM) across the rat everted gut sacs.

Experiments	EH		TC		GS		EA	
	Control	Test	Control	Test	Control	Test	Control	Test
V_{max} ($\mu\text{M hr}^{-1}$)	108.2 \pm 10.6	112.1 \pm 6.6	98.09 \pm 7.9	69.42 \pm 6.9	170.7 \pm 15.9	87.03 \pm 9.8	154.1 \pm 12.6	103.35 \pm 8.63
	K_m (μM)	24.75 \pm 5.3	24.39 \pm 6.1	22.26 \pm 6.6	22.22 \pm 5.1	53.34 \pm 13.6	53.37 \pm 10.1	32.25 \pm 6.30

The everted gut sacs were incubated in Krebs- Henseleit buffer (pH= 7.4) at 37 °C.

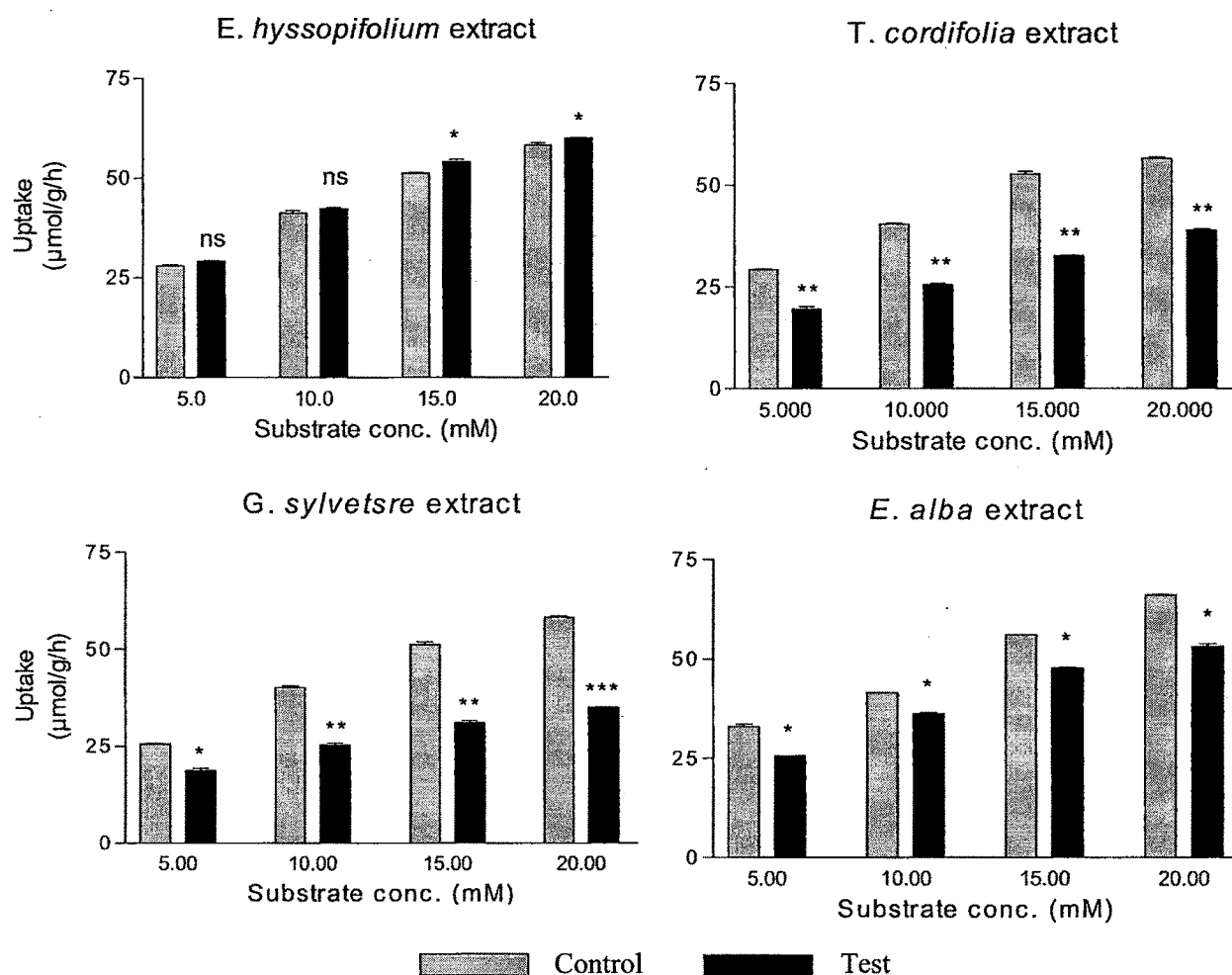


Figure 64 Effect of extracts on D (+)-glucose uptake across rat everted gut sac.

ns: not significant, * $p < 0.05$, ** $p < 0.001$, *** $p < 0.0001$.

Out of these four extract, GS leaf extract showed excellent inhibition of glucose uptake at intestinal level. Gymnemic acid, a major constituent present in the extract was checked along with its genin moiety, gymnemagenin at different dose levels in the same experimental set up. Results are depicted in table 19 and graph 65. Gymnemagenin as such did not possess any inhibition of glucose uptake whereas gymnemic acid showed 24.12, 28.38, 41.92% inhibition at 1, 5 and 10 mg/ml dose respectively.

Table 19 Biochemical parameters obtained for the effect of plant extracts on the transport of D (+)-glucose at different concentrations (1-10 mg/ml) across the rat everted gut sacs.

Sample conc. (mg/ml)	Substrate conc. in the medium (mM)	Uptake ($\mu\text{mol/g}$ tissue wet wt/h) Control (n=3)	Uptake ($\mu\text{mol/g}$ tissue wet wt/h) In presence of Gymnemic acid (n=3)	Uptake ($\mu\text{mol/g}$ tissue wet wt/h) In presence of Gymnemagenin (n=3)
1	5	19.6 \pm 0.11	15.4 \pm 0.23	18.8 \pm 0.16
	10	22.8 \pm 0.16	18.5 \pm 0.21	21.6 \pm 0.15
	15	31.5 \pm 0.31	25.1 \pm 0.30	30.3 \pm 0.27
	20	41.1 \pm 0.14	33.6 \pm 0.16	40.2 \pm 0.30
5	5	25.2 \pm 0.15	22.6 \pm 0.24	24.9 \pm 0.36
	10	30.5 \pm 0.22	23.5 \pm 0.36	28.6 \pm 0.16
	15	42.6 \pm 0.16	28.6 \pm 0.25	41.1 \pm 0.28
	20	46.2 \pm 0.31	33.0 \pm 0.18	45.3 \pm 0.19
10	5	29.2 \pm 0.15	19.5 \pm 0.66	28.3 \pm 0.29
	10	40.4 \pm 0.23	25.6 \pm 0.51	41.6 \pm 0.13
	15	52.8 \pm 0.55	32.6 \pm 0.21	48.5 \pm 0.38
	20	56.6 \pm 0.26	38.9 \pm 0.25	58.3 \pm 0.22

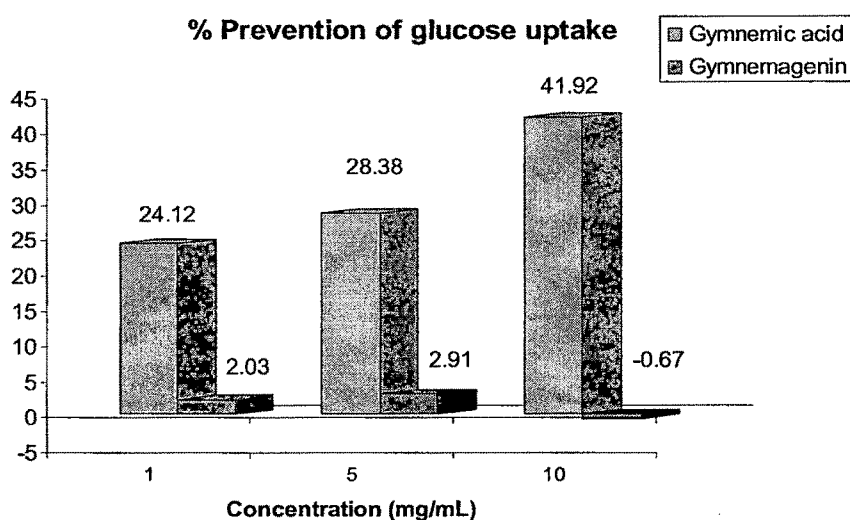


Figure 65 Effect of crude gymnemic acid and gymnemagenin on prevention of glucose uptake.

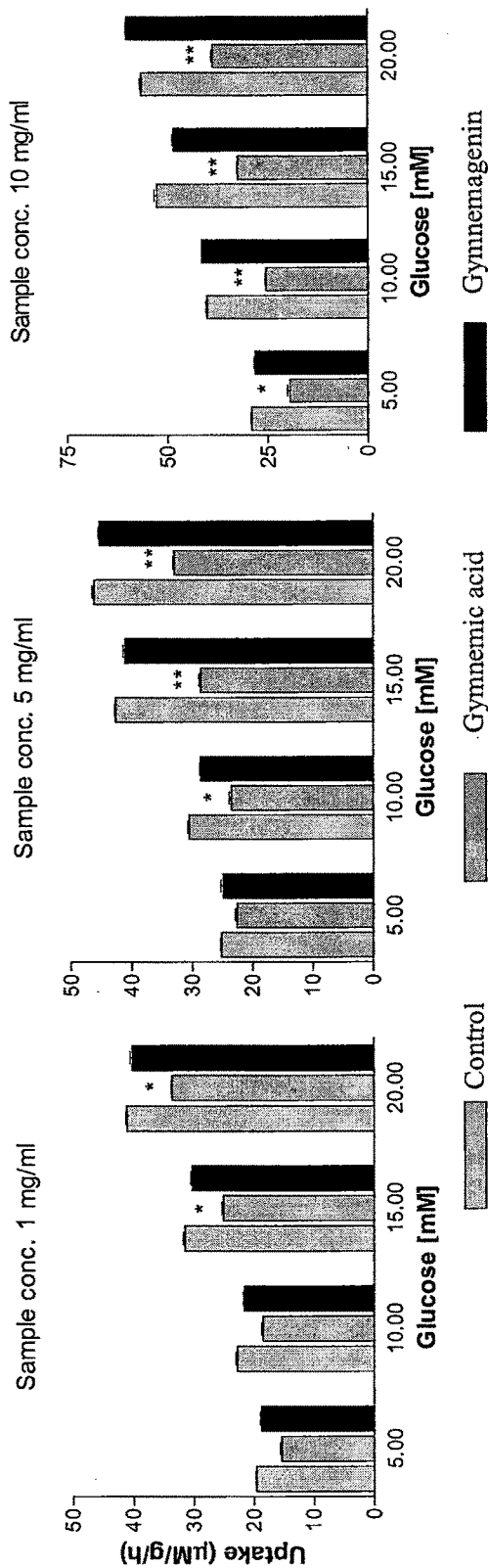


Figure 66 A comparison of gymnemic acid and gymnemenin as an inhibitor of glucose uptake in rat everted gut sac study

Table 20 Kinetic parameters obtained for the effect of gymnemic acid on the transport of D (+)-glucose across the rat everted gut sacs.

Experiments	Gymnemic acid		
	1 mg/ml	5 mg/ml	10 mg/ml
V_{max} ($\mu\text{M hr}^{-1}$)	Control 108.2 \pm 12.1 Test 82.1 \pm 18.6	Control 144.1 \pm 20.3 Test 103.2 \pm 14.5	Control 198.09 \pm 29.6 Test 109.42 \pm 11.3
K_m (μM)	Control 24.75 \pm 6.3 Test 24.39 \pm 5.3	Control 27.02 \pm 7.1 Test 27.26 \pm 9.4	Control 22.26 \pm 6.6 Test 22.22 \pm 5.1

Gymnemic acid, a major oleanane triterpenoid saponin, possessed a potent inhibitory effect on glucose uptake at small intestine. Glucose transport through biological membranes requires specific transport proteins. Active transport of glucose through the apical membrane of intestinal and kidney epithelial cells depends on the presence of secondary active Na⁺/glucose symporters, SGLT-1 and SGLT-2, which concentrate glucose inside the cells, using the energy provided by co-transport of Na⁺ ions down their electrochemical gradient (Hediger and Rhoads, 1994). Passive transport (facilitated diffusion) of glucose through the cellular membrane is otherwise catalyzed by glucose carriers (protein symbol GLUT) (Henderson, 1993). GLUT 2, a transmembrane carrier protein of GLUT family, located in basolateral membrane of small intestine, is very efficient carrier of glucose at small intestine level. Some investigators suggested that flavonoids decreased glucose uptake by a sodium-dependent pathway *via* the sodium-dependent glucose transporter 1, SGLT1. It is most probable that active phytochemicals present in the studied extracts (like gymnemic acid of GS leaf) binds on the glucose transporters thus may lead to wash out of glucose from the body. It may be one of the mechanisms for the hypoglycemic phenomenon after administration of these extracts noted by various investigators in animals or subjects.

4.6.2 *Alpha amylase Inhibitory Activity*

Starch as the predominant ingredient of human food is rapidly degraded in the gastrointestinal tract by salivary and pancreatic α -amylase to maltose which is further hydrolyzed by maltase localized in the brush border of the small intestine to glucose. Glucose is immediately absorbed leading to hyperglycemia and consequently to hyperinsulinemia. Both phenomena are undesirable in diabetics and in obese patients. Inhibition of the digestion of starch leads to a decrease and a retardation of glucose absorption. In nature, α -amylase inhibitors are found in wheat and other grains (Shainkin and Birk 1970).

Inhibition of α -Amylase activity was measured by determination of the reducing groups arising from hydrolysis of soluble starch by α -amylase. Glucose produced as a result of starch hydrolysis was measured spectrophotometrically at 505 nm using glucose oxidase kit. Inhibition of starch hydrolysis by an α -amylase inhibitor results in a diminished absorbance at 505 nm in comparison with the controls.

Methanol extract of EA, EH, TC and GS were first screened for their alpha amylase inhibitory activity. EA extract showed complete inhibition of enzyme at the conc. of 400

$\mu\text{g/ml}$ and above, in the set parameters of experiment. GS extract also possessed moderate inhibitory effect. Results are shown in table 21 and in figure 67.

Table 21 Alpha amylase inhibitory activity of methanol extracts.

Concentration ($\mu\text{g/ml}$)	% Inhibition			
	EA *	EH *	TC *	GS *
25	27.46 \pm 3.61	2.02 \pm 0.10	1.43 \pm 0.12	10.65 \pm 0.82
50	42.34 \pm 1.05	2.50 \pm 0.23	3.21 \pm 0.62	18.52 \pm 1.01
75	59.20 \pm 0.19	3.31 \pm 0.51	4.03 \pm 1.12	20.62 \pm 0.35
100	77.65 \pm 0.92	4.10 \pm 1.20	10.21 \pm 0.26	32.12 \pm 0.87
200	86.52 \pm 3.02	5.32 \pm 2.43	9.96 \pm 1.62	43.56 \pm 1.21
300	99.82 \pm 1.48	4.83 \pm 0.61	9.85 \pm 0.98	45.33 \pm 0.23
400	100	5.16 \pm 0.38	10.51 \pm 1.52	40.51 \pm 1.36
500	100	6.03 \pm 1.55	16.39 \pm 1.23	42.50 \pm 1.84

* Each value is mean \pm SEM of five observations.

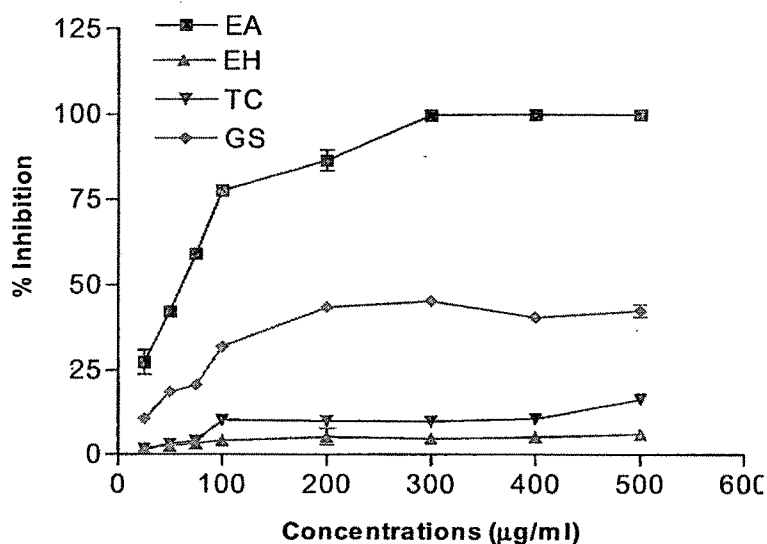


Figure 67 The effect of methanol extract of EA, EH, TC and GS on alpha amylase activity. Values are mean of five determinations.

Major constituents present in the active extracts were prepared as fractions like phenolic fraction and sterol fraction of EA, crude gymnemic acid and gymnemagenin from GS methanol extract. Data of their activity are presented in table 22 and figure 68.

Table 22 A dose dependent alpha amylase inhibitory activity of fractions and isolated compounds from *E. alba* and *G. sylvestre* extract (n=5).

Conc. (µg/ml)	EA Phenolic fraction	Wedelolactone	EA Sterol fraction	EA002	Crude Gymnemic acid	Gymnema-genin
5	0.00 ± 0.00	0.00 ± 0.00	8.36 ± 0.82	25.96 ± 0.65	0.00 ± 0.00	2.30 ± 0.49
10	10.10 ± 0.88	1.66 ± 0.55	24.66 ± 1.06	39.00 ± 1.21	0.00 ± 0.00	1.36 ± 0.64
20	22.00 ± 1.04	4.46 ± 0.20	40.26 ± 1.44	52.42 ± 0.68	0.00 ± 0.00	2.10 ± 1.07
30	30.08 ± 0.49	8.14 ± 0.51	55.38 ± 1.20	64.84 ± 1.39	1.86 ± 0.26	2.36 ± 0.74
40	39.16 ± 0.78	14.06 ± 0.89	64.84 ± 1.33	78.94 ± 0.58	13.36 ± 1.11	3.18 ± 0.82
50	49.36 ± 0.73	17.68 ± 0.74	76.78 ± 0.58	97.90 ± 0.97	25.40 ± 0.73	1.56 ± 0.71
60	54.20 ± 1.59	24.10 ± 1.07	83.72 ± 1.06	100.00 ± 0.00	35.60 ± 0.99	2.48 ± 0.71
70	62.24 ± 0.98	35.22 ± 1.07	95.58 ± 0.31	100.00 ± 0.00	45.86 ± 0.89	2.54 ± 0.56
80	64.22 ± 1.08	48.00 ± 0.49	99.78 ± 0.16	100.00 ± 0.00	55.30 ± 1.25	1.32 ± 0.35
90	67.96 ± 0.94	56.56 ± 0.58	100.00 ± 0.00	100.00 ± 0.00	59.98 ± 1.01	3.18 ± 0.66
100	70.36 ± 0.68	68.96 ± 1.56	100.00 ± 0.00	100.00 ± 0.00	72.06 ± 1.29	2.86 ± 0.73

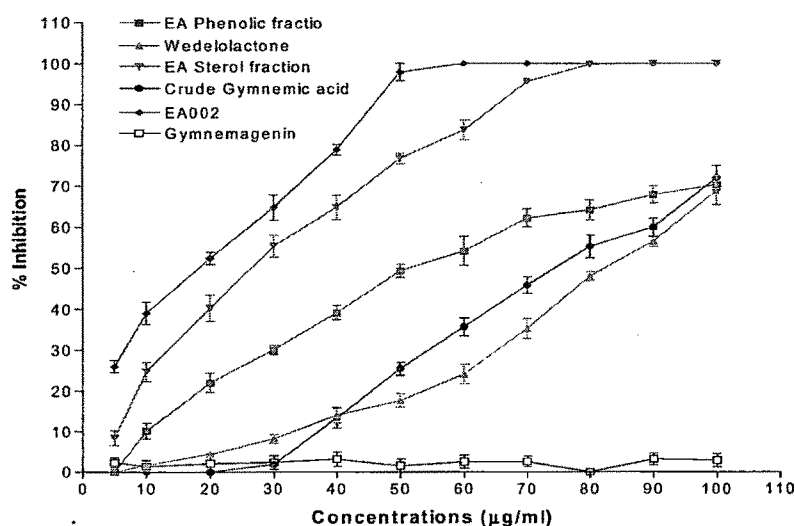


Figure 68 Alpha amylase inhibitory effect of fractions and isolated compounds of *E. alba* and *G. sylvestre*. Values are mean of five determinations.

Sterol fraction of EA inhibits the enzyme at 90 $\mu\text{g/ml}$ concentration. A compound isolated from this fraction EA002 found to block the enzyme at 60 $\mu\text{g/ml}$ concentration. Phenolic fraction and its major phenolic compound wedelolactone also showed good activity. Phenolic fraction found to be more potent than wedelolactone alone. It reveals that wedelolactone is not the principle compound which is responsible for the activity of phenolic fraction. TLC study confirms the presence of EA002 in phenolic fraction which could be the possible compound responsible for the activity. IC_{50} values of fractions and isolated compounds are depicted in table 23. Crude gymnemic acid showed IC_{50} value, 74.63 $\mu\text{g/ml}$, where as gymnemagenin found to be totally ineffective as alpha amylase inhibitor.

Table 23 Alpha amylase inhibitory activities of fractions and compounds isolated from aerial parts of *Eclipta alba* and leaves of *Gymnema sylvestre*.

Sample	IC_{50} ($\mu\text{g/ml}$)
Phenol fraction (EA)	51.10
Sterol fraction (EA)	26.35
Wedelolactone	82.50
EA002	18.20
Crude gymnemic acid (GS)	74.63
Gymnemagenin	-

A kinetic study has been performed for the potent alpha amylase inhibitor EA002 from EA extract. Biochemical parameters of this study are shown in table 88. A decrease of 24.73% in V_{max} was observed in presence of EA002. It renders Michaelis-Menten constant (K_m) unchanged revealing the type of enzyme inhibition non competitive.

Table 24 Biochemical parameter obtained for the effect of EA002 on the kinetics of alpha amylase.

Kinetic Parameter	Control	EA002
V_{max}	0.930 ± 0.008	0.700 ± 0.009 *
K_m (mM)	1.78 ± 0.01	1.78 ± 0.03

V_{max} is reported as mM glucose produced/30 min.

* indicate a statistically significant difference from the values in the absence of sample ($p < 0.001$). Values are mean \pm standard error mean ($n=5$).

The effect of formulations on alpha amylase activity was studied. Data are presented in the form of figure 69. The formulations were evaluated in the concentration range of 10 – 100 µg/ml. The maximum inhibition (27.06%) was observed with formulation F3 at 100 µg/ml. Their relative activity were in the order being F3>F1>F4>F2.

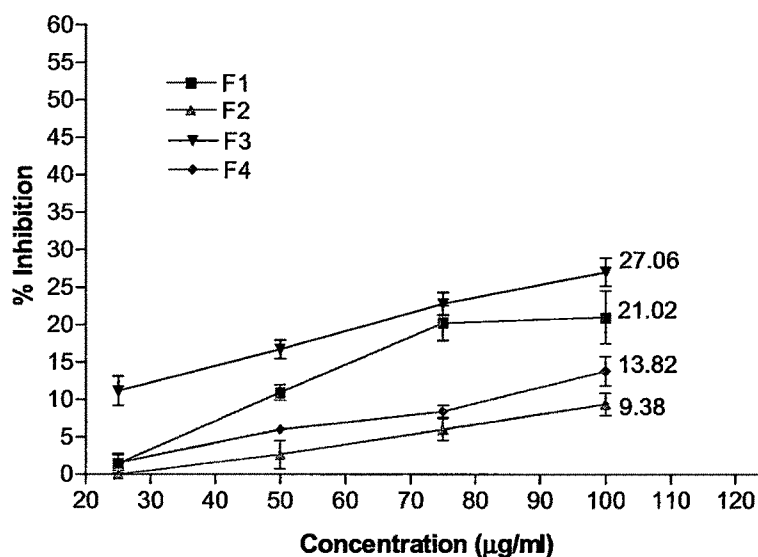


Figure 69 The inhibitory effect of formulations on alpha amylase activity.

Values are mean of five determinations.

4.6.3 Aldose Reductase Inhibitory Activity

Diabetes is one of the major risk factors for cataractogenesis and cataract is the leading cause of blindness worldwide. Increased blood sugar levels influence the refractive power of the lens in diabetics, and can lead to diabetic cataract. Surplus glucose induces accumulation of the sugar alcohol within the cells, thus generating disturbances of the osmotic balance and finally causing cataract. The enzyme aldose reductase (AR) is the first enzyme of the polyol pathway that reduces excess D-glucose into D-sorbitol with concomitant conversion of NADPH into NADP⁺ (Kador, 1988; Tomlinson et al, 1994; Crabbe and Goode, 1998; Yabe-Nishimura, 1998; Carper et al, 1989). AR has been reported to play an important role in sugar-induced cataract. Bio guided fractionation was performed and inhibitory effect of plant extracts, their fractions and isolated compounds was studied.

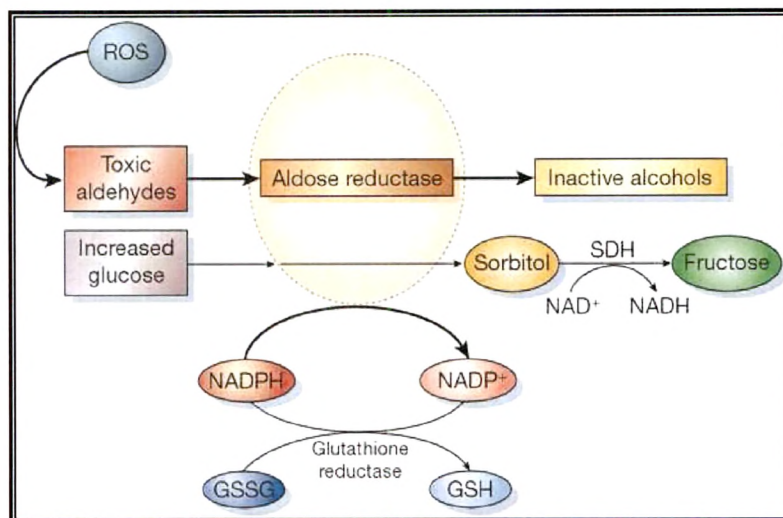


Figure 70 Polyol pathway.

An enzyme preparation contained 3.1 mg/ml protein. In the screening part, methanol extract of EA, EH, TC and GS were studied. Out of these only EH and TC showed interesting results as depicted in table 25. Data reveals 86.03% and 96.58% inhibition with 400 $\mu\text{g/ml}$ dose each of EH and TC extract respectively.

Table 25 AR Inhibitory activity of extracts

Concentration ($\mu\text{g/ml}$)	% Inhibition			
	EA *	EH *	TC *	GS *
25	0.00 \pm 0.00	12.45 \pm 1.57	19.66 \pm 2.42	7.70 \pm 0.32
50	6.29 \pm 0.73	25.75 \pm 1.47	34.00 \pm 1.91	8.70 \pm 0.71
75	15.16 \pm 1.74	35.82 \pm 1.90	49.15 \pm 3.02	10.70 \pm 0.83
100	17.75 \pm 0.72	49.43 \pm 1.43	71.20 \pm 2.04	12.70 \pm 1.37
200	26.31 \pm 2.03	77.62 \pm 1.42	89.80 \pm 2.49	13.27 \pm 1.59
300	32.82 \pm 1.48	84.67 \pm 2.55	92.72 \pm 3.44	11.05 \pm 0.94
400	33.82 \pm 1.18	86.03 \pm 2.45	96.58 \pm 1.77	12.60 \pm 1.44

* Each value is mean \pm SEM of three observations.

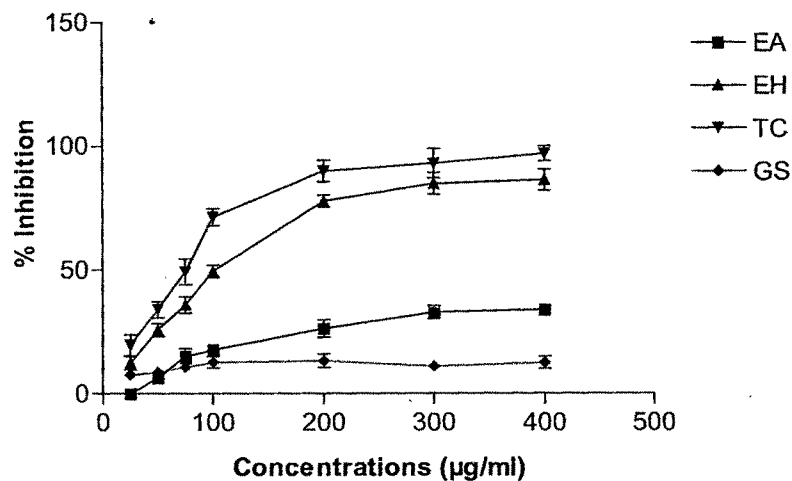


Figure 71 The effect of TC, EH, EA and GS on AR activity

EH bitter fraction and flavonoid fraction along with their major constituents viz., swertiamarin and swertisin were evaluated. As shown in figure 71, EH flavonoid fraction and swertisin showed better activity with IC_{50} value 1.32 and 1.23 $\mu\text{g/ml}$ respectively.

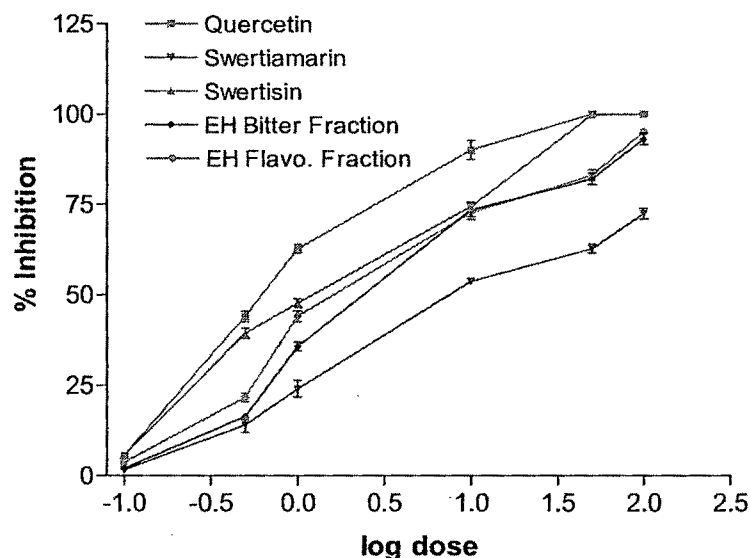


Figure 72 The inhibitory effects of quercetin, swertisin, swertiamarin, EH bitter fraction and EH Flavonoid fraction on aldose reductase activity.

TC alkaloid fraction and its isolated alkaloids (TCY, TCB and TCA) were studied simultaneously in one set of experiment. Their effect is shown in figure 70, where all alkaloid individually found to be more effective than their mixture (alkaloid fraction). Individual

alkaloid showed their activity in order of TCA>TCB>TCY with IC₅₀ value 1.89, 2.68, and 3.71 µg/ml respectively.

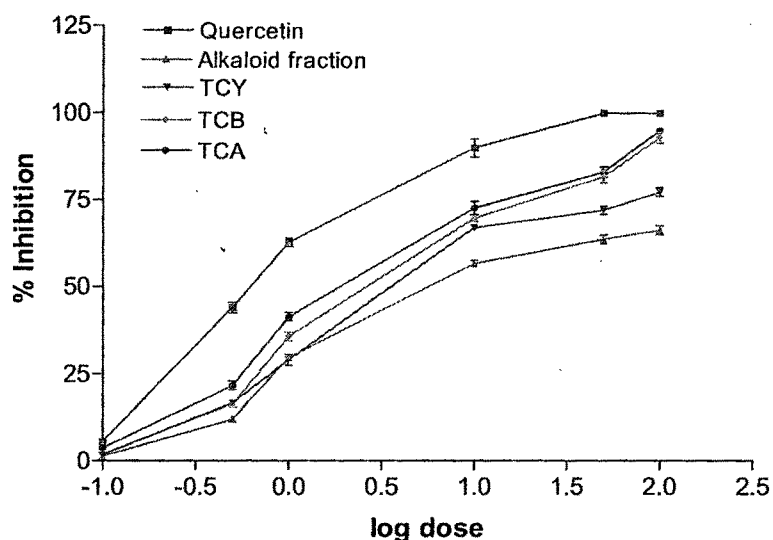


Figure 73 The inhibitory effects of quercetin, alkaloid fraction, TCY, TCB and TCA on aldose reductase activity.

Marketed formulations were studied for their aldose reductase inhibitory property in their extract form. Results are presented in figure 74.

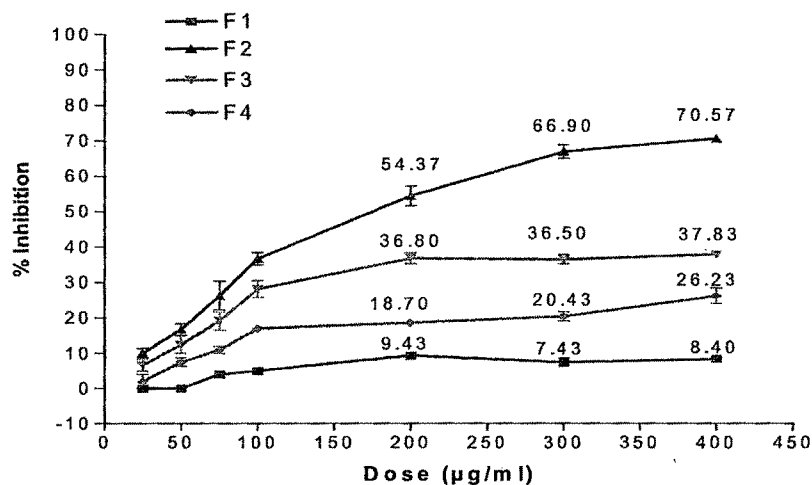


Figure 74 The inhibitory effects of formulations on aldose reductase activity.

Values are mean of three determinations.

Table 26 Aldose reductase inhibitory activities of compounds isolated from aerial parts of *Enicostemma hyssopifolium* and stem of *Tinospora cordifolia*

Sample	IC ₅₀ ($\mu\text{g/ml}$)
Bitter fraction (EH)	2.40
Flavonoid fraction (EH)	1.32
Swertiamarin	7.59
Swertisin	1.23
Alkaloid fraction (TC)	5.76
Alkaloid TCY	3.71
Alkaloid TCB	2.68
Alkaloid TCA	1.89
Quercetin (Positive control)	0.62

A study conducted to evaluate the effect of methanol extract, their fractions and isolated compounds gave very much promising results for swertisin and TCA with 56.00 and 49.20% polyol accumulation respectively as compare to control. The effect is similar to that of positive control quercetin (with 57.17% galactitol). Results in graphical form is presented in figure 75.

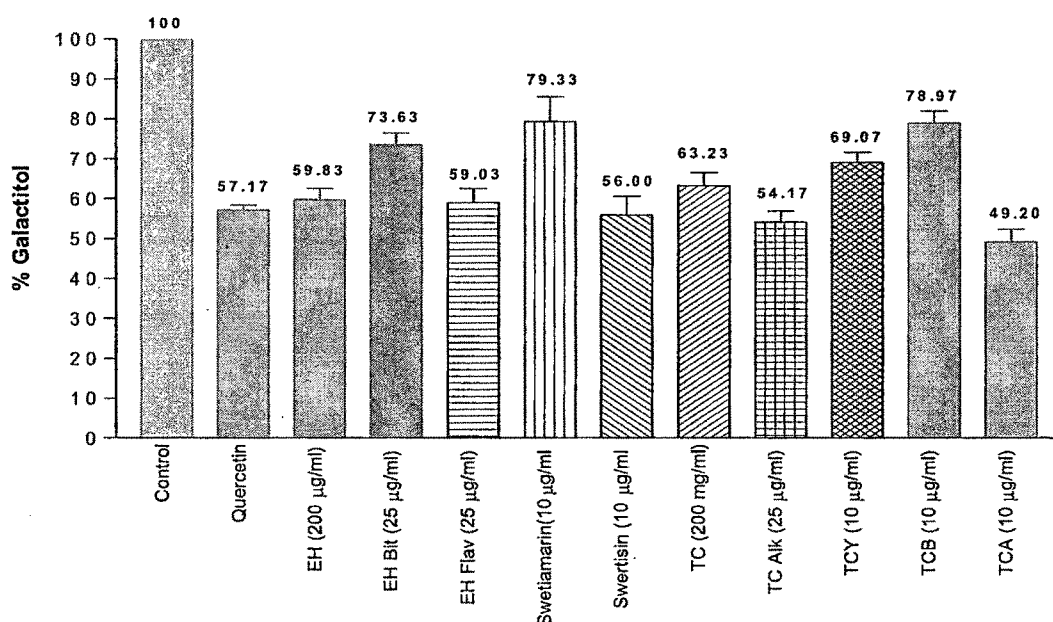


Figure 75 The effect of EH and TC on polyol accumulation in lenses cultured in a GAL-medium (n=3).

Kinetic parameters like K_m and V_{max} have been estimated to understand the nature of inhibition of AR by swertisin and an alkaloid TCA. Table 27 lists the kinetic parameters of sheep lens aldose reductase *in vitro*. The K_m and V_{max} were calculated in the absence as well as in the presence of swertisin or TCA. Data analysis revealed that V_{max} decreased ($P < 0.001$) by $0.037 \mu\text{M}/\text{min}/\text{mg}$ protein in the presence of the swertisin. In contrast, the apparent K_m (0.035 Mm) remained unaltered ($P > 0.05$) in the presence of the swertisin. Decreased V_{max} with D-Xylose as substrate indicates that swertisin inhibit AR in a non-competitive manner. Where as in case of TCA V_{max} decreased by $0.055 \mu\text{M}/\text{min}/\text{mg}$ protein and a K_m value did not decreased significantly ($p > 0.05$) is again an indicative of non-competitive inhibition of sheep lens aldose reductase by TCA.

Table 27 Maximal velocity (V_{max}) and Michaelis menten value (K_m) for swertisin and TCA

Kinetic Parameter	Contro (no treatment)	Swertisin	TCA
V_{max}	0.112 ± 0.02	$0.075 \pm 0.009 *$	$0.0565 \pm 0.005 *$
K_m (mM)	0.035 ± 0.004	0.034 ± 0.003	0.031 ± 0.002

V_{max} is reported as $\mu\text{moles NADPH oxidized}/\text{min}/\text{mg}$ protein.

* indicate a statistically significant difference from the values in the absence of sample ($p < 0.001$). Values are mean \pm standard error mean ($n=5$).

The polyol pathway plays a significant role in the development of sugar-induced cataractogenesis followed by cataract. Accumulation of a high concentration of polyol in the lens leads to an increase in the intracellular ionic strength resulting in excessive hydration, eventually loss of membrane integrity and leakage of free amino acids, glutathione and myo-inositol etc. (Heyningen, 1959). The hyperosmotic theory of sugar cataract identifies AR as the primary factor responsible for this pathological condition. Human genetic and biochemical data also suggested a strong link between raised AR activity and strongly altered risk of diabetic complications such as cataract, nephropathy, retinopathy and neuropathy (Collier and Small, 1991). These results together with recent clinical, experimental and pharmacological data provide powerful new support for the rationale for research and development of AR Inhibitors.

There are many reports of plant's inhibitory actions on aldose reductase, published in relation to diabetes mellitus, such as *Eugenia borinquensis*, *Mangifera indica*, *Eucalyptus deglupta*,

Development of Methods for Chemical and Biological Evaluation of Some Polyherbal Antidiabetic Formulations

and *Syzygium malaccense* (Guzman and Guerrero, 2005). In the leaves of *Myrciaria dubia*, ellagic acid and two of its derivatives were found as potent aldose reductase inhibitors (Ueda et al, 2004). Three flavonoids isolated from *Brickellia arguta* showed anticataract activity in rats (Rosler et al, 1984). Acteoside, an active aldose reductase inhibitor phenolic glycoside was discovered from a 70 % acetone extract of *Monochasma savatierii* (Kohda et al, 1989). Monoterpene glycosides, perillosides A and C isolated from the leaves of *Perilla frutescens* were found to be excellent aldose reductase inhibitors (Kohda et al, 1995). Some sulfated flavonoids in *Polygonum hydropiper* were discovered to show potent inhibition against bovine lens aldose reductase (Haraguchi et al, 1996). Other studies showed that flavonoid glycosides (Haraguchi et al, 1998), isoflavonoids (Jung et al, 2002), flavanone glucosides (myrciacitrins III) (Suryanarayana et al, 2004), protocatechualdehyde (Matsuda et al, 2002) and tannoid principles (Lee et al, 2005) had strong inhibitory activity.

Medicinal plants which are rich in polyphenols and bioflavonoids are reported to reduce the AR activity. The above results indicate presence of bioactive compounds in two plants that prevent cataractogenesis via a possible inhibition of aldose reductase. In relation to these two active plants, it has been found that swertisin present in *E. hyssopifolium* is the bioactive molecule responsible for inhibitory effect of the both i.e., plant flavonoid fraction and bitter fraction. It has shown IC_{50} value of 1.23 $\mu\text{g/ml}$. Swertisin may be employed as a lead molecule in the quest of novel aldose reductase inhibitors. An alkaloid fraction of *T. cordifolia* contains a water soluble alkaloid TCA which shows a moderate inhibition of aldose reductase (IC_{50} 1.89 $\mu\text{g/mL}$). Marketed formulation (F2) showed 70.57% inhibition at the dose of 400 $\mu\text{g/mL}$. Composition of F2 contains high amount of *E. hyssopifolium* and *T. cordifolia* extract, which could be the possible reason for this positive action. The rest of the formulations did not show any significant inhibition.

4.6.4 Alpha Glucosidase Inhibitory Activity

One of the therapeutic approaches for reducing postprandial hyperglycemia in patients with DM is to prevent absorption of carbohydrates after food uptake. Only monosaccharides, such as glucose and fructose, can be transported out of the intestinal lumen into the bloodstream. Complex starches, oligosaccharides, and disaccharides must be broken down into individual monosaccharides before being absorbed in the duodenum and upper jejunum. This digestion is facilitated by enteric enzymes, including pancreatic α -amylase, and α -glucosidases that are attached to the brush border of the intestinal cells. Acarbose and miglitol are competitive

inhibitors of intestinal α -glucosidases and reduces the postprandial digestion and absorption of starch and disaccharides (Davis and Granner, 1996). Screening of α -glucosidases inhibitors from plants and synthetic sources is increasing. Inhibitors of these enzymes have been recently developed from natural sources (Shim et al., 2003).

In the screening of methanol extract of EH, EA, TC and GS as an alpha glucosidase inhibitor, EH and EA methanol extract found to possess a dose dependent inhibitory activity. Data are depicted in table 28. A positive standard voglibose was used in the concentration range of 0.5 – 10 $\mu\text{g/ml}$ and the extracts were studied in the range of 5 – 100 $\mu\text{g/ml}$. The activity was evaluated against two substrate i.e., sucrose and maltose.

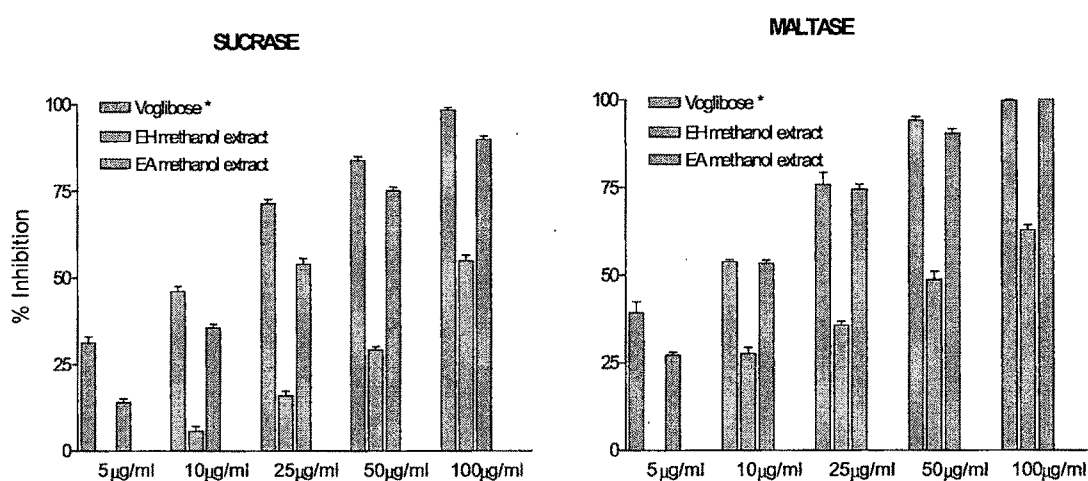


Figure 76 Sucrase and maltase inhibitory activity of EH and EA methanol extracts.

* Voglibose studied in the conc. range of 0.5 – 10 $\mu\text{g/ml}$.

Data reveals that methanol extract of EH and EA possesses moderate to potent activity. EA methanol extract totally inhibit the maltase activity at 100 $\mu\text{g/ml}$ concentration. At this concentration it showed effect that is comparable to 10 $\mu\text{g/ml}$ of positive control, voglibose (figure 76). Fractions of EA (phenolic fraction) and EH (bitter and flavonoid fraction) along with their marker components wedelolactone, swertiamarin and swertisin were evaluated in the same experimental set up.

Table 28 Alpha glucosidase inhibition by methanol extracts.

Sample	% Inhibition																				
	Substrate	Sucrose	Maltose	Sucrose	Maltose	Sucrose	Maltose	Sucrose	Maltose	Sucrose	Maltose	Sucrose	Maltose								
Voglibose	0.5 µg/ml	31.1 ± 1.79	0.5 µg/ml	39.2 ± 3.17	1 µg/ml	46.0 ± 1.42	1 µg/ml	53.8 ± 0.62	2.5 µg/ml	71.36 ± 1.29	2.5 µg/ml	75.9 ± 3.39	5 µg/ml	83.9 ± 1.11	5 µg/ml	94.1 ± 1.01	10 µg/ml	98.4 ± 0.70	10 µg/ml	99.62 ± 0.273	
	5 µg/ml		5 µg/ml		10 µg/ml		10 µg/ml		25 µg/ml		25 µg/ml		25 µg/ml		50 µg/ml		50 µg/ml		100 µg/ml		100 µg/ml
EH methanol extract	0.00		0.00		27.60 ± 1.68	5.60 ± 1.50	27.60 ± 1.68	15.88 ± 1.43	35.62 ± 1.56	29.08 ± 0.92	48.74 ± 2.33	54.80 ± 1.72	62.80 ± 1.48								
TC methanol extract	0.0		0.0		0.0	0.0	0.0	0.0	0.0	0.0	0.0	0.0	0.0	0.0	0.0	0.0	0.0	0.0	0.0	0.0	0.0
EA methanol extract	14.00 ± 1.12		27.14 ± 0.89		35.58 ± 0.94		53.38 ± 0.89		53.93 ± 1.67		74.46 ± 1.45		75.04 ± 1.07		90.34 ± 1.32		89.76 ± 1.07		100 ± 0.00		
GS methanol extract	0.0		0.0		0.0	0.0	0.0	0.0	0.0	0.0	0.0	0.0	0.0	0.0	0.0	0.0	0.0	0.0	0.0	0.0	0.0

Values are mean ± SEM of three determinations.

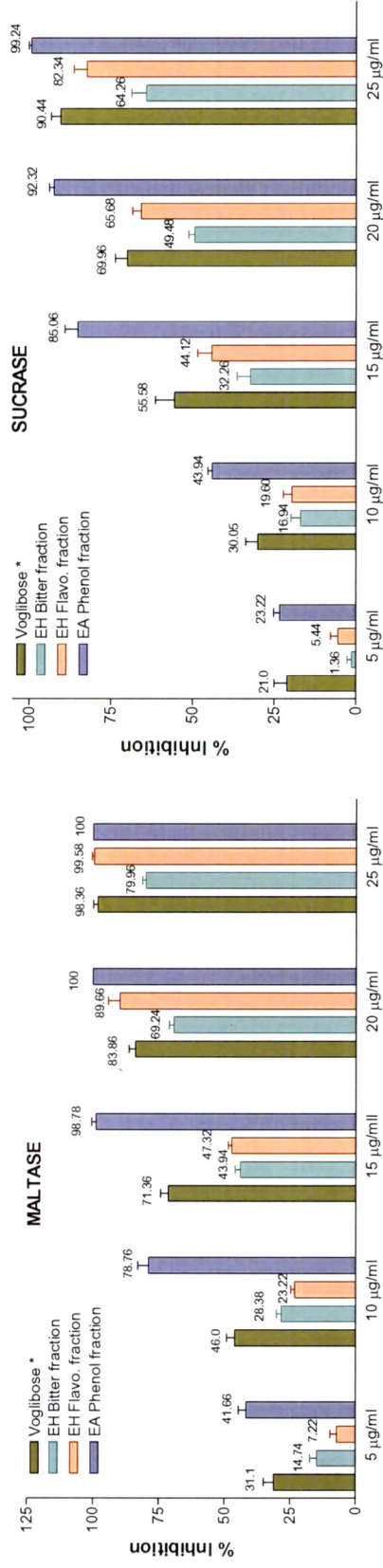


Figure 77 Alpha glucosidase inhibition by bio active fractions of EH and EA. * Voglibose studied in the conc. range of 0.5 – 10 µg/ml.

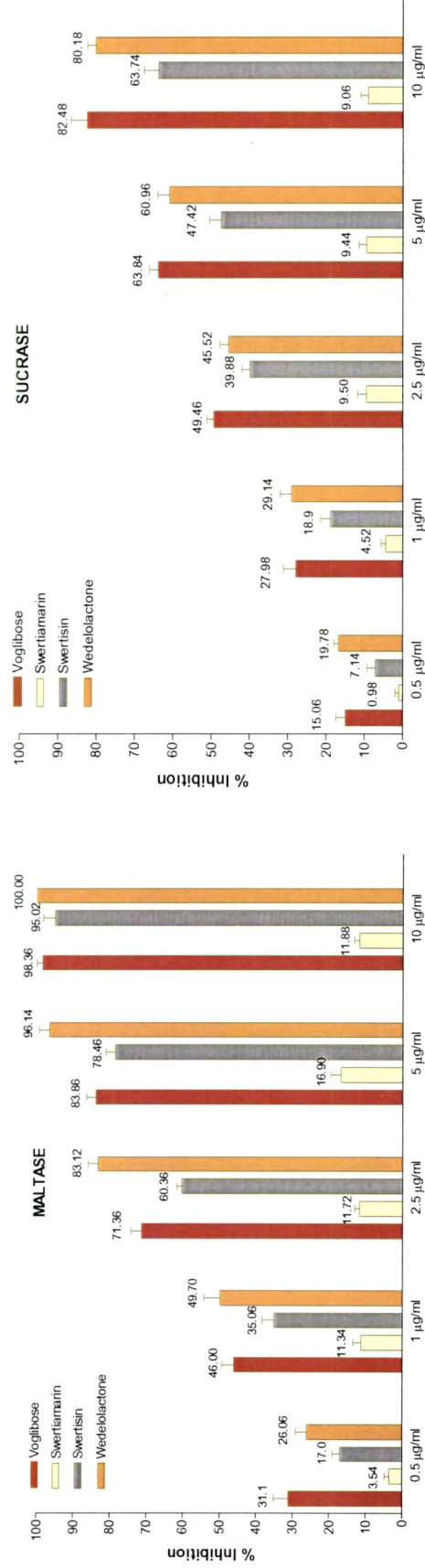


Figure 78 Alpha glucosidase inhibition by swertisin, swertiamarin and wedelolactone.

The activity of fractions and isolated compound against sucrase and maltase are presented in figure 77 and 78. Since swertiamarin, a bitter principle did not inhibit either maltase or sucrase, the activity of EH bitter and EH flavonoid fraction was probably due to presence of swertisin. As swertisin alone produced 95.02% and 63.74% inhibition of maltase and sucrase activity respectively at 10 $\mu\text{g/ml}$ concentration.

A sterol fraction of EA did not showed any activity but the phenolic fraction was found to have an excellent potential to inhibit both maltase and sucrase activity. A principle component of this fraction, wedelolactone possessed an activity equivalent to that of voglibose. IC_{50} values of these fractions and compounds are reported in table 29. Wedelolactone with an IC_{50} value of 1.0 $\mu\text{g/ml}$ (voglibose – 1.23 $\mu\text{g/ml}$) for maltase inhibition and 3.20 $\mu\text{g/ml}$ (voglibose – 2.58 $\mu\text{g/ml}$) for sucrase inhibition proved to be a comparable inhibitor of alpha glucosidase to a positive standard voglibose.

Table 29 Maltase and sucrase inhibitory activity of fractions and isolated compounds.

Sample	IC_{50} ($\mu\text{g/ml}$)	
	Maltase	Sucrase
Voglibose (Positive control)	1.23	2.58
Bitter fraction (EH)	16.19	20.13
Flavonoid fraction (EH)	15.31	16.38
Swertiamarin	> 42.60	> 33.52
Swertisin	1.89	5.74
Phenolic fraction (EA)	6.14	10.75
Wedelolactone	1.00	3.20

A kinetic study has been performed to understand the nature of inhibition of alpha glucosidase by swertisin and wedelolactone. The effect was checked on both sucrase and maltase activity of alpha glucosidase using sucrose and maltose as substrate respectively. Data is presented in tabular form in table 30. The K_m and V_{max} values were estimated in the absence (control) as well as in the presence either of swertisin or wedelolactone. When using sucrose as substrate, a significant decrease in V_{max} ($P < 0.001$) by 0.13 and 0.2 mM glucose formed/30 min was observed in the presence of swertisin and wedelolactone respectively.

Quite similar effect was observed in case of maltose as substrate (V_{\max} decreased by 0.18 and 0.2 mM glucose/30 min by swertisin and wedelolactone respectively).

Michaelis-Menten constant, K_m remained unchanged in the presence of the swertisin. Decreased V_{\max} with both substrates and constant K_m indicate that swertisin inhibit alpha glucosidase in non-competitive manner. Where as in case of wedelolactone, decreased V_{\max} along with K_m value with both substrates is an indicative of competitive inhibition of alpha glucosidase.

Table 30 Effect of swertisin and wedelolactone on alpha glucosidase kinetics.

Substrate	Kinetic Parameter	Control (no treatment)	Swertisin	Wedelolactone
Sucrose	V_{\max}	0.49 ± 0.004	0.36 ± 0.003 *	0.29 ± 0.006 *
	K_m (mM)	9.93 ± 0.31	9.93 ± 0.78	4.88 ± 0.6
Maltose	V_{\max}	0.59 ± 0.03	0.41 ± 0.009 *	0.39 ± 0.005 *
	K_m (mM)	8.32 ± 0.006	8.31 ± 0.003	5.68 ± 0.002

Substrates were studied in the concentration range of 10 – 50 µg/ml.

V_{\max} is reported as mM glucose formed/30 min.

* indicate a statistically significant difference from the values in the absence of sample ($p < 0.001$). Values are mean ± standard error mean ($n=5$).

Similarly, all formulations were also tested for their sucrase and maltase inhibitory effect. Results are presented in graphical form in the figure 79. Maltase inhibitory activity was observed in the order of F2>F1>F3 with 52.80, 44.80, and 34.75% inhibition at 400 µg/ml concentration. Formulation F4 was found to be ineffective as maltase inhibitor. Potential as sucrase inhibitor was in the order of F2>F3>F1 having 45.64, 22.56 and 30.68% inhibition at 400 µg/ml concentration. Formulation F4 did not showed inhibition of sucrase activity of alpha glucosidase.

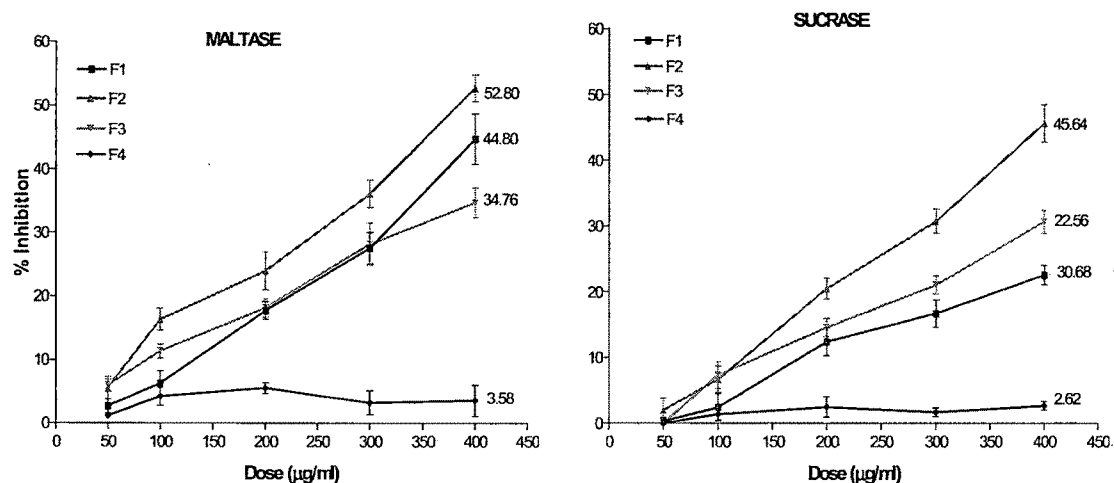


Figure 79 The inhibitory effect of formulations on alpha glucosidase (maltase and sucrase) activity.

Values are mean of five determinations.

4.6.5 Cytoprotective Activity (MTT Assay)

Oxidative stress is suggested as a mechanism underlying the complications of diabetes (Halliwell and Gutteridge, 1989). Reactive oxygen species (ROS) have been implicated in the pathology of various disease states, including diabetes mellitus and it is well known that superoxide anion is the radical formed by the reduction of molecular oxygen that may lead to ROS such as hydrogen peroxide and hydroxyl radical (Baynes 1991). In the streptozotocin (STZ)-induced rat diabetes model, an activated oxygen species was proposed to be formed and involved in the death of the β -cells (Schmezer et al, 1994). STZ (*N*-(methyl nitro carbamoyl)-D-glucosamine) is a potent DNA methylating agent and acts as a free radical donor in the pancreas where the β -cells are particularly sensitive to damage from free radicals because of a low level of free radical scavenging enzymes (Lukic et al, 1998, Spinass 1999). Medicinal plants are currently being investigated for their pharmacological properties in the regulation of blood glucose and apoptosis induced by oxidative stress, a process which is pivotal in the pathology of diabetes mellitus (Kinloch et al, 1999, Latha et al, 2004). Investigation for the protective effects of plant extracts, fractions and isolated phytoconstituents has been carried out on oxidative stress induced by STZ on the pancreatic β -cellline (RINm5F).

Measurement of cell viability and proliferation forms the basis for numerous *in vitro* assays of a cell population's response to external factors. The reduction of tetrazolium salts is now widely accepted as a reliable way to examine cell proliferation. The yellow tetrazolium MTT (3-(4, 5-dimethylthiazolyl-2)-2, 5-diphenyltetrazolium bromide) is reduced by metabolically active cells, in part by the action of dehydrogenase enzymes, to generate reducing equivalents such as NADH and NADPH. The resulting intracellular purple formazan can be solubilized and quantified by spectrophotometric means. The MTT Cell Proliferation Assay measures the cell proliferation rate and conversely, when metabolic events lead to apoptosis or necrosis, the reduction in cell viability. The number of assay steps has been minimized as much as possible to expedite sample processing. The MTT Reagent yields low background absorbance values in the absence of cells.

The purpose of this study was to conduct a preliminary evaluation of the cytoprotective effect of the fractions and isolated phytomolecules from commonly used antidiabetic herbs in an *in vitro* assay using RINm5F cells.

The difference in the mean values for cell viability of EH flavonoid fraction, EH bitter fraction, EA phenol fraction and gymnemic acid treated cells were greater than those treated only with STZ. It was found to be statistically significant ($P < 0.001$). In contrast, neither the mean values among the different levels of TC alkaloid fraction nor the EA sterol fraction was significantly different.

Cell viability data for fractions is summarized in table 31. The EC_{50} value for bioactive fraction and compound was calculated by plotting dose vs cell viability curve (Table 32).

Study confirms the cytoprotective activity of EH bitter fraction, EH flavonoid fraction, EA phenolic fraction and crude gymnemic acid as well ($p < 0.001$ in all cases when compared with control cells), with their EC_{50} values being 86.5, 63.1, 95 and 53.2 μg respectively. TC alkaloid fraction did not have any effect on this cell line as protective agent. EA sterol fraction on the negative side, showed cyto-toxic effect and reduces the cell viability even below that of STZ treatment. Therefore, these two fractions were dropped out for the next study on RINm5F cells. Further the major constituents which presents in bio active fractions were taken for the same study in the concentration range of 2.5 - 50 $\mu\text{g}/200 \mu\text{l}$. Data clearly indicated that swertisin present in EH possess potent cytoprotective activity against STZ induced damage in RINm5F cell line. Since swertiamarin, a major bitter iridoid glycoside of

EH showed no effect as protective agent, it could be said that even the bitter fraction showed activity due to presence of swertisin. EC₅₀ value of swertisin was determined to be 9.2 µg. Phenolic fraction of EA showed positive response to the cytoprotection assay henceforth the isolated coumestan, wedelolactone was chosen to study its potential as cytoprotective to RIN cells and found to have EC₅₀ value 32.5µg. Both, swertisin and wedelolactone were found to be effective in dose dependent manner and are responsible for the activity. Gymnemagenin, a genin part of gymnemic acid when studied for MTT assay, didn't possess any protection (figure 81).

Formulations when tested for their activity as cyto-protective, F-1, F-2 and F-3 showed good activity where as F-4 did not show any significant difference as compare to STZ treated cells. Data are shown in figure 82 and table 34. Formulations having GS (F-1) or EH (F-2 and F-3) as one of the ingredient possesses positive activity.

Table 31 Cytoprotective activity of different fraction in the dose ranges 10 – 100 µg.

Percent Cell Viability						
Dose (µg)	EH Bitter	EH Flavonoid	TC Alkaloid	EA Phenolic	EA Sterol	Crude Gymnemic acid
10	11.54 ± 0.47	10.45 ± 0.63	9.50 ± 0.43	10.98 ± 0.27	5.94 ± 0.33	11.97 ± 0.35
20	12.79 ± 0.35	12.03 ± 0.35	10.00 ± 0.25	12.02 ± 0.20	6.02 ± 0.32	13.96 ± 0.04
30	14.45 ± 0.46	16.55 ± 0.45	10.42 ± 0.44	13.03 ± 0.06	7.05 ± 0.43	15.55 ± 0.22
40	14.99 ± 0.32	23.11 ± 1.12	7.70 ± 0.92	14.05 ± 0.10	5.50 ± 0.08	27.06 ± 0.51
50	19.37 ± 0.58	31.73 ± 0.74	9.12 ± 0.30	16.19 ± 0.19	6.00 ± 0.07	44.98 ± 0.33
60	25.37 ± 0.48	44.26 ± 0.99	9.44 ± 0.49	19.59 ± 0.32	6.92 ± 0.04	59.93 ± 0.38
70	32.42 ± 0.83	64.21 ± 0.84	10.30 ± 0.14	21.14 ± 0.39	7.54 ± 0.26	62.12 ± 0.20
80	42.18 ± 0.70	82.91 ± 1.14	9.80 ± 0.32	32.93 ± 0.82	6.43 ± 0.11	63.36 ± 0.64
90	54.44 ± 0.28	90.92 ± 0.36	10.83 ± 0.18	43.36 ± 0.51	5.70 ± 0.25	64.18 ± 0.97
100	63.53 ± 0.69	92.93 ± 0.43	8.64 ± 0.42	55.19 ± 0.82	6.16 ± 0.29	66.07 ± 0.51

Values are mean of three determinations ± SEM

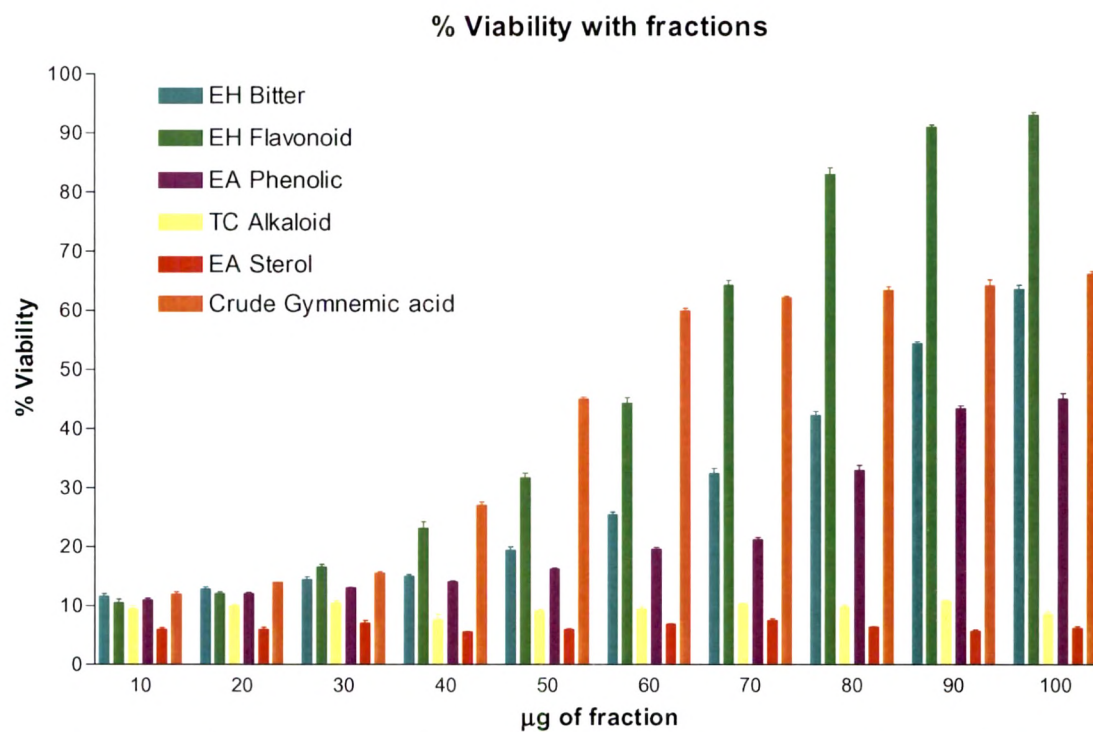


Figure 80 Effect of fraction on % cell viability of rat insulinoma cell line RIN5mF.

Table 32 Cytoprotective actions of fractions and isolated compounds.

Sample	EC 50 (µg)
EH Bitter Fraction	86.5
EH Flavonoid Fraction	63.1
TC Alkaloid Fraction	-
EA Phenolic Fraction	95.0
EA Sterol Fraction	-
Crude Gymnemic acid	53.2
Swertisin	9.2
Wedelolactone	32.5

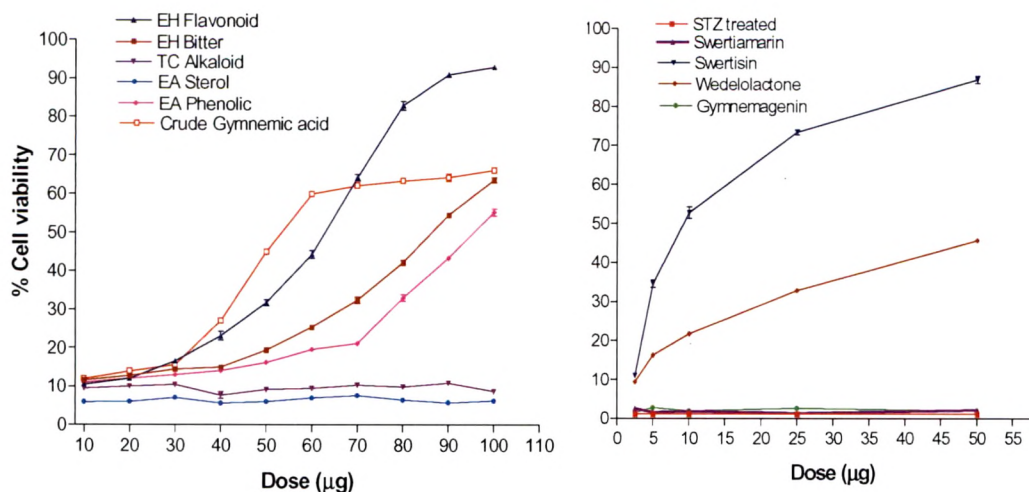


Figure 81 Dose dependent cytoprotective activity of fractions and isolated compounds.

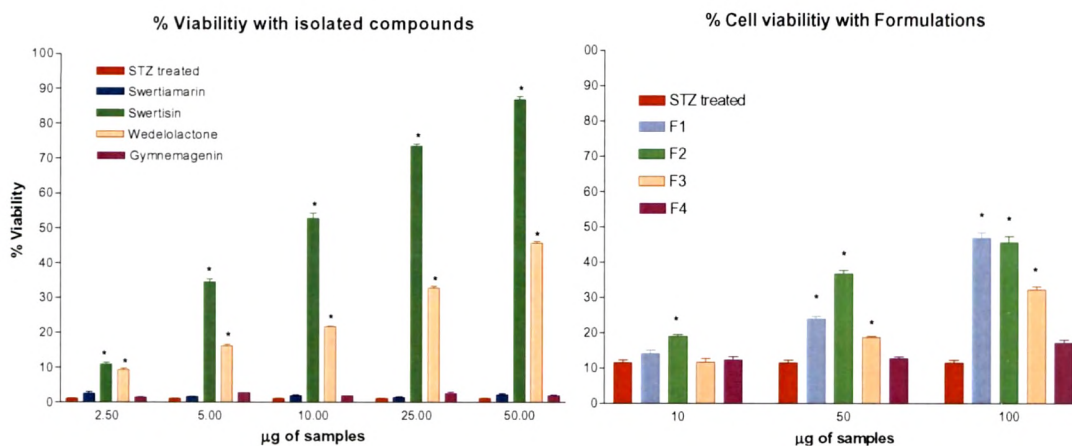


Figure 82 Percent cell viability in presence of isolated compounds and formulations at different doses. * p < 0.001

Table 33 Cytoprotective effect of isolated compounds on RINm5F cells.

Dose (µg)	Percent Protection			
	Swertiamarin	Swertisin	Wedelolactone	Gymnemagenin
2.5	2.54 ± 0.56	11.05 ± 0.45	9.36 ± 0.50	1.48 ± 0.09
5	1.59 ± 0.17	34.57 ± 0.90	16.25 ± 0.43	2.77 ± 0.03
10	1.88 ± 0.24	52.75 ± 1.49	21.71 ± 0.24	1.95 ± 0.05
25	1.38 ± 0.18	73.46 ± 0.66	32.84 ± 0.42	2.62 ± 0.29
50	2.14 ± 0.38	86.91 ± 0.88	65.16 ± 1.02	1.92 ± 0.24

Table 34 Cytoprotective effect of formulations on RINm5F cells.

Dose (μg)	F-1	F-2	F-3	F-4
10	14.13 \pm 0.92	18.95 \pm 0.54	11.70 \pm 1.00	12.40 \pm 0.76
50	23.88 \pm 0.87	36.83 \pm 0.81	18.73 \pm 0.31	12.72 \pm 0.48
100	46.86 \pm 1.53	45.52 \pm 1.75	32.24 \pm 0.87	17.12 \pm 0.94

4.6.6 Glucose Production Assay in Rat Hepatocytes

Isolated hepatocytes have become a useful model for pharmacological, toxicological, metabolic and transport studies of xenobiotics since the development of techniques for high yield isolation of rat hepatocytes (Skett, 1994).

The prolonged and uncontrolled diabetes is presumably predominated by an increase in gluconeogenesis and overproduction of glucose from the liver; therefore it would be of interest to find out the effect of compounds on this process. The aim of this study was to determine the effect of prepared fractions and isolated compounds on glucose production in rat hepatocytes cultured *in vitro*. Results are presented as percentages relative to the glucose produced by DEX + pCPT-cAMP treated hepatocytes (100%).

Table 35 Inhibition of gluconeogenesis in rat hepatocytes in presence of fractions

Treatment (n=3)	Glucose production (% of control) mean \pm SEM
Control (No treatment)	7.2 \pm 0.43
DEX/pCPT-cAMP + Insulin	19.8 \pm 0.78
DEX/pCPT-cAMP + EH Bitter fraction [#]	78.9 \pm 1.94
DEX/pCPT-cAMP + EH Flavonoid fraction [#]	44.9 \pm 2.37
DEX/pCPT-cAMP + TC Alkaloid fraction [#]	47.1 \pm 0.91
DEX/pCPT-cAMP + EA Phenolic fraction [#]	57.4 \pm 2.56
DEX/pCPT-cAMP + EA Sterol fraction [#]	100.3 \pm 2.23
DEX/pCPT-cAMP + Gymnemic acid [#]	97.6 \pm 2.67

[#] Samples were tested at the concentration of 100 $\mu\text{g}/\text{ml}$.

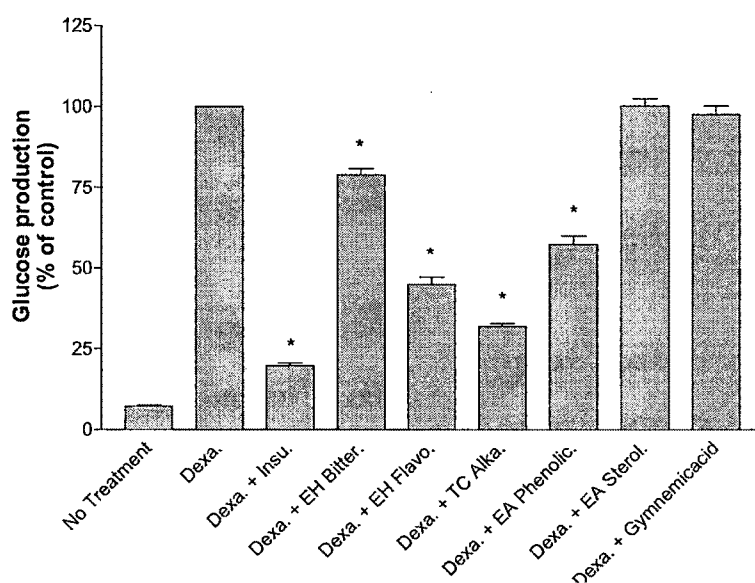


Figure 83 Effect of fractions on hepatic glucose production

Results are presented as percentages relative to the glucose produced by DEX + pCPT-cAMP treated hepatic cells (100%).

Data represent the mean of three experiments \pm SEM (* $p < 0.001$).

The production of glucose in response to insulin (at physiological conc. 10 nM) or different fractions (100 μ g/ml) was examined in rat hepatocytes incubated in medium containing pyruvate and lactate as substrates for gluconeogenesis. Hepatocytes produce glucose in response to hormone dexamethasone and pCPT-cAMP. The cells were treated with a combination of 500 nM DEX and 0.1 mM of pCPT-cAMP in the presence or absence of insulin or samples. A significant ($p < 0.001$) inhibition of glucose production was observed in hepatocytes after treatment with EH bitter, EH flavonoid, TC alkaloid and EA phenolic fractions at the concentration of 100 μ g/ml (figure 83), but not after treatment with EA sterol and gymnemic acid. Insulin clearly inhibits the gluconeogenesis. While studying the effect of swertiamarin, swertisin, wedelolactone and gymnemagenin in dose dependent manner (10, 50 and 100 μ g/ml) swertiamarin and wedelolactone gave excellent response where as swertisin produced a significant inhibition only at 100 μ g/ml concentration (figure 84).

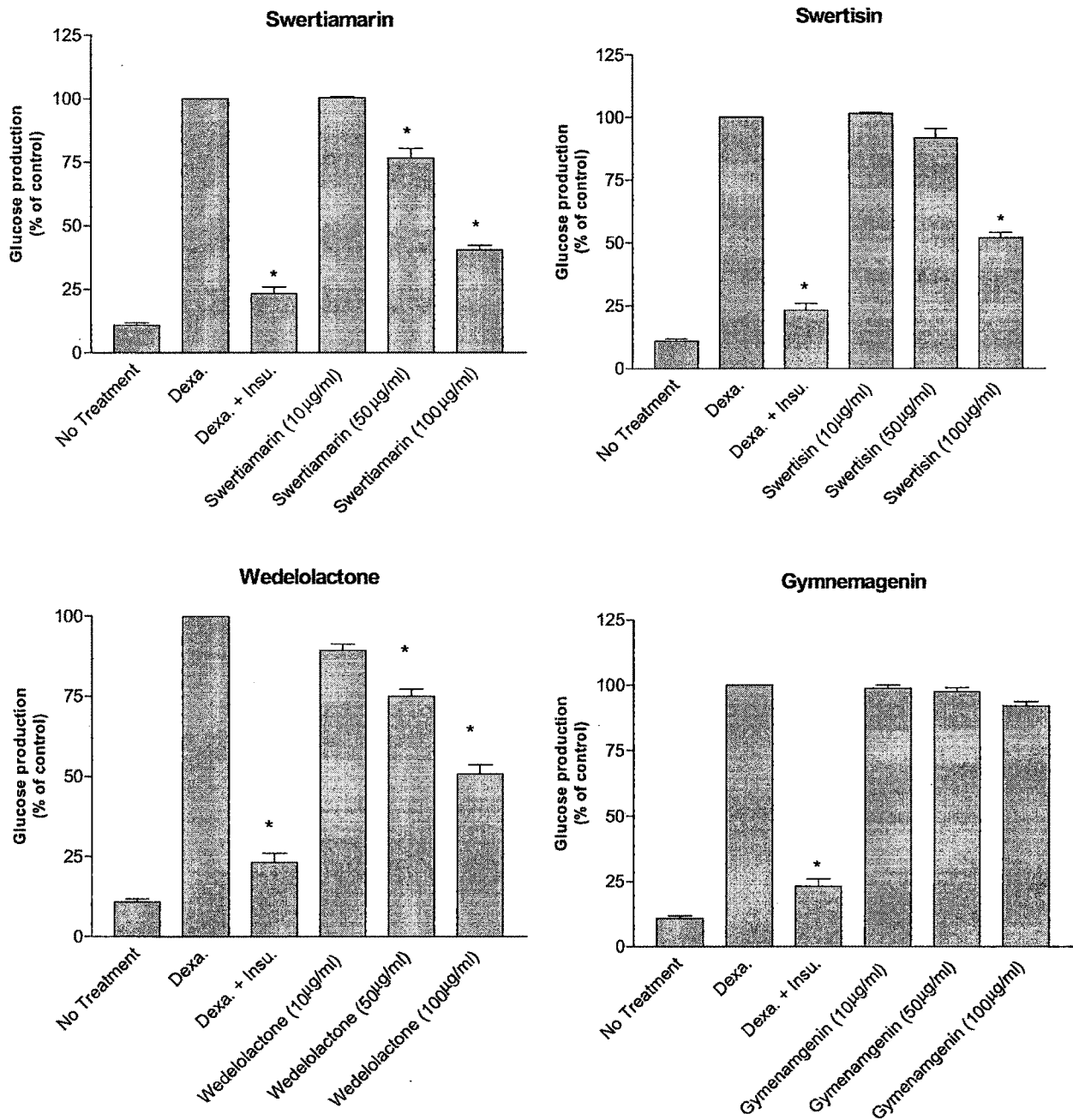


Figure 84 Inhibition of hepatic glucose production in rat hepatocytes in presence of swertiamarin, swertisin, wedelolactone and gymnemenin.

* $p < 0.001$ as compare to hepatocytes treated only with DEX/pCPT-cAMP.

Table 36 Inhibition of gluconeogenesis in rat hepatocytes in presence of isolated compounds.

Treatment (n=3)	Glucose production (% of control) mean \pm SEM		
	10 μ g/ml	50 μ g/ml	100 μ g/ml
Control		10.8 \pm 0.87	
DEX/pCPT-cAMP + Insulin		23.1 \pm 2.84	
Swertiamarin	100.4 \pm 0.43	76.5 \pm 3.74	40.4 \pm 1.78
Swertisin	101.4 \pm 0.55	91.7 \pm 3.72	52.0 \pm 2.14
Wedelolactone	89.4 \pm 1.95	75.1 \pm 2.14	50.8 \pm 2.84
Gymnemagenin	98.83 \pm 1.17	97.57 \pm 1.45	92.03 \pm 1.70

Data represent the mean of three experiments \pm SEM.

A study was undertaken to observe the effect of combination of these bio active constituents in the equivalent proportion they present in the mixture of their extracts in formulations. As shown in figure 85, combination of swertiamarin, swertisin and wedelolactone produced an equal response to that of 10 nM insulin.

Table 37 Effects of combination of bio active markers on hepatic glucose production.

Treatment (n=3)	Glucose production (% of control) mean \pm SEM
Control	17.5 \pm 2.60
Dexa + Insulin	31.7 \pm 1.78
Swertiamarin (100 μ g/ml)	65.5 \pm 2.0
Swertisin (100 μ g/ml)	75.9 \pm 3.13
Wedelolactone (100 μ g/ml)	65.2 \pm 0.72
Combination [#]	31.6 \pm 1.82

[#] Contains swertiamarin : swertisin : wedelolactone (40 : 35 : 25 μ g/ml).

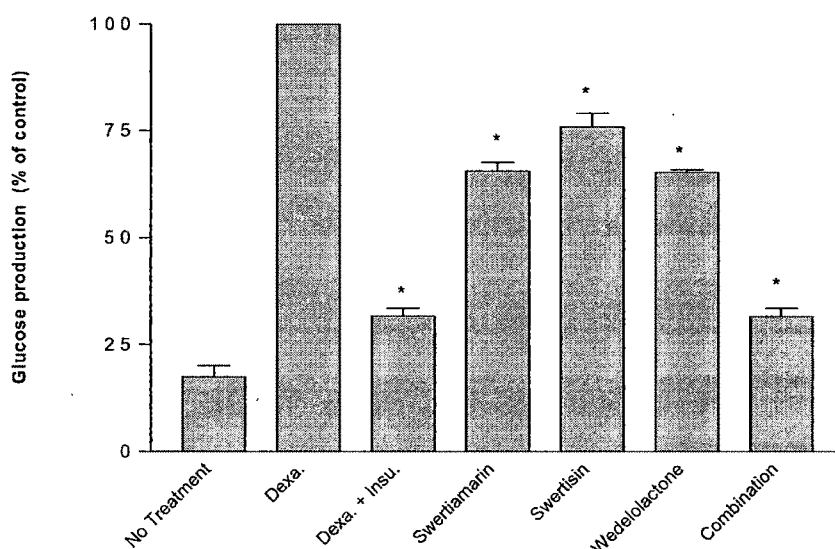


Figure 85 Effect of bio active compounds alone and in combination on Inhibition of hepatic glucose production in rat hepatocytes.

Amongst the studied formulations (100 $\mu\text{g/ml}$) none produced any significant inhibition rather they showed a very high glucose concentration may be because of presence of reducing sugars in formulations itself. A sample blank and treatment group did not show any significant change in glucose concentration. Experimental data are shown in graphical form in figure 86.

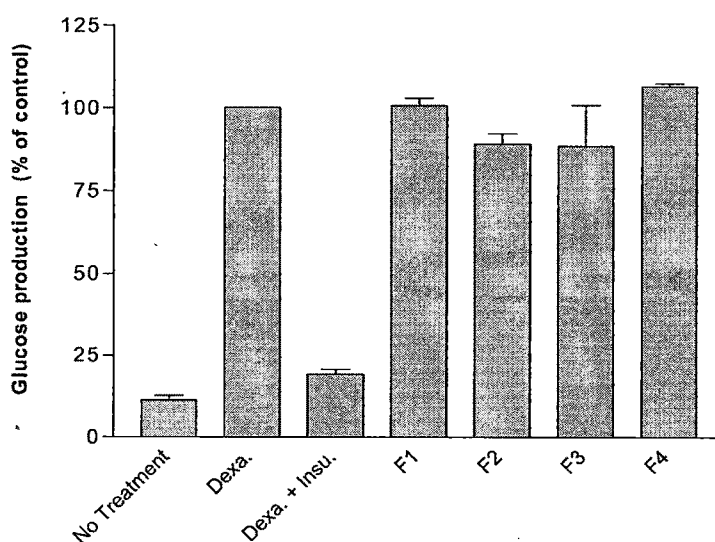


Figure 86 Effect of formulations on Inhibition of hepatic glucose production in rat hepatocytes.

4.6.7 Insulin Secreting Activity

Insulinotropic drugs have been used as hypoglycemic agents that stimulate insulin secretion by pancreatic β -cells in the treatment of NIDDM for almost 45 years. These drugs, namely tolbutamide, glibenclamide and glimepiride trigger insulin secretion primarily through binding to the sulfonylurea receptor subunit on the β -cell membrane (Sheeham, 2003; Rendell, 2004). The possibility of exploiting the rat pancreatic cell lines to study the insulinotropic effects is currently considered with much enthusiasm in developing new anti-diabetic agents (Mathews et al., 2006; McClenaghan, 2007). Considerable potential is also afforded for rapid screening and isolation of novel anti-diabetic entities from plants and other natural resources based on insulinotropic activities using pancreatic β -cell lines.

The effect of different fractions was tested at 1.1 and 16.7 mM glucose on insulin secretion from RINm5F cell line. The results are shown in table 38. Graphical presentation of the data is shown in figure 84. None of the fraction found to raise insulin level significantly at 1.1 mM glucose concentration when compared with respective control. EH flavonoid fraction and TC alkaloid fraction evoked insulin secretion from RINm5F cells in hyperglycemic condition (16.7 mM glucose) as compare to control (without fraction). Positive standard tolbutamide (10 μ g/ml) found to raise insulin secretion significantly ($p < 0.001$) even at hypoglycemic condition i.e, 1.1 mM glucose.

Table 38 Effects of the fraction on insulin secretion from RINm5F cells.

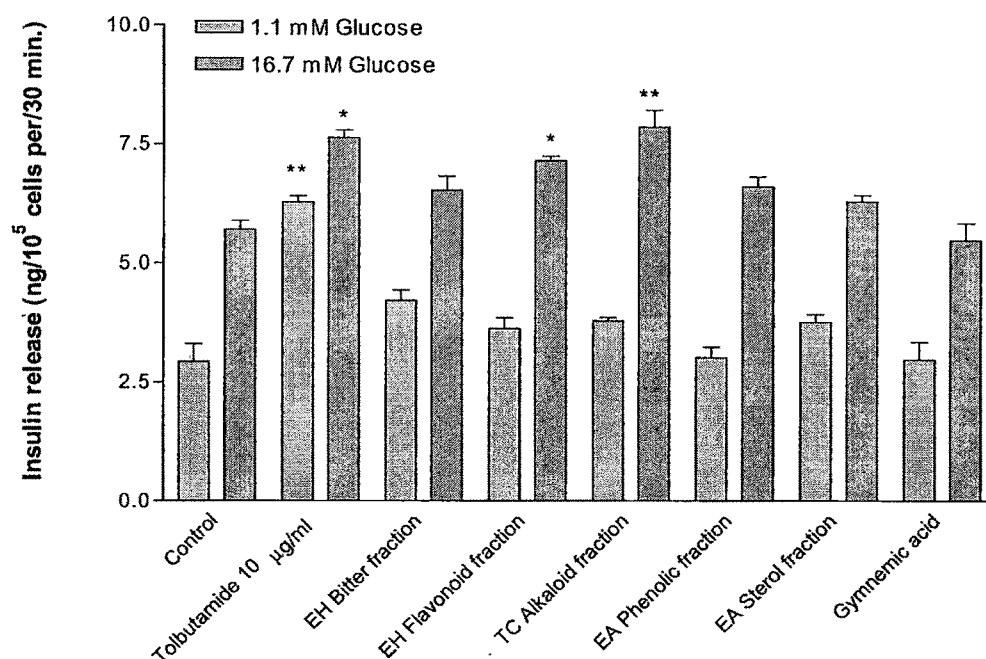
Sample	Insulin content (ng/10 ⁵ cells per/30 min.)	
	1.1 mM Glucose	16.7 mM Glucose
Control	2.93 \pm 0.37	5.70 \pm 0.18
Tolbutamide (10 μ g/ml)	6.28 \pm 0.13	7.63 \pm 0.17
EH Bitter fraction #	4.21 \pm 0.22	6.52 \pm 0.30
EH Flavonoid fraction #	3.61 \pm 0.23	7.14 \pm 0.10
TC Alkaloid fraction #	3.78 \pm 0.06	7.85 \pm 0.35
EA Phenolic fraction #	3.01 \pm 0.22	6.59 \pm 0.21
Gymnemic acid #	2.96 \pm 0.38	5.46 \pm 0.36

Samples were tested at the concentration of 100 μ g/ml.

Table 39 Effects of isolated compounds on insulin secretion from RINm5F cells.

Sample	Insulin content (ng/10 ⁵ cells per/30 min.)					
	1.1 mM Glucose			16.7 mM Glucose		
	10 µg/ml (n=3)	50 µg/ml (n=3)	100 µg/ml (n=3)	10 µg/ml (n=3)	50 µg/ml (n=3)	100 µg/ml (n=3)
Control		1.63 ± 0.02			3.17 ± 0.03	
Tolbutamide	3.28 ± 0.08 ^a	4.68 ± 0.07 ^b	5.38 ± 0.05 ^c	6.26 ± 0.05 ^a	6.85 ± 0.06 ^b	7.57 ± 0.03 ^c
Swertiamarin	1.70 ± 0.02	1.83 ± 0.01	1.90 ± 0.02	2.90 ± 0.04	3.54 ± 0.04	3.76 ± 0.03
Swertisin	1.65 ± 0.01	1.65 ± 0.02	1.73 ± 0.01	3.56 ± 0.04	3.77 ± 0.03	3.90 ± 0.13
TCY	2.33 ± 0.04	2.57 ± 0.05	2.97 ± 0.05	6.31 ± 0.04	6.65 ± 0.05	6.93 ± 0.05
TCB	2.56 ± 0.06	2.86 ± 0.02	3.04 ± 0.05	5.56 ± 0.06	5.83 ± 0.03	6.51 ± 0.10
TCA	1.60 ± 0.03	1.68 ± 0.02	1.68 ± 0.03	6.48 ± 0.10	7.03 ± 0.06	7.24 ± 0.04
Gymnemagenin	1.61 ± 0.02	1.68 ± 0.02	1.63 ± 0.03	4.38 ± 0.04	4.64 ± 0.04	4.75 ± 0.04

^a sample tested at the concentration of 1 µg/ml; ^b sample tested at the concentration of 5 µg/ml; ^c sample tested at the concentration of 10 µg/ml.

**Figure 87** Effects of the fraction on insulin secretion in presence of 1.1 mM and 16.7 mM glucose from RINm5F cells.

* P < 0.05 ** P < 0.001 when compared with respective control group.

The bioactive fraction EH flavonoid fraction and TC alkaloid fraction were further screened for insulin secreting compound. A major constituent from EH flavonoid fraction swertiamarin

and swertisin; an isolated alkaloids TCY, TCB and TCA; and a genin part of gymnemicacid, gymnemagenin were selected for evaluation as an insulin secretagogue. The samples were tested at three dose level i.e., 10, 50 and 100 $\mu\text{g/ml}$. The positive control tolbutamide was studied at 1, 5 and 10 $\mu\text{g/ml}$ concentration (table 39). Results are presented in graphical form in figure 88. Swertiamarin showed dose dependent response in both hypo and hyperglycemic condition. Swertisin also showed significant increase in insulin secretion in hyperglycemic state and not in hypoglycemic state. At higher concentration of 100 $\mu\text{g/ml}$ swertisin showed moderate activity in hypoglycemic state. Alkaloids TCY and TCB both found to increase insulin secretion by about 1.8 fold in presence of 1.1 mM glucose. They also gave positive activity in presence of 16.7 mM glucose i.e., 2.19 (TCY) and 2.05 (TCB) fold high secretion as compare to control at 100 $\mu\text{g/ml}$ concentration. TCA was found to possess a significant ($p < 0.001$) insulin secretion activity in hyperglycemic condition (2.31 fold higher compare to control at 100 $\mu\text{g/ml}$ concentration). Very interestingly unlike gymnemic acid, gymnemagenin found to raise insulin secretion by 1.5 times as compare to control at the concentration of 100 $\mu\text{g/ml}$.

To study the effect of combination of bioactive molecules, swertisin, TCA and gymnemagenin were selected as thrice of them were found to possessed potent insulin secreting action in hyperglycemic condition only. They were mixed in the proportion of 65 : 35 : 15 respectively to produce a final solution of 100 $\mu\text{g/ml}$ mixture. The direct comparison was done with 100 $\mu\text{g/ml}$ solution of individual constituent. In this case, the results were obtained only with 16.7 mM glucose exposure. Results are depicted in table 40. Combination of biomarker increases insulin secretion by 2.97 fold as compare to control and it also showed significant activity as compare to individual component studied alone. No additive effect was observed but the enhancement of activity in combination is very clear. Combination did not show any secretary effect in the absence of stimulus (1.1 mM glucose).

All four formulations in their extract form were studied at the concentration of 100 $\mu\text{g/ml}$. None of them found to produce any significant activity.

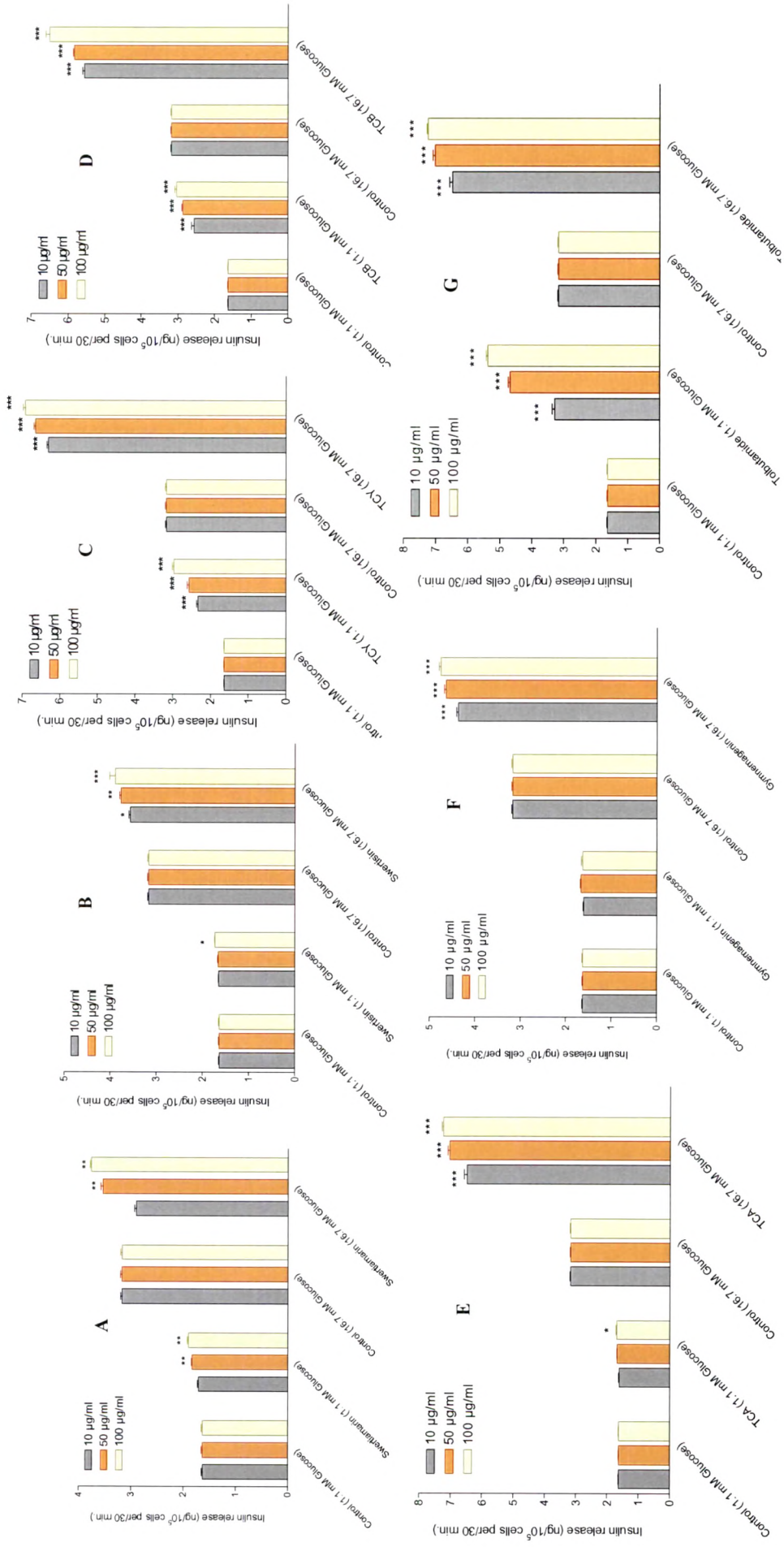


Figure 88 Effects of different concentrations of (A) swertiamarin (B) swertiamarin (C) TCY (D) TCB (E) TCA (F) gymnemagenin, isolated from bioactive fractions and (G) toltubamide, on insulin release from RINm5F cells. Results are means \pm S.E.M. of three observations. * $P<0.05$, ** $P<0.01$, *** $P<0.001$ compared with respective control.

Table 40 Effects of combination of bio active markers on insulin secretion from RINm5F cells.

Sample	Insulin content (ng/10 ⁵ cells per/30 min.)
Control	1.55 ± 0.04
Tolbutamide (10 µg/ml)	4.65 ± 0.05
Swertisin	2.73 ± 0.05
TCA	4.25 ± 0.06
Gymnemagenin	2.75 ± 0.04
#Combination (with 16.7 mM glucose)	4.61 ± 0.10
#Combination (with 1.1 mM glucose)	1.48 ± 0.08

contains swertisin : TCA : gymnemagenin (65 : 35 : 15) in 100 µg/ml concentration.

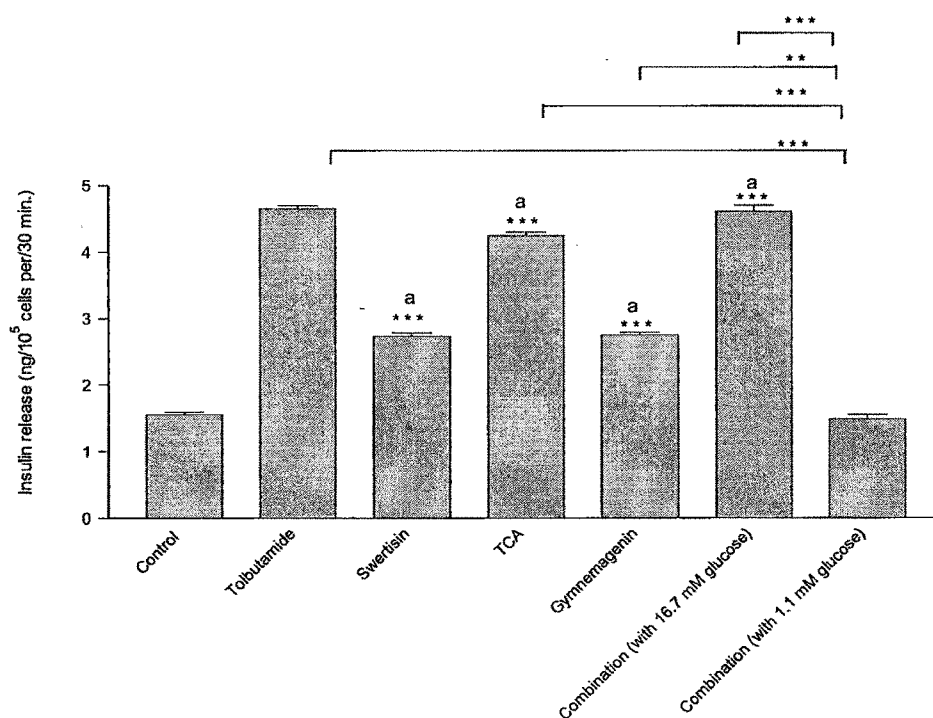


Figure 89 Comparative effects of combination and individual biomarker on insulin release from RINm5F cells. Results are means ± SEM of three observations.

a – compared with control group. ** $P < 0.05$, *** $P < 0.001$.

Results shown in figure 90 and 91 are presenting the effect of isolated compounds (as individual and in combination) on serum glucose level and insulin release of rat respectively.

Table 41 Hypoglycemic effect of isolated compounds in rat.

Sample	Glucose level (mg/dl)	
	0 min.	60 min.
Control	54.2 ± 2.19	98.2 ± 2.52
Tolbutamide (10 mg/kg)	59.2 ± 1.17	59.7 ± 1.89
Swertisin (10 mg/kg)	48.8 ± 1.38	80.4 ± 2.49
TCA (10 mg/kg)	54.8 ± 1.93	57.8 ± 1.87
Gymnemagenin (10 mg/kg)	52.2 ± 1.77	74.4 ± 1.83
#Combination	50.0 ± 2.27	56.3 ± 2.67
F-1 (100 mg/kg)	52.4 ± 1.44	92.5 ± 0.88
F-2 (100 mg/kg)	53.2 ± 1.17	93.6 ± 1.58
F-3 (100 mg/kg)	59.4 ± 1.63	82.4 ± 2.58
F-4 (100 mg/kg)	58.2 ± 2.62	78.3 ± 3.80

contains swertisin : TCA : gymnemagenin (65 : 35 : 15).

An alkaloid TCA found to restore the normoglycemic condition in 60 min after glucose administration. The activity was comparable to that of positive standard tolbutamide at the same dose i.e., 10 mg/kg. Swertisin and gymnemagenin also showed significant ($p < 0.001$) hypoglycemic effect but the normoglycemic condition was not reach after 60 min. Combination of these three biomarkers also found to exhibit significant ($p < 0.001$) glucose lowering effect but the data didn't lead to the conclusion of being additive or synergism of due to the combination of markers. Out of studied formulation at the dose of 100 mg/kg p.o., formulation F-3 and and F-4 found to decrease serum glucose level significantly. Formulation F-1 and F-2 at this dose did not showed any significant decrease in serum glucose level.

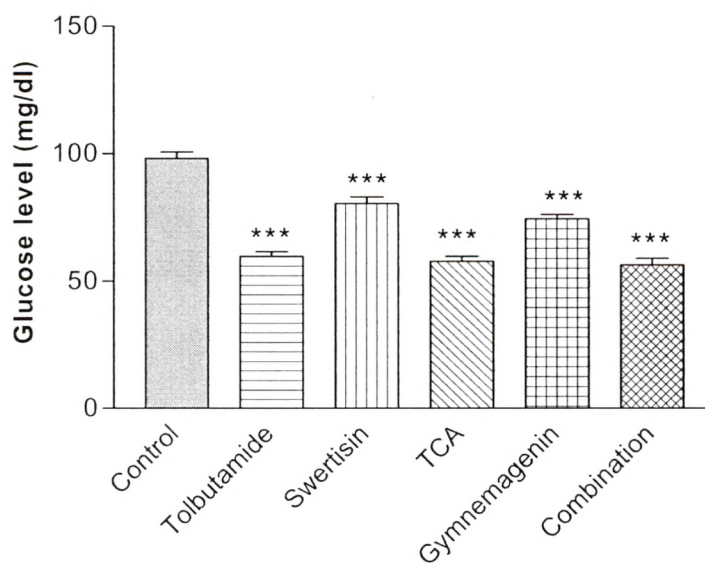


Figure 90 Serum glucose levels after single dose (intraperitoneal injection) of vehicles/compounds in rats (*in vivo*). All values are mean \pm SEM, n = 5.

*** p < 0.001 versus control animals (60 min after oral glucose).

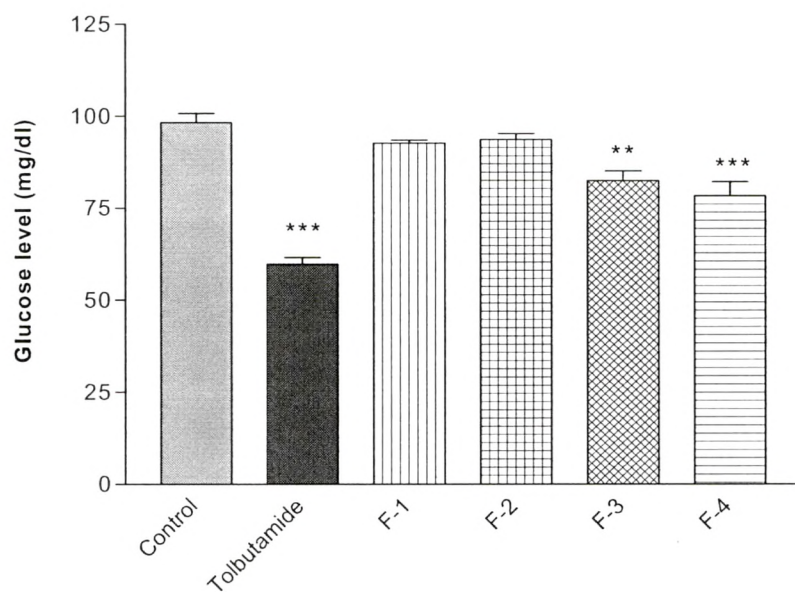


Figure 91 Serum glucose levels after single dose (100 mg/kg, p.o.) of formulations in rats (*in vivo*). All values are mean \pm SEM, n = 5.

** p < 0.01, *** p < 0.001 versus control group (60 min after oral glucose).

Table 42 Insulin secretagogue action of isolated compounds in rat.

Sample	Insulin content (ng/ml)
Control	0.49 ± 0.04
Tolbutamide (10 mg/kg)	1.50 ± 0.07
Swertisin (10 mg/kg)	0.89 ± 0.09
TCA (10 mg/kg)	1.48 ± 0.08
Gymnemagenin (10 mg/kg)	0.67 ± 0.04
#Combination	1.55 ± 0.05

contains swertisin : TCA : gymnemagenin (65 : 35 : 15).

In vivo insulin secreting activity of compound alone and in their combination is presented in table 42. Gymnemagenin showed no significant ($p > 0.05$) insulin secreting activity when compared with control group. Swertisin and TCA both possessed significant ($p < 0.001$) insulin secretagogue activity. Similarly the combination thereof also showed excellent activity. Thus the hypoglycemic potential of swertisin and TCA may be owing to their activity on pancreatic β -cells. Hypoglycemic activity of gymnemagenin is well observed *in vivo*, which may be due to some other mechanism except insulin releasing activity.

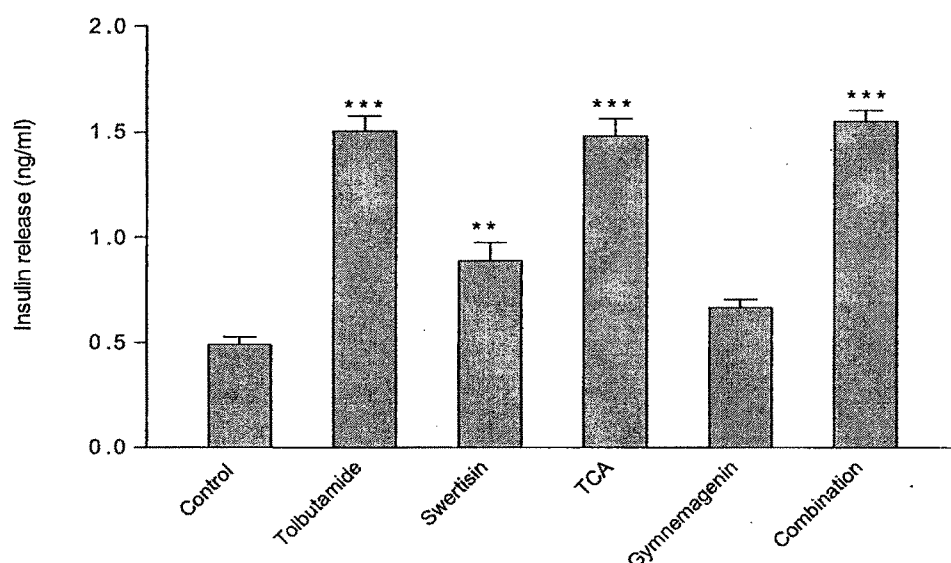


Figure 92 The serum insulin levels after single dose (intraperitoneal injection) of vehicle/test compounds in wistar rats (*in vivo*). ** $p < 0.01$, *** $p < 0.001$.

4.6.8 Characterization of Bioactive Molecules

Isolated compounds which were found to have promising activity on either of the studied models were subjected to various spectroscopic studies for their identification.

Enicostemma hyssopifolium

Thin layer chromatographic studies on precoated HPTLC plates (Merck, Germany) confirm the presence of two major components in EH. EH001 (R_f 0.71) and EH002 (R_f 0.57) were identified as a secoiridoid glycoside and C-glycosyl flavonoid respectively (figure 93). EH002 was identified as swertiamarin by spectral comparison with reference substance procured from Wako Pure Chem. Ind. Ltd, Osaka, Japan. EH001 was identified as C-glycosyl flavone (6- β -D-glucopyranosyl; 4'-5-dihydroxy, 7-methoxy flavone). This flavonoid, swertisin was already reported in literature (Ghosal and Jaiswal, 1980). Identification was done on the basis of phytochemical, elemental, IR and UV spectrum analysis.

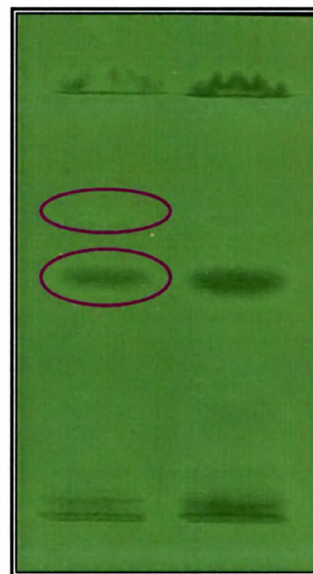


Figure 93 HPTLC Plate of EH methanol extract

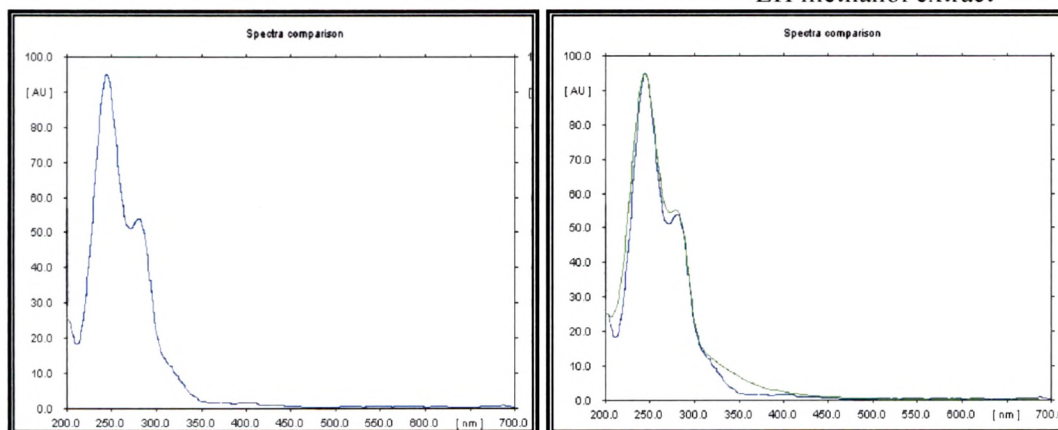


Figure 94 Ultra violet spectrum of (A) standard swertiamarin (B) overlain spectra of swertiamarin standard and compound 1 isolated from EH

Swertisin ($C_{22}H_{22}O_{10}$): Yellow crystalline powder, mp. 242 °C (decomp.), color test: $FeCl_3$, brown; $Mg-HCl$, yellow; $Zn-HCl$; pink. Its R_f value on paper, 0.54 (butanol:acetic acid:water - 4:2:1), U V λ_{max} (methanol) nm: 272, 332. U V λ_{max} (methanol + $AlCl_3$) nm: 280, 300, 344. U V λ_{max} (methanol+ $AlCl_3$ + HCl) nm: 280, 300, 345. U V λ_{max} (methanol + sodium

methoxide) nm: 273, 390. U V λ_{max} (methanol + sodium acetate) nm: 271, 335. U V λ_{max} (methanol + sodium acetate + boroc acid) nm: 271, 333. CH percentage calculated for $\text{C}_{22}\text{H}_{22}\text{O}_{10}$: C, 59.19; H, 4.97. Found: C, 59.56; H, 5.04. The IR spectrum was also found to be superimposable with that of swertisin reported in literature.

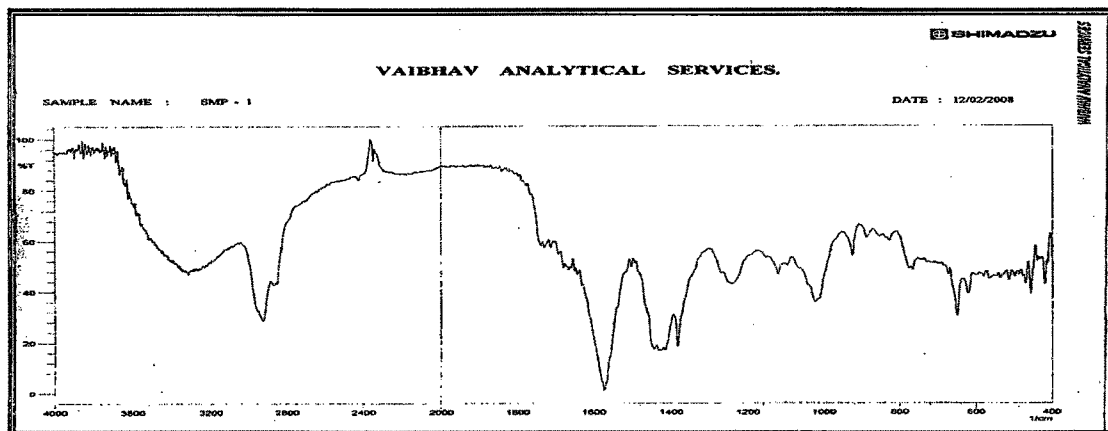


Figure 95 IR spectrum of compound 2 (EH)

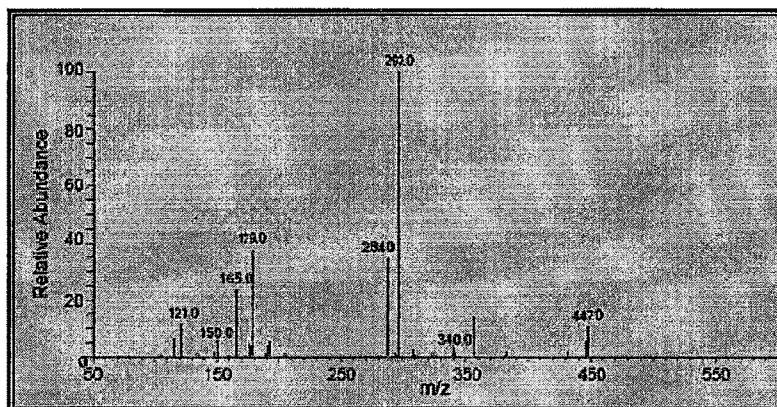


Figure 96 Mass spectrum of compound 2 (EH).

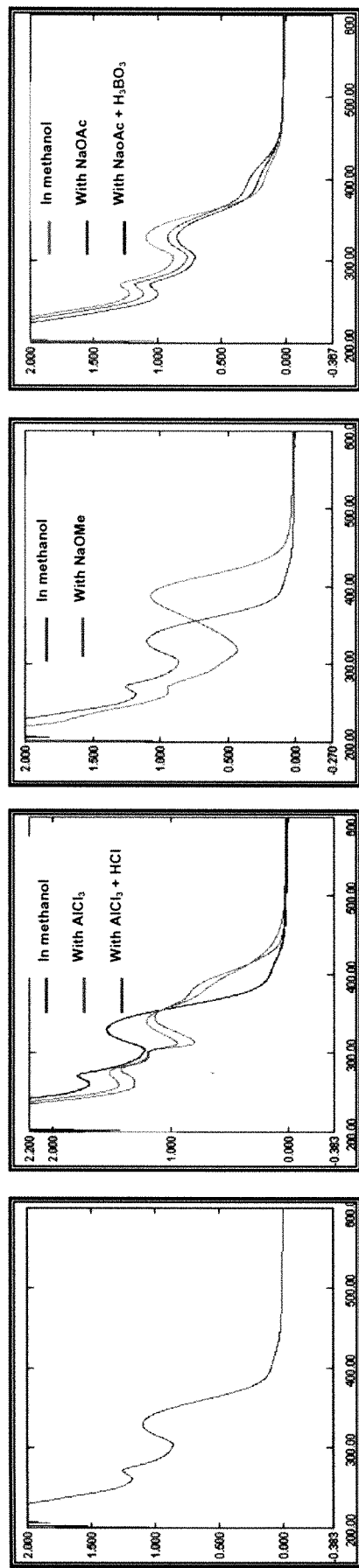
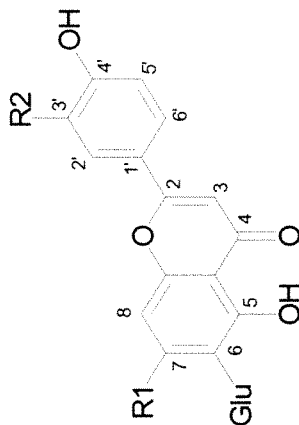


Figure 97 Ultraviolet absorption spectra of isolated compound 2

Table 43 Bathochromic shifts of isolated compound 2 (EH)

Reagent	λ max. (nm)observed	Observation	Inference	
Methanol	272	Bathochromic shift and stability with HCl of band I (i.e, 332 nm)	Free 5-OH group is present	
Methanol + AlCl ₃	280	300	344	
Methanol + AlCl ₃ + HCl	280.5	300.5	346	
NaOMe	273	390	Absence of bathochromic shift of band II (i. e, 271 nm)	No free OH group at 7 th position
NaOAc	271	335		
NaOAc + H ₃ BO ₃	271	333	Absence of bathochromic shift of band I (i. e, 332 nm)	No O-dihydroxy system in B ring



R1=R2=H, 6-C-glucopyranosyl apigenin

Mass spectrum

The based ion 447 $[M + H]^+$ was observed. Base peak observed at 297 (aglycone + CH_2^+), this ion may be stabilized by rearrangement to a tropylium structure. A peak of medium intensity was observed (m/e 284) of aglycone. Peaks at m/e 179, 121, 118 are justified in figure 15.5.

Isolated flavonoid is confirmed to have 6-C-glucosyl flavone as the peak m/e 298 $[M-148]^+$ is of about 65% of the intensity of the peak m/e 297 $[M-149]^+$. In case of 8-C it is usually of 25% intensity. For higher intensity of $[M-148]^+$ proposed mechanism involves the transference of hydrogen atom from the 5-OH group of the 4-keto function followed by the abstraction of a hydrogen atom from the 2-OH group of the sugar to give ultimately the cleaved ion at m/e $[M-148]$. The ion subsequently loses a hydrogen atom to yield the $[M-149]^+$ ion which is equivalent to $[M-149]^+$ ion produced directly.

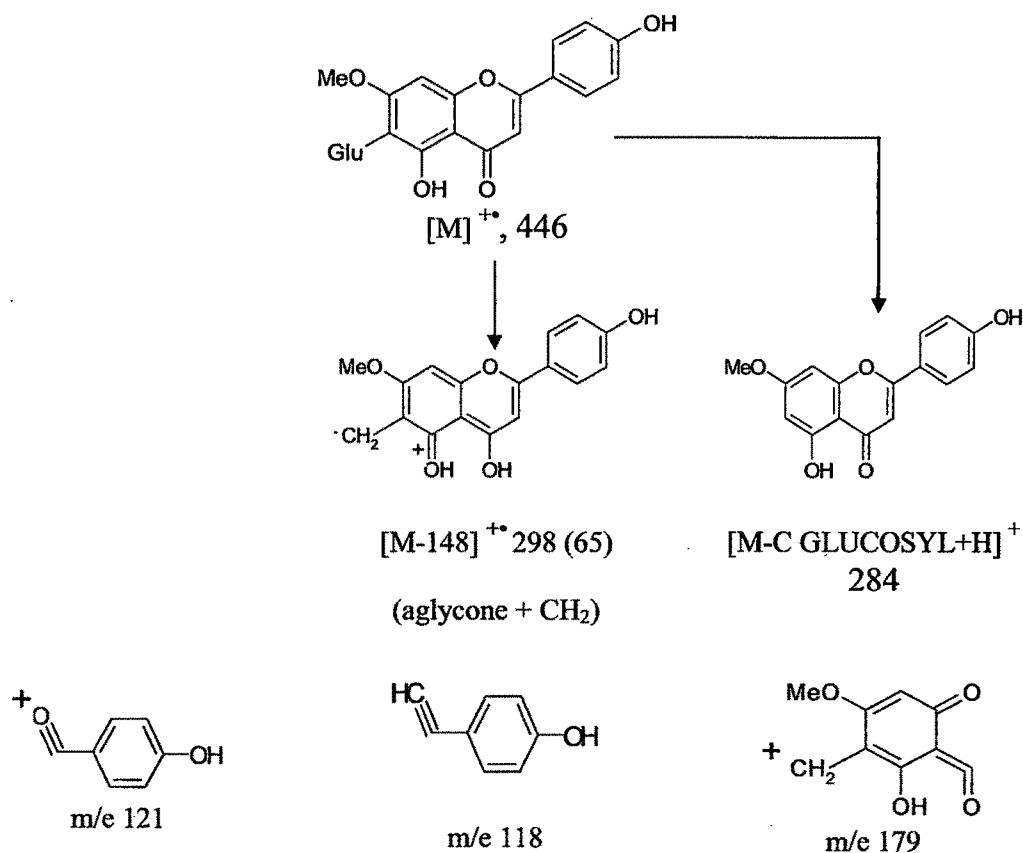


Figure 98 Mass fragments of compound 2 (EH)

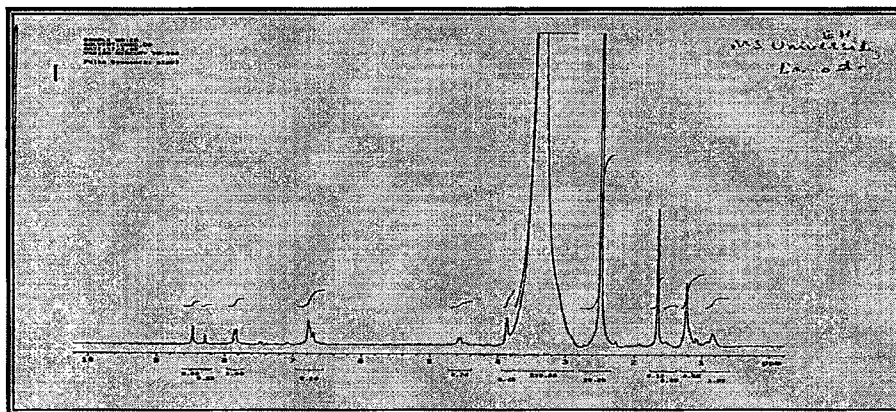


Figure 99 Proton NMR spectrum of compound 2 (EH)

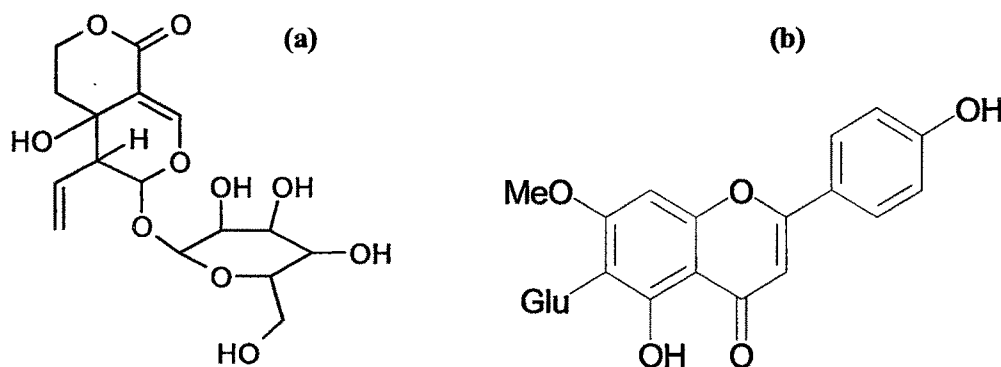
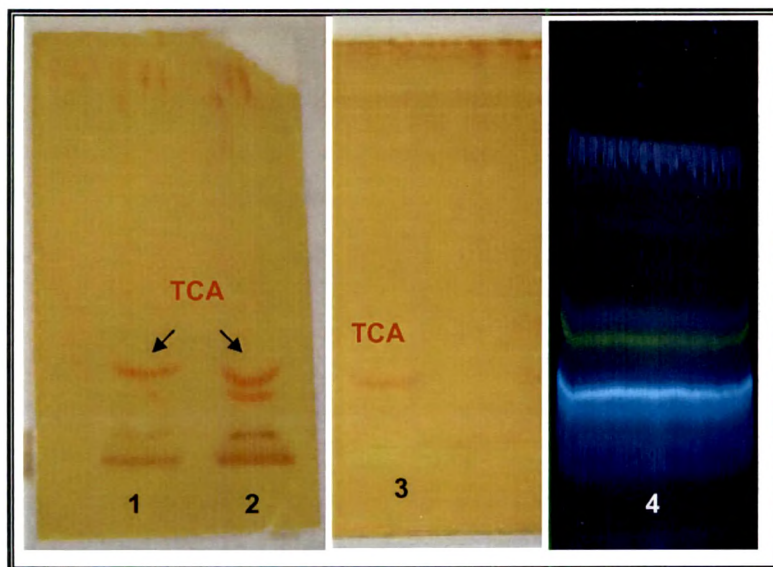


Figure 100 Chemical structure of (a) compound 1 - swertiamarin (b) compound 2 - swertisin.

Tinospora cordifolia

Three alkaloids TCY, TCB and TCA were isolated from TC stem. TCA was found to be present in both aqueous and methanol extract of TC stem.



Characterization of the isolated alkaloids was done using different spectroscopic studies viz., UV, IR, NMR, mass.

HPTLC chromatogram (figure 101) represents their R_f values when TLC plates developed in mobile phase ethyl acetate : formic acid : acetic acid : water (10 : 1.1 : 1.1 :3.2) and scanned under fluorescence mode at 366 nm.

Figure 101 Presence of TCA in (1) aqueous and (2) methanol extract of TC (3) Isolated TCA (4) alkaloid fraction under 366 nm.

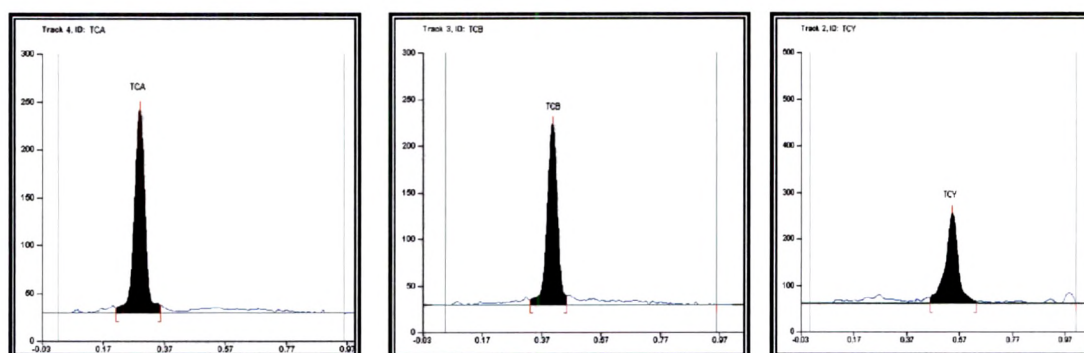


Figure 102 HPTLC chromatogram of isolated alkaloids TCA, TCB and TCY.

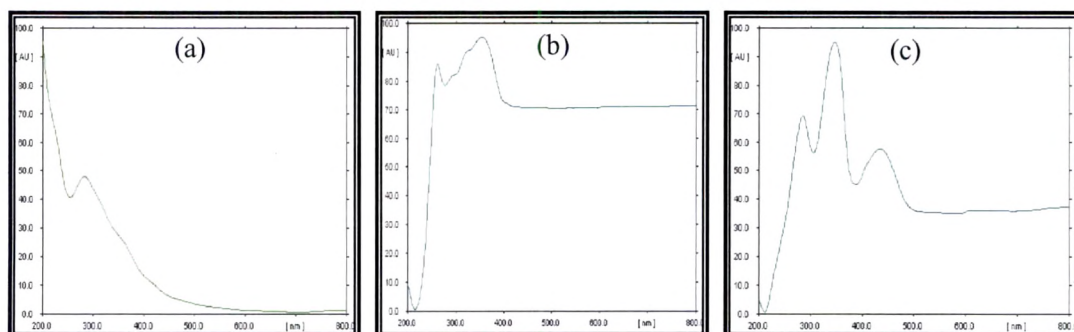


Figure 103 UV spectrum of (a) TCA (b) TCB and (c) TCY.

Characterization TCA ($C_{20}H_{24}O_4N^+$, mw. 342.41) was made by UV, IR, CHN and mass spectroscopy and identified as an aporphine alkaloid. Identification was made by comparison with literature data (Pachaly, 1988).

Physical properties and spectral data of TCA

Colorless amorphous powder.

UV (MeOH) λ_{max} nm : 282 .

IR KBr max cm^{-1} : 3391, 2957, 1603, 1396, 1365, 804, 771.

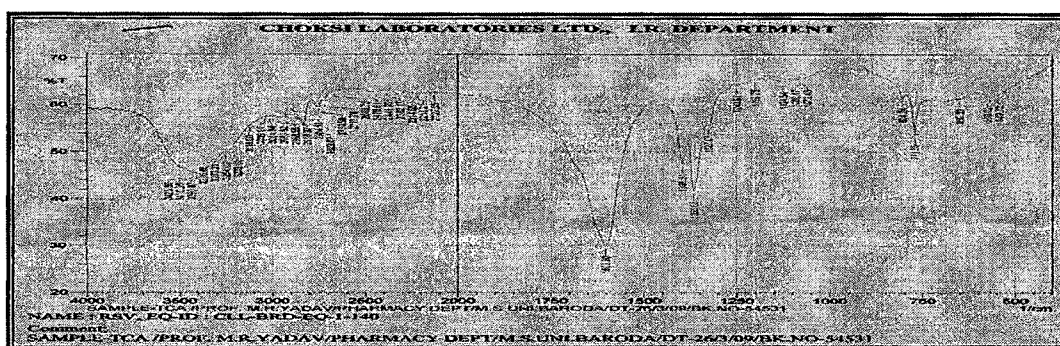


Figure 104 IR spectrum of TCA.

CHN percentage calculated for $C_{20}H_{24}NO_4$: C 70.18; H, 7.02; N, 4.09. Found: C, 69.75; H, 7.04; N, 4.1.

Mass: 342, 341, 327, 301, 263, 273, 262, 253, 227, 210, 163, 131, 58, 43.

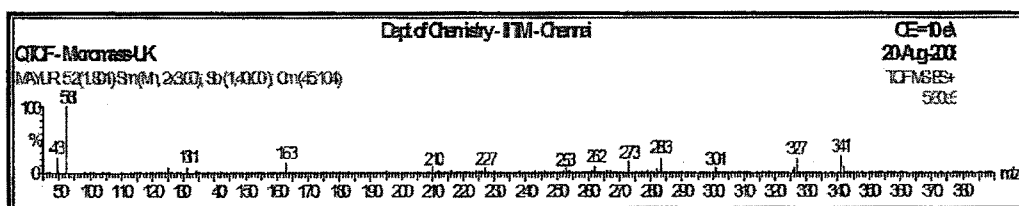


Figure 105 Mass spectrum of TCA.

Physical properties and spectral data of TCB

yellow needles, m.p. 195-198°C (decomposed).

UV λ_{max} (MeOH) nm: 268, 280, 324, 350.

IR ν_{\max} (KBr) cm^{-1} : 3410, 2826, 2741, 1604, 1384, 1352, 1342, 790, 762, 679.

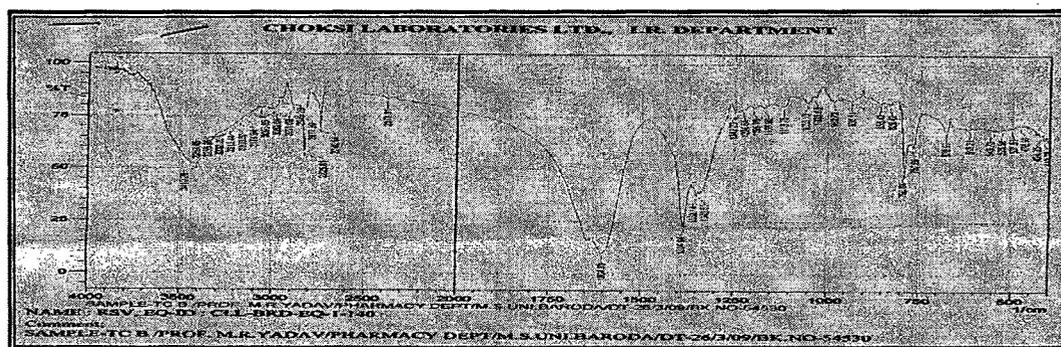


Figure 106 IR spectrum of TCB.

CHN percentage calculated for $\text{C}_{21}\text{H}_{22}\text{NO}_4$: C 71.59; H, 6.25; N, 3.98. Found: C, 70.35; H, 6.14; N, 3.7.

Mass spectrum: 352, 336, 323, 321, 115, 55, 43.

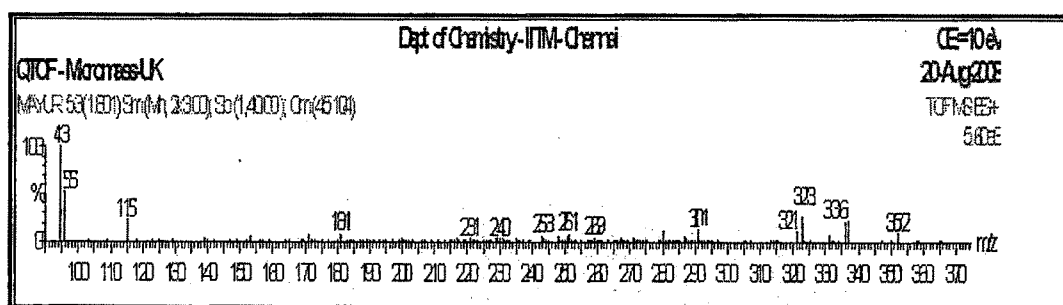


Figure 107 Mass spectrum of TCB.

Physical properties and spectral data of TCY

Orange powder, m.p. 194-196°C

UV λ_{\max} (MeOH): nm: 286, 346, 432.

IR (KBr) cm^{-1} : 3427, 2926, 2852, 2825, 1647, 1604, 1415, 1384, 1354, 1261, 1107, 1022, 790, 653.

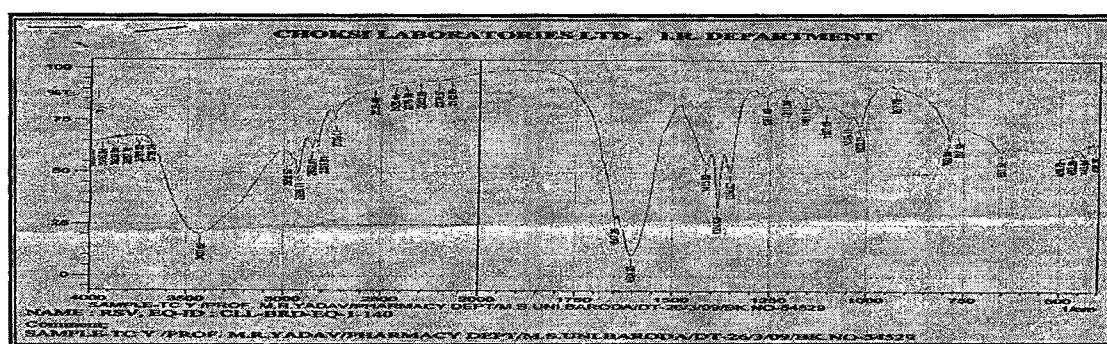


Figure 108 IR spectrum of TCY.

CHN percentage calculated for $C_{20}H_{20}NO_4$: C, 71.00; H, 6.09; N, 4.14. Found: C, 70.60; H, 5.83; N, 4.10.

Mass spectrum: 339, 338, 337, 336, 324, 323, 322, 294, 161, 50, 36

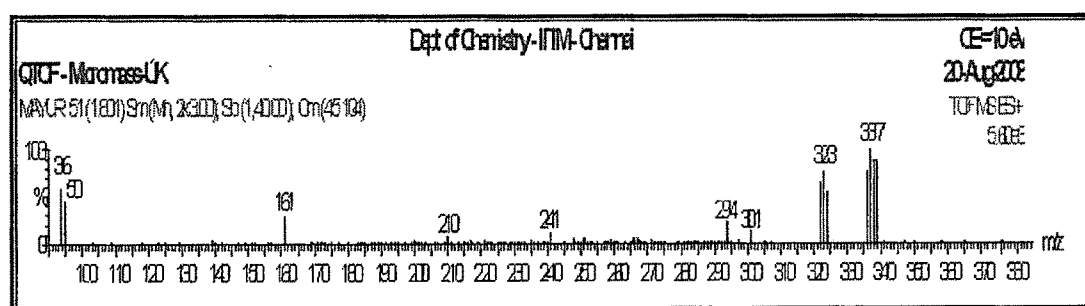


Figure 109 Mass spectrum of TCY.

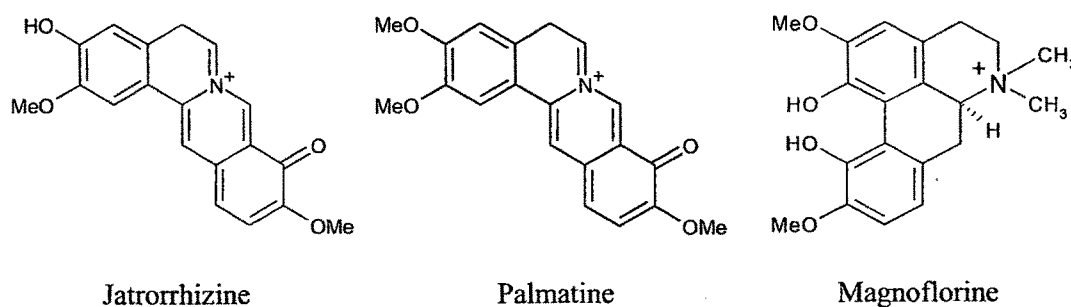


Figure 110 Chemical structures of TCY (jatorrhizine), TCB (palmatine) and TCA (magnoflorine).

Gymnema sylvestre

Crude gymnemic acid was used to isolate gymnemagenin. It was characterized by IR NMR, mass CHN and mass spectroscopy by comparing the spectral data with available in literature.

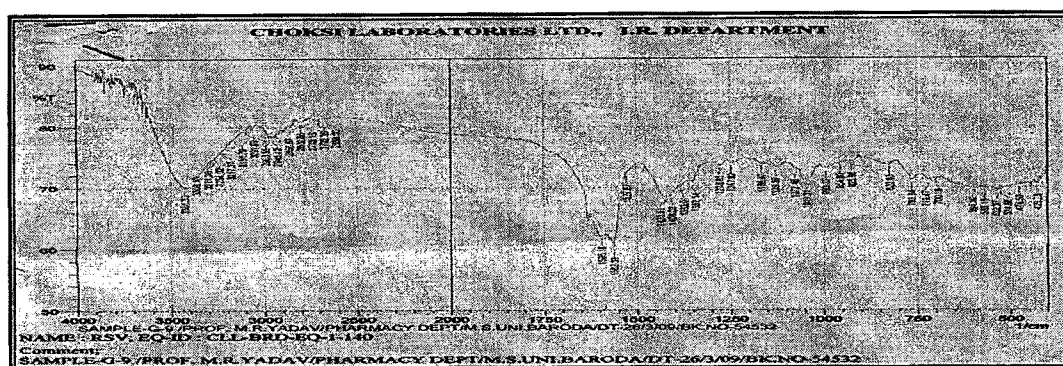


Figure 111 IR spectrum of gymnemagenin.



Figure 112 ¹H NMR of gymnemagenin.

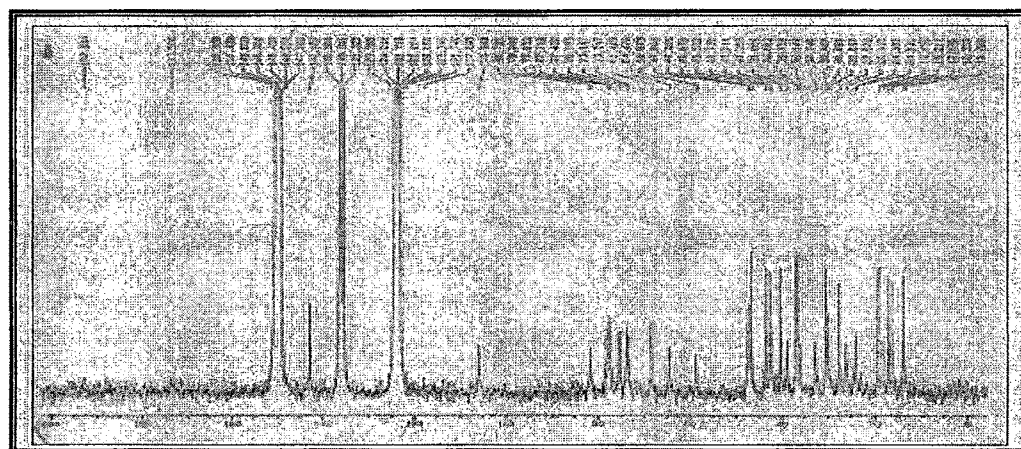


Figure 113 ¹³C NMR spectrum of gymnemagenin.

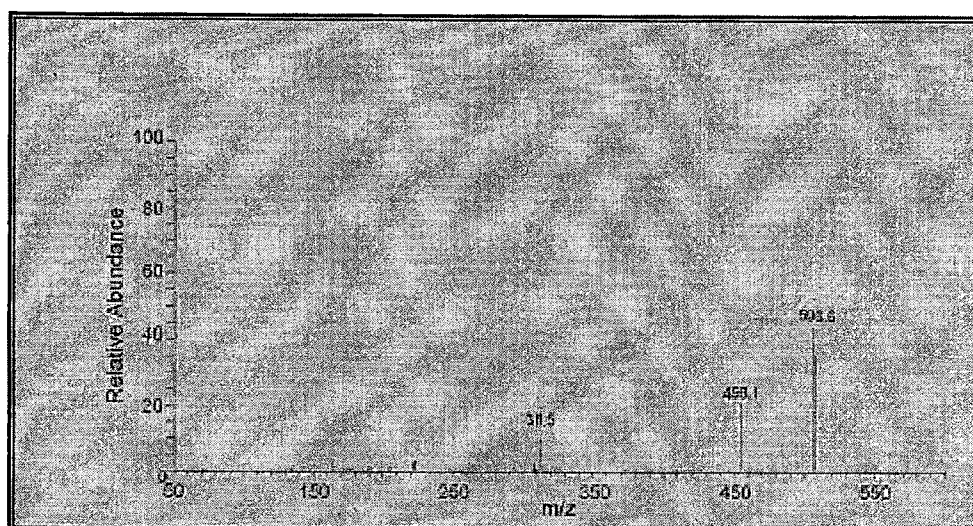
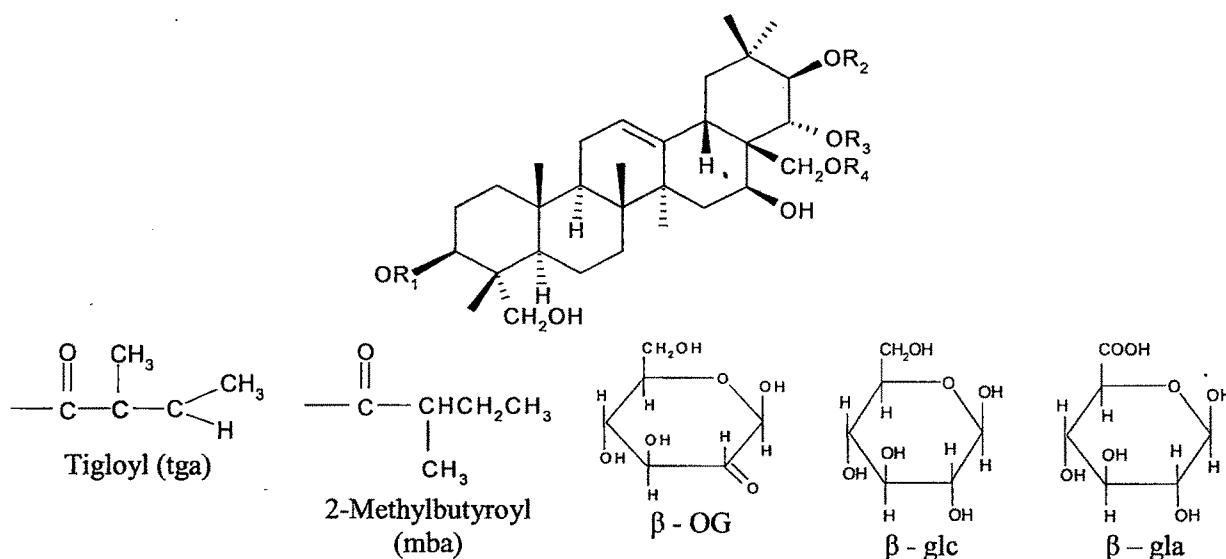


Figure 114 Mass spectrum of gymnemagenin.

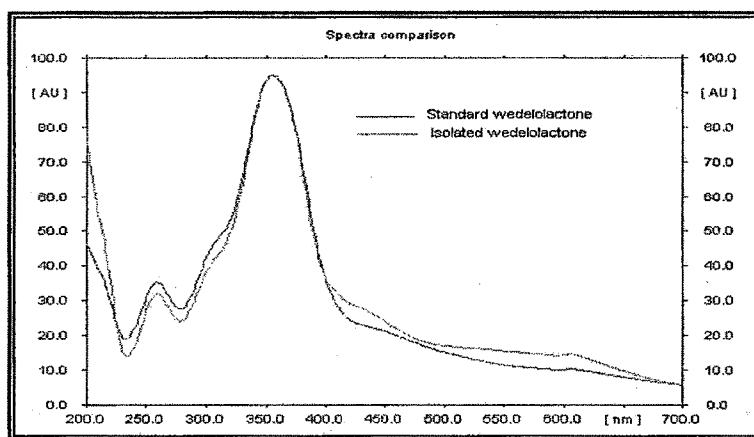
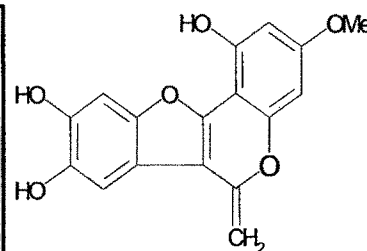
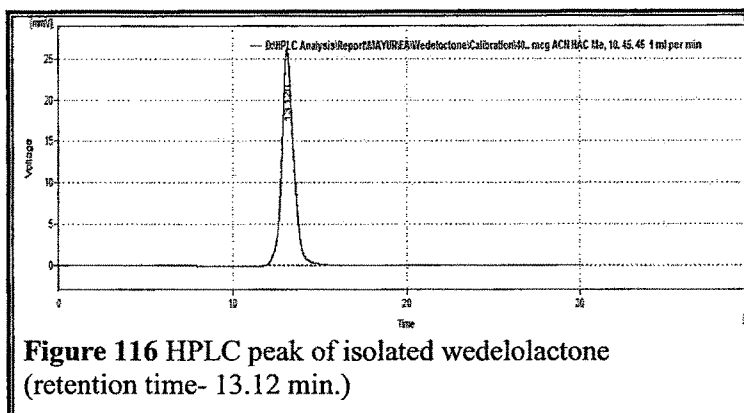


	R1	R2	R3	R4
Gymnemagenin	H	H	H	H
Gymnemic acid I	β - gla	tga	tga	tga
Gymnemic acid II	β - gla	mba	mba	mba
Gymnemic acid III	β - gla	mba	mba	mba
Gymnemic acid VI	β - gla	tga	tga	tga
Gymnemic acid V	β - gla	tga	tga	tga
Gymnemic acid VI	β - gla ³ - β - glc	tga	tga	tga
Gymnemic acid VIII	β - gla ³ - β - OG	mba	mba	mba
Gymnemic acid IX	β - gla ³ - β - OG	tga	tga	tga
Gymnemic acid X	β - gla	H	H	H
Gymnemic acid XI	β - gla	tga	tga	tga
Gymnemic acid XII	β - gla ³ - β - glc	tga	tga	tga
Gymnemic acid XIII	β - gla	H	H	H
Gymnemic acid XIV	β - gla	H	H	H

Figure 115 Chemical structure of Gymnemagenin and gymnemic acid.

*Eclipta alba**Wedelolactone*

An isolated yellow solid with melting point 300 °C (dec.) was identified as wedelolactone by matching the R_f value on TLC plate with that of standard wedelolactone. UV spectrum of isolated wedelolactone was also found to be superimposed on UV spectrum of standard. The purity estimated by HPLC was 97-98%.

*EA002**Physical properties and spectral data of EA002*

Light greenish waxy powder.

UV λ_{max} (MeOH) nm: 261, 361

IR ν_{max} (KBr) cm^{-1} : 3047, 2866, 2656, 2358, 2094, 1621, 1437, 1231, 1078, 1037, 937, 861, 732, 703.

CHN percentage calculated for $\text{C}_{19}\text{H}_{22}\text{O}_3$: C 76.51; H, 7.38; O, 16.11. Found: C, 77.35; H, 7.14; O, 17.10.

Mass spectrum: 298, 277, 276, 269, 261, 258, 240, 231, 210.

^1H NMR (400 MHz, CDCl_3): 6.24 (1H, d, $J = 9.6$ Hz, H-3), 7.64 (1H, d, $J = 9.6$ Hz, H-4), 7.20 (1H, s, H-5), 6.97 (1H, s, H-8), 3.40 (2H, d, $J = 7.2$ Hz, H-1'), 5.30 (1H, m, H-2'), 2.08–2.14 (4H, m, H-4', H-5' _), 5.10 (1H, m, H-6'), 1.69 (3H, s, H-8'), 1.61 (3H, s, H-9'), 1.75 (3H, s, H-10').

^{13}C NMR (100 MHz, CDCl_3): 162.2 (C-2), 112.4 (C-3), 144.1 (C-4), 128.3 (C-5), 125.5 (C-6), 158.5 (C-7), 103.3 (C-8), 154.2 (C-9), 112.3 (C-10), 28.5 (C-1'), 120.8 (C-2'), 138.9 (C-3'), 39.7 (C-4'), 26.4 (C-5'), 123.8 (C-6'), 131.9 (C-7'), 25.8 (C-8'), 17.7 (C-9'), 16.2 (C-10').

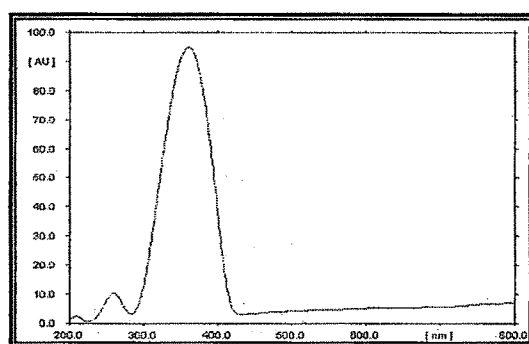


Figure 119 UV spectrum of EA002.

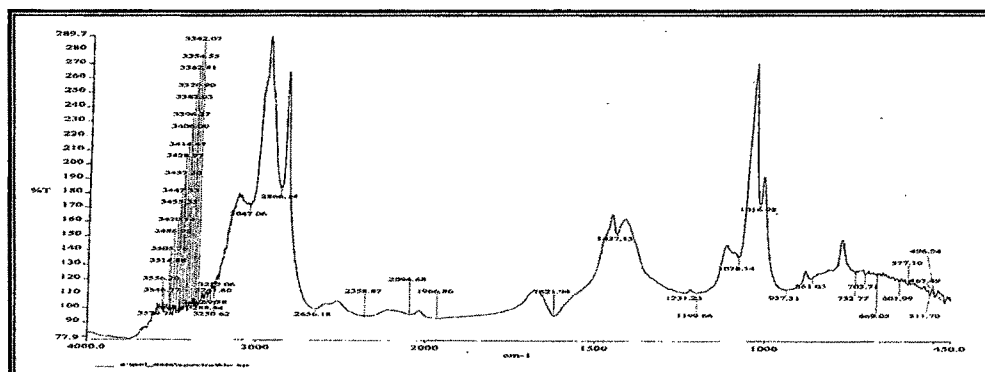


Figure 120 IR spectrum of EA002.

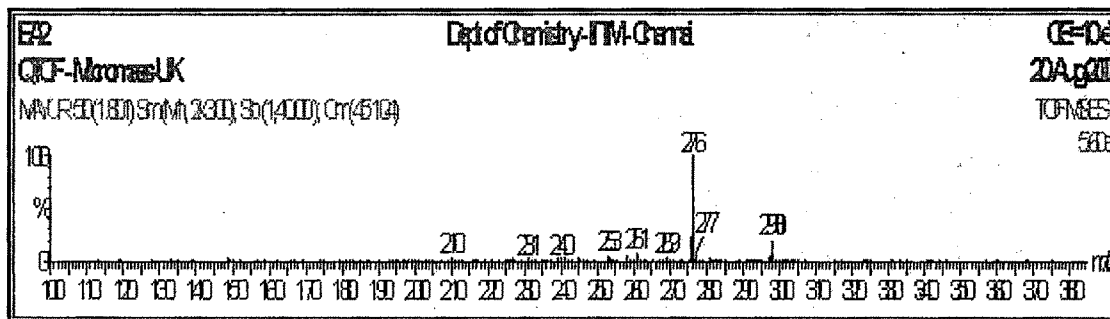


Figure 121 Mass spectrum of EA002.

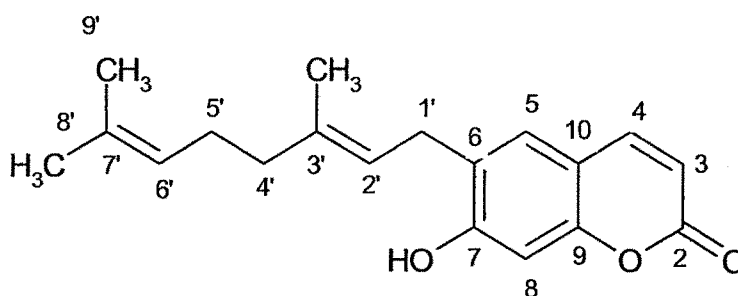
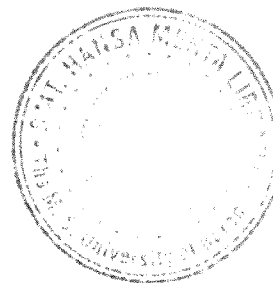


Figure 122 Probable chemical structure of EA002

EA002 is proposed to be a coumarin derivative. Probable chemical structure elucidated from spectral data of EA002 is shown in figure 122. EA002 was found to be toxic during MTT assay and hence it was not evaluated for antidiabetic property.



CHAPETR 5

SUMMARY AND CONCLUSION

Indian traditional system of medicine depends mainly on plants for maintenance of health and also for treatment of diseases. A lot of such formulations based on plant products either in powder form or whole organ or the extracts thereof in combination form are prescribed by physician practicing traditional system of medicine. Many such combinations are prepared based on the methods prescribed in text or sometimes prepared by using formulations based on experience of physicians. Thus the market is full of such remedies claimed to be effective in many diseases. These claims, however, are either based only on the traditional knowledge or on the database of information gathered or on the information passed through one individual to another for their efficacy. Such preparations although are providing relief to some extent and therefore could sustain their place in therapy, but need to be subjected for assessment of their quality, safety and efficacy which may provide convincing argument regarding their usage and also getting a medicament scientifically screened for its specific application in therapy.

Diabetes Mellitus as the name itself suggests is formed for two words Diabetes and mellitus meaning excessive honeyed micturation. Diabetes, commonly known as a disorder of sugar assimilation in human body causing various types of disorders of functional organs. There are so many claimed medicaments in different system of therapy throughout the world including plant and animal origin traditionally to treat this disorder. *Ayurveda*, an Indian traditional system of medicine described this disorder as "madhuprameha" and identified so

many plants having a curative property and also recommended in their standard text many such combinations as composite system containing different herbs or herbal extracts as polyherbal combinations. Assessment of bioactivity of such combinations as described in *ayurveda* for the efficacy was entirely based on parameters which are physically seen like wound healing or level of suagr in urine etc. In order to evaluate the efficacy of some such system which are recommended for majority of diseases and for their recognition as medicament these are required to be subjected for some evaluation. WHO has recognized the value of traditional system of medicine prevailing in different countries and has taken up excercises of different level to provide guidelines defining various criteria for evaluation of the quality, safety and efficacy of individual plant component as well as their combinations. These criteria involve main aspect for identification of correct plant sources, preparation of extracts, incorporation of extracts and their chemoprofiling to know probable chemical entities may be responsible for the biological activity. WHO has provided parameters for screening the raw material and finished products and also for standardizing the processes as well as the products.

The present studies therefore, were undertaken, to develop methods for chemical and biological evaluation of some such polyherbal formulations available in market and prescribed by traditional physician to treat diabetes. The formulations were selected taking in to consideration the utility and the plants used are common in all the four selected formulations. The plants were commonly designated in the literature possessing the activity therefore understanding the synergistic effect of these extracts when prescribed in combination was another very important factor required to be assessed and taken in to consideration. The present studies were planned first to evaluate individual plant which constituted the polyherbal formulation for their individual assessment and then similarly the formulations were subjected for the studies. Plants were collected and subjected for studies as per WHO guidelines for identification purpose. The preparation of extract and fractions, identification of chemical markers was done using various standard procedures. The quantitation of marker was also taken up using HPTLC and HPLC. The biological activity of fraction was and bio active fractions were subjected for isolation and characterization of chemical entities responsible for bio efficacy of the product. These procedures were performed for the formulations containing these plants which inturn provide justification of these combinations. Four proprietary marketed formulations; three in tablet form and one in capsulated form containing extract of selected plants were evaluated using above information.

The plants which were selected were first evaluated for their correct identity by studying their pharmacognostic parameters. Their morphological, microscopical was studied. Whole herbs of *Enicostemma hyssopifolium* (EH), *Gymnema sylvestre* (GS), *Tinospora cordifolia* (TC), and *Eclipta alba* (EA) were collected and authenticated. Transverse sections of leaf and stem of all these plants were observed for their microscopic studies. EH leaf was isobilateral, having anisocytic stomata present on both the epidermis and did not showed presence of trichomes. EH stem showed collenchymatous cortex and bicollateral vascular bundle with central pith. GS leaf was dorsiventral with multicellular covering trichomes on both the epidermis. Lamina portion showed presence of spheraphide of calcium oxalate. T.S. of GS stem also showed numerous multicellular trichomes, collenchymatous hypodermis and large pith at centre. Below cortex there was a sclerenchymatous pericyclic fibers arranged in a ring like fashion. Leaf of TC was dorsiventral and epidermis showed presence of anomocytic stomata. Stem showed parenchymatous cortex followed by sclerenchymatous pericycle forming a continuous circle of arches. Below each arch there was an open collateral vascular bundle present. Cells of cortex and pith contain abundant starch grains. EA consists of dorsiventral leaf with 2 layers of collenchyma below upper and above lower epidermis. Rarely covering trichomes were observed. It consists of bicollateral vascular bundle in the midrib. EA stem showed presence of uniseriate multicellular trichomes. Inner cortex was made up of aerenchyma. Vascular bundles were capped with sclerenchymatous bundle sheath. All these features were found to be in accordance with that reported earlier and hence confirms the identity of respective plants.

Physicochemical parameters described in WHO guidelines were estimated. Determination of total ash value indicated higher ash value in *E. alba* (24.09% w/w). A higher alcohol soluble extractive value in case of *E. hyssopifolium* (37.25 % w/w) and higher water soluble extractive value in case of *E. alba* (35.40 %w/w) was found. Determination of inorganic elements, including the trace elements and heavy metals has gained outstanding importance in the life sciences. The recent report on the potential deleterious effect of some *ayurvedic* medicines due to presence of unacceptable levels of metals and metalloids such as lead, arsenic, mercury etc. and their possible chronic toxicological effects, have caused much concern not only among the herbal practitioners, but also among large population who still depend on the medicinal plants for their health care needs. Thus it has become necessary that all the medicinal plant material should be assessed for the content of heavy metals and other inorganic elements. The plant material under study were found to be devoid of arsenic and

cadmium but were found to contain traces of lead in *E. hyssopifolium* and *E. alba* (5.6 and 7.8 ppm respectively). Traces of mercury found only in *E. alba* (6.9 ppm).

Preliminary phytochemical screening showed the presence of flavonoids, phenolics, terpenoids, saponins, sterols and very less amount of alkaloid in *E. hyssopifolium*. Saponins, flavonoids, tri-terpenoids were found to be present in *G. sylvestre*. High amount of alkaloid was present in *T. cordifolia*, where as *E. alba* found to contain higher amount of phenolic and sterols. Most of these constituents were found to present in total ethanol extract. The same extract was therefore been used for fingerprinting study. The characteristic TLC fingerprint was obtained in three different solvent system, one being non polar (hexane : ethyl acetate , 4 : 1), another medium polar (chloroform : methanol, 4.5 : 0.5) and third was polar in nature (ethylacetate : acetic acid : formic acid : water, 25 : 2.75 : 2.75 : 6.5). Developed tracks were scanned under 254 nm (absorption mode), 366 nm (fluorescence mode) and 540 nm (after derivatization with anisaldehyde sulphuric acid reagent). A complete TLC fingerprint of the resolved compounds comprising of typical chromatogram, R_f value and the percentage proportion of the individual components in extract was recorded.

DNA fingerprinting of herbal drugs for authentication for medicinal plant species and for ensuring better quality herbs seems to be a promising tool. In the present studies an attempt has been made to isolate pure genomic DNA of the selected plants which was subsequently subjected to RAPD (random amplified polymorphic DNA) fingerprinting. Ten random primers were selected and PCR (polymerase chain reaction) amplification was performed. Amplified DNA fragments were separated by gel electrophoresis and the pattern was photo documented. A few common bands of identical base pair were observed after amplification with specific primers (5'-GTGACATGCC-3' and 5'-GGTGCGGGAA-3') in plant DNA isolated from different locations.

Studied plants were extracted with methanol and then fractionated for the purpose of bioactivity guided fractionation. Identification of major constituents present in the prepared fractions was checked by HPTLC and derivatization with different detecting reagents. Two fractions constituted of bitter principles and flavonoids respectively were prepared from *E. hyssopifolium* methanol extract. A bitter principle (secoiridoid glycoside) namely swertiamarin and C-glycosyl flavonoid, swertisin was identified as a major constituents of bitter and flavonoid fraction from *E. hyssopifolium* and they were isolated by various steps of chromatography. A fraction rich in alkaloid content was prepared from *T. cordifolia* stem

powder. Three alkaloids were isolated from this fraction by preparative thin layer chromatography. Crude gymnemic acid was isolated from the methanol extract of leaf of *G. sylvestre* by precipitation at acidic pH. A genin part, gymnemagenin was cleaved by alkali and acid hydrolysis, partitioned in chloroform and then purified on TLC. *E. alba* powder was extracted and fractionated to give two fractions one being rich in phenolic constituents and another in sterol constituents. Wedelolactone was isolated as one of the major phenolics present in *E. alba* from phenolic fraction. Sterol fraction showed presence of high amount of one bright blue fluorescent compound which was named EA002 and isolated by preparative TLC.

Four formulations available in market for treatment of diabetes mellitus type II were selected. For their chemical evaluation an attempt has been made to identify and/or quantify the marker constituent in the methanol extract of these formulations. Analytical methods were developed and validated for the estimation of marker constituents by HPTLC and HPLC.

Biomarkers identified in *E. hyssopifolium* were swertiamarin and swertisin. Quantitation of these markers was performed using HPTLC. Stationery phase, precoated silicagel 60F₂₅₄ HPTLC plates and mobile phase, ethyl acetate : methanol : water (77 : 15 : 8) was used. Detection was performed by scanning densitometrically at 238 nm. Swertisin was quantified keeping all HPTLC parameters same as in case of swertiamarin except scanning wavelength i.e. 342 nm. The developed and validated method was applied for estimation of swertiamarin in root (0.230 %w/w), stem (0.521 %w/w), leaf (0.556 %w/w), methanol extract of aerial part (1.404 %w/w), bitter fraction (18.65 %w/w), flavonoid fraction (19.54 %w/w) and in polyherbal formulation-F2 (not detected). Content of swertisin estimated was 0.660 %w/w in root, 0.730 %w/w in stem, 0.820 %w/w in leaf, 2.100 %w/w in methanol extract of aerial part, 12.37 %w/w in bitter fraction, 25.82 %w/w in flavonoid fraction and 0.0095 %w/w in polyherbal formulation-F2. An attempt has also been made to quantify both of these markers simultaneously in methanol extract of aerial parts and it found to contain swertiamarin 2.14 % and swertisin 1.77 % w/w. The result of simultaneous estimation was not matched with that of measured individually. The scanning wavelength used for simultaneous estimation (254 nm) could be the reason as in case of individual estimation UV_{max} (λ_{max}) of respective compound was selected for scanning purpose. HPLC estimation has performed for quantitation of these markers and they found to contain swertiamarin 0.46 % and swertisin

0.73 % in aerial part of *E. hyssopifolium*. Results obtained by two different chromatographic methods were comparable to each other. HPTLC method found to be more economic and less time consuming than that of HPLC. Reproducibility and recovery in HPLC method was better than HPTLC method.

In case of *T. cordifolia* a nor-clerodane glucoside, tinosporaside was quantified in methanol and aqueous extracts. An alkaloids isolated were found to be less stable while used in solution form for quantification. Linearity of their calibration was questionable and hence those alkaloids were not considered for the said purpose. Tinosporaside was estimated after densitometry scan at 254 nm. Development of HPTLC plate was performed in chloroform : methanol (4 : 1). The method was applied for quantification of tinosporaside in stem methanol extract, stem aqueous extract, and polyherbal formulation F2, F3 and F4 and they found to contain 0.085, 0.032, 0.003, 0.006, and 0.039 % w/w respectively. HPLC fingerprint of alkaloid fraction, aqueous extract and chromatogram of alkaloid TCA was obtained.

HPTLC quantification of gymnemagenin in methanol and aqueous extract of *G. sylvestre* was performed after hydrolysis of sample. Chloroform : methanol : acetic acid (5 : 1 : 1) was used as mobile phase and plates were scanned at 450 nm after derivatization with AS reagent under absorption mode. Formulations (F1 and F3) were analysed for their gymnemagenin content using same set of parameters. Content of gymnemagenin was found to be 5.62, 2.81 %w/w in methanol and aqueous extract respectively. Formulation F1 contains 0.008 % of gymnemagenin where as formulation F3 does not contain a measurable amount of gymnemagenin. HPLC fingerprint of methanol extract was obtained using acetonitrile : 0.1% KH_2PO_4 (40 : 60) as mobile phase at flow rate of 0.8 ml/min. Detection was performed at 210 nm.

Wedelolactone, a marker constituent of *E. alba*, was quantified in aerial parts and phenolic fraction by HPTLC method. Toluene : acetone : formic acid (11 : 6 : 1) was used as mobile phase. Plates were scanned at 351 nm under fluorescence mode. Content of wedelolactone was found to be 1.879 and 19.69 %w/w in aerial parts and phenolic fraction respectively. HPLC method was also performed to quantify this marker and the percentage of wedelolactone was found to be 1.52. An isolated compound EA002 was quantified by HPLC method using acetonitrile as mobile phase at flow rate of 0.8 ml/min. Detection was performed at 360 nm using UV detector. Aerial parts of *E. alba* found to contain 0.05 %w/w of EA002.

Biological screening of medicinal plants is of vital importance, not only to provide a scientific basis for their continued usage but also justify their traditional utilization. Additionally, these studies aid to correlate the activity with some components present in the plant. Biological screening, thus provide additional mean of standardization of a plant drug and also lead to have an active phytomolecules which could be the lead molecule in the path of new drug discovery. The studies were aimed to screen methanol extract, fractions and isolated compounds on various *in vitro* and *in vivo* models to justify their usage as antidiabetic agent alone and their combinations and to evaluate the mechanism of action for their bio activity.

For studying the effect of the plant extracts on the uptake of glucose, a preparation of isolated small intestine was used. Intestinal segments (5 ± 1 cm) were everted and sacs were prepared by tying it at both ends and filling it with sufficient fluid to distend the wall. Inhibitory effect of plant extracts were studied at various substrate (glucose) concentrations. Out of the studied extracts *G. Sylvestre* leaf extract showed excellent inhibition of glucose uptake at intestinal level. Gymnemic acid and its genin moiety, gymnemagenin were tested for their effect on glucose uptake. Gymnemic acid showed 24.12, 28.38, 41.92% inhibition at 1, 5 and 10 mg/ml dose respectively whereas gymnemagenin found to be ineffective as an inhibitor of glucose uptake at intestine level. As a part of the study biochemical parameters like maximal velocity (V_{max}) and Mechaelis-Menten constant (K_m) were calculated. Decreased V_{max} and unaltered K_m in presence of gymnemic acid is an indicative of a non-competitive type of inhibition of glucose uptake at the level of the small intestine.

Inhibitory effect of extracts at various doses (25 – 500 $\mu\text{g/ml}$) was studied on hydrolysis of soluble starch by α -amylase. *E alba* extract showed complete inhibition of enzyme at the 400 $\mu\text{g/ml}$ and above concentration. *G. Sylvestre* extract also possessed moderate inhibitory effect as compare to *T. cordifolia* and *E. hyssopifolium*. At fraction level sterol fraction showed complete inhibition of the enzyme activity at 90 $\mu\text{g/ml}$ concentration. An isolated compound from this sterol fraction blocks the enzyme at 60 $\mu\text{g/ml}$ concentration. IC_{50} value calculated for sterol fraction and EA002 are 26.35 and 18.20 $\mu\text{g/ml}$ respectively. Phenolic fraction also found to show good activity with IC_{50} value of 51.10 $\mu\text{g/ml}$. Wedelolactone, a major phenolic constituents showed inhibition of lesser extent (IC_{50} 82.5 $\mu\text{g/ml}$). The activity of phenolic fraction may think because of presence of EA002. When effect of EA002 was observed on kinetics of α -amylase reaction, V_{max} was decrease by 24.73% in presence of

EA002 but Michaelis-Menten constant (K_m) unchanged revealing the type of enzyme inhibition non competitive. The effect of formulations on alpha amylase activity was studied. Studied formulations were evaluated in the concentration range of 10 – 100 $\mu\text{g/ml}$. The maximum inhibition (27.06%) was observed with formulation F3 at 100 $\mu\text{g/ml}$. Their relative activity were in the order being $F3 > F1 > F4 > F2$.

The enzyme aldose reductase (AR) is the enzyme of the polyol pathway that reduces excess D-glucose into D-sorbitol. This enzyme plays an important role in sugar-induced cataract. An inhibitory effect of *E. hyssopifolium* and *T. cordifolia* methanol extract on AR isolated from sheep lens was found to be significant. Further screening of fractions showed that flavonoid rich fraction from *E. hyssopifolium* and alkaloid fraction from *T. cordifolia* possessed excellent inhibitory effect on AR with IC_{50} value of 1.32 and 5.76 $\mu\text{g/ml}$ respectively. An isolated flavonoid swertisin showed IC_{50} value 1.23 $\mu\text{g/ml}$ and an alkaloid from *T. cordifolia* alkaloid fraction, TCA showed IC_{50} value 1.86 $\mu\text{g/ml}$. Both of these active components were checked for their action on kinetic of aldose reductase activity. Swertisin decrease V_{max} by 33% but did not alter K_m value. TCA also significantly decrease V_{max} by 49.5% and showed no alteration of K_m value is an indicative of inhibition being non-competitive type. Marketed formulation (F2) showed 70.57% inhibition at the dose of 400 $\mu\text{g/mL}$. Composition of F2 contains high amount of *E. hyssopifolium* and *T. cordifolia* extract, which could be the possible reason for this positive action. The rest of the formulations did not show any significant inhibition.

Screening of α -glucosidase inhibitors from studied plants and formulations was performed. Two substrates namely sucrose and maltose were used to evaluate sucrase and maltase inhibitory activity respectively. Methanol extract of *E. hyssopifolium* and *E. alba* showed promising effect. *E. hyssopifolium* methanol extract showed dose dependent alpha glucosidase inhibition in the concentration range of 5 -100 $\mu\text{g/ml}$. It showed 54.8 and 62.8 % inhibition of sucrase and maltase activity respectively at 100 $\mu\text{g/ml}$ concentration. Flavonoid fraction showed somewhat better activity than bitter fraction of *E. hyssopifolium*. Swertiamarin did not significantly inhibit maltase ($IC_{50} > 42.60 \mu\text{g/ml}$) or sucrase ($IC_{50} > 33.52 \mu\text{g/ml}$) activity, the activity of bitter and flavonoid fraction was probably due to presence of swertisin. Swertisin alone produced 95.02% and 63.74% inhibition of maltase and sucrase activity respectively at 10 $\mu\text{g/ml}$ concentration. IC_{50} value of swertisin as maltase and sucrase inhibitor was 1.89 and 5.74 $\mu\text{g/ml}$ respectively. *E. alba* methanol extract showed

complete inhibition of maltase activity at 100 $\mu\text{g/ml}$ concentration. Phenolic fraction of *E. alba* was active fraction ($\text{IC}_{50} = 6.14 \mu\text{g/ml}$). A major constituent from this fraction, wedelolactone with an IC_{50} value of 1.0 $\mu\text{g/ml}$ for maltase inhibition and 3.20 $\mu\text{g/ml}$ for sucrase inhibition proved to be a comparable inhibitor of alpha glucosidase to a positive standard voglibose. Effect of swertisin and wedelolactone was studied on alpha glucosidase kinetics. In case of sucrose as substrate, a significant decrease in V_{max} ($P < 0.001$) by 0.13 and 0.2 mM glucose formed/30 min was observed in the presence of swertisin and wedelolactone respectively. When maltose was used as substrate, V_{max} decreased by 0.18 and 0.2 mM glucose/30 min in presence of swertisin and wedelolactone respectively. Michaelis-Menten constant (K_m) remained unchanged in the presence of the swertisin indicate that swertisin inhibit alpha glucosidase in non-competitive manner. Where as in case of wedelolactone, decreased V_{max} along with K_m value with both substrates is an indicative of competitive inhibition of alpha glucosidase. Formulations were tested for their sucrase and maltase inhibitory effect. Maltase inhibitory activity was observed in the order of F2>F1>F3 with 52.80, 44.80, and 34.75% inhibition at 400 $\mu\text{g/ml}$ concentration. Formulation F4 was found to be ineffective as maltase inhibitor. Potential as sucrase inhibitor was in the order of F2>F3>F1 having 45.64, 22.56 and 30.68% inhibition at 400 $\mu\text{g/ml}$ concentration. Formulation F4 did not showed inhibition of sucrase activity of alpha glucosidase

Investigation for the protective effects of fractions and isolated phytoconstituents has been carried out on oxidative stress induced by streptozotocin (STZ) on the pancreatic β -cellline (RINm5F). Cell viability was measured by MTT assay. Cells were cultivated in liquid growth media of RPMI-1640 supplemented with 2 mM L-glutamine adjusted to contain 1.5 g/L sodium bi carbonate, 4.5 g/L glucose, 10 mM HEPES, and 1.0 mM sodium pyruvate, 90%; fetal bovine serum 10% in 5% CO_2 atmosphere at 37 $^{\circ}\text{C}$. Bitter fraction and flavonoid fraction derived from *E. hyssopifolium*, phenolic fraction of *E. alba* and gymnemic acid possessed significant protection of cells against STZ with EC_{50} values 86.5, 63.1, 95 and 53.2 μg respectively. Sterol fraction of *E. alba* found to have cytotoxic action on this cells. Principle constituents from these fractions were also screened in the same set of experiment. Swertiamarin, swertisin, wedelolactone and gymnemagenin were evaluated and out of them swertisin and wedelolactone were found to show significant protection with EC_{50} values 9.2 and 32.5 μg respectively. All the formulation were evaluated for their cytoprotective effect at three dose level i.e., 10, 50 and 100 μg . F-1, F-2 and F-3 showed good activity where as F-4 did not show any significant difference as compare to STZ treated cells.

A study has been performed to evaluate prepared fraction and isolated compounds on glucose production in rat hepatocytes cultured *in vitro*. The glucose production was measured by incubating hepatocytes in glucose free RPMI-1640 medium. The glucose release in to the medium was determined enzymatically with glucose oxidase. Rat hepatocytes were treated with 500 nM of dexamethasone (DEX) and 0.1mM of 8-(4-chlorophenylthio) adenosine 3', 5'-cyclic monophosphate sodium salt (pCPT-cAMP) in the presence or absence of insulin (10 nM) or test samples for 5 h at 37 °C. A significant ($p < 0.001$) inhibition of glucose production was observed after treatment with bitter and flavonoid fraction from *E. hyssopifolium*, alkaloid fraction of *T. cordifolia* and phenolic fraction of *E. alba* at the concentration of 100 µg/ml. While studying the effect of swertiamarin, swertisin, wedelolactone and gymnemagenin in dose dependent manner (10, 50 and 100 µg/ml) swertiamarin and wedelolactone gave excellent response where as swertisin produced a significant inhibition only at 100 µg/ml concentration. A study was undertaken to observe the effect of combination of these bio active constituents in the equivalent proportion they present in the mixture of their extracts in formulations. Swertiamarin, swertisin, wedelolactone and combination thereof (at 100 µg/ml dose) showed 65.5, 75.9, 65.2 and 31.6 % glucose production as compare to control. Combination of swertiamarin, swertisin and wedelolactone produced an equal response to that of 10 nM insulin. Amongst the studied formulations none produced any significant inhibition.

An insulin secretion effect of fractions and isolated compounds was studied on RINm5F cell line. The effect of was tested at 1.1 and 16.7 mM glucose concentration independently. None of the fraction found to raise insulin level significantly at 1.1 mM glucose concentration when compared with respective control where as flavonoid fraction of *E. hyssopifolium* and alkaloid fraction of *T. cordifolia* evoked insulin secretion from RINm5F cells at 16.7 mM glucose. A major constituent from flavonoid fraction swertiamarin and swertisin; an isolated alkaloids TCY, TCB and TCA; and a genin part of gymnemic acid, gymnemagenin were evaluated as an insulin secretagogue. Swertiamarin and swertisin showed significant increase in insulin secretion in hyperglycemic state and not in hypoglycemic state. Alkaloids TCY and TCB both found to increase insulin secretion by about 1.8 fold in presence of 1.1 mM glucose. They also produced positive activity in presence of 16.7 mM glucose at 100 µg/ml concentration, i.e., 2.19 (TCY) and 2.05 (TCB) fold high secretion as compare to control group. Unlike gymnemic acid, gymnemagenin found to raise insulin secretion by 1.5 times as compare to control at 100 µg/ml

concentration. The effect of combination of bioactive molecules, swertisin, TCA and gymnemagenin were studied as thrice of them were found to possessed potent insulin secreting action in hyperglycemic condition only. The direct comparison was done with 100 $\mu\text{g/ml}$ solution of individual constituent. Combination of biomarker increases insulin secretion by 2.97 fold as compare to control and it also showed significant activity as compare to individual component studied alone. The enhancement of activity in combination is very clear. Combination did not show any secretary effect in the absence of stimulus (1.1 mM glucose). None of the studied formulations found to produce any insulin secreting activity *in vitro*. This study was extrapolated to *in vivo* activity of isolated compounds and combination thereof on rats. Group treated with tolbutamide (10 mg/kg) was kept as positive control. In rats fasted overnight, vehicle (normal saline)/test/standard compounds were administered intraperitoneally (i.p.) on a body weight basis 90 min before the i.p. injection of glucose (3 g/kg body weight). Soon after the administration of glucose (0 min.) and subsequently after 60 min blood samples were collected. Serum insulin and glucose content were measured. Swertisin ($p < 0.05$) and TCA ($p < 0.001$) both possessed significant insulin secretagogue activity as compare to control group. The effect of TCA is supported by its glucose lowering action. Swertisin and gymnemagenin also showed significant ($p < 0.05$) hypoglycemic effect but the normoglycemic condition was not reach after 60 min. Combination of these three biomarkers also found to exhibit significant ($p < 0.001$) glucose lowering effect but the data didn't lead to the conclusion of being additive or synergism of due to the combination of markers. Hypoglycemic activity of swertisin and TCA may be owing to their activity on pancreatic β -cells. Hypoglycemic activity of gymnemagenin is well observed *in vivo* without sinificant increase of insulin secretion led to conclusion that gymnemagenin possessed hypoglycemic action due to some other mechanism except insulin releasing activity. Out of the studied formulation at the dose of 100 mg/kg p.o., formulation F-3 and and F-4 found to decrease serum glucose level significantly. F-1 and F-2 at this dose did not showed any significant decrease in serum glucose level.

Screening for biological activities ultimately gave few phytomolecules which acts via different mechanisms in treatment of diabetes mellitus. Characterization of the identified bioactive molecules was performed using various analytical techniques. In case of *E. hyssopifolium*, swertiamarin was identified by spectral comparison with reference standard. Another molecule was identified as C-glycosyl flavonoid which was characterized as swertisin by UV spectrophotometry/bathochromic shift studies. Three alkaloids have been

isolated from *T. cordifolia* stem. They were termed as TCA, TCY and TCB at the time of isolation and they have been characterized as magnoflorine, jatrorrhizine and palmatine respectively by CHN analysis, UV, IR and mass spectrometry. Gymnemagenin was identified by R_f value and spectral comparison with reported values. Further characterization was performed by IR, and NMR spectroscopy. Two compounds from *E. alba* were isolated one of which was confirmed as wedelolacone (by R_f value and spectral comparison with reference standard) and another compound (EA002) was identified as C-prenylated coumarin.

In conclusion, a C-glycosyl flavonoid, swertisin from EH contributed as one of the major constituent which acts via different mechanism to achieve normoglycemic status as presented in figure 123. Alkaloid from *T. cordifolia* also exerts hypoglycemic action via various mechanisms. Aldose reductase inhibition by alkaloid fraction and isolated alkaloids viz., magnoflorin, palmatine and jatrorrhizine was promising. This is in support of reported action of isoquinoline alkaloids as inhibitor of aldose reductase (Lee HS, 2002) and thus justifying the use of *T. cordifolia* in prevention of long term complication (cataract) of DM. In the study performed on rat hepatocytes, it produced a significant inhibition of dexamethasone and pCPT-cAMP induced glucose production. In an insulin secretagogue activity sulfonylurea compound (tolbutamide) was used as a positive standard which stimulate insulin secretion by blocking ATP-sensitive K^+ channels (K^+ -ATP channels) of the β -cell membrane, thereby causing depolarization, Ca^{2+} influx, and rise in cytoplasmic Ca^{2+} concentration (Mariot P et al., 1998). When treated with tolbutamide, RINm5F cells showed significant rise in insulin secretion both at 1.1 mM and 16.7 mM glucose exposure. In contrast, TC alkaloid fraction did not exhibit much rising effect in insulin secretion at 1.1 mM glucose concentration but a dose dependent insulin secreting activity was observed at hyperglycemic condition, i.e, 16.7 mM glucose. This study revealed that the mechanism by which TC alkaloid fraction act as insulin secretagogue may not be exactly same as that of tolbutamide. TC alkaloid fraction may remain inactive in hypo or normoglycemic condition and show its effect only in hyperglycemic environment.

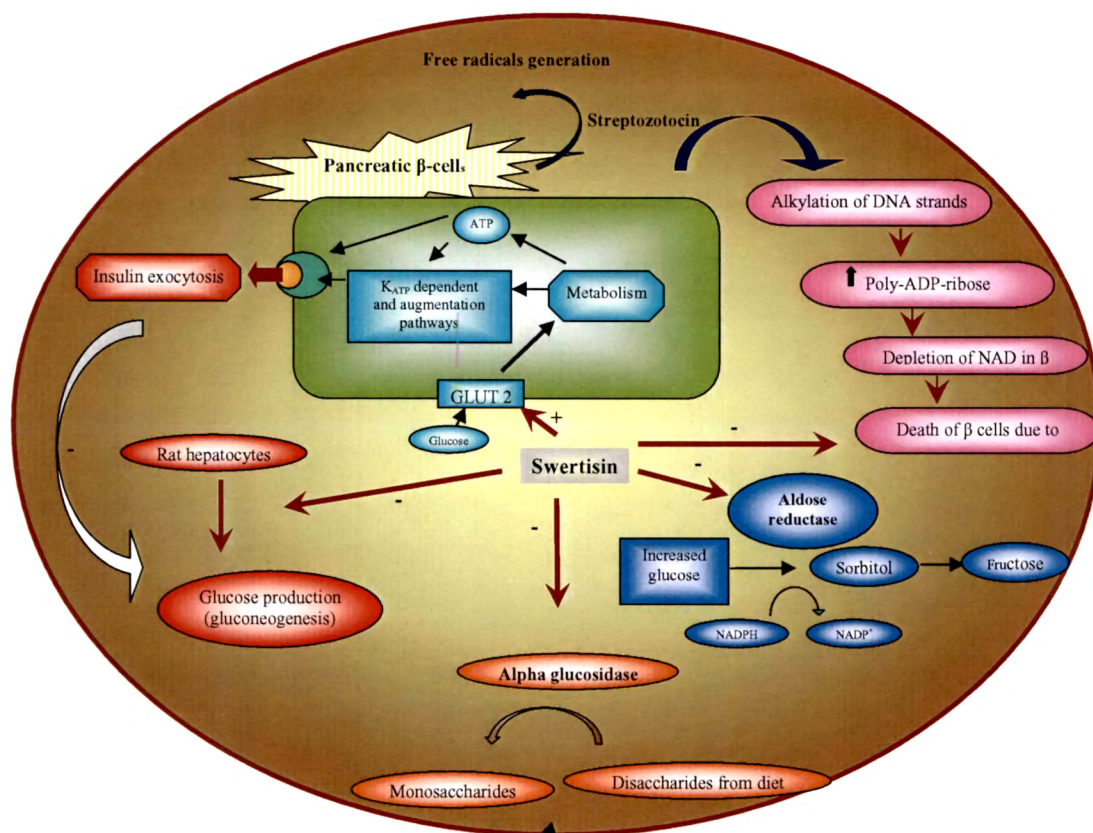


Figure 123 Mechanism of action of swertisin

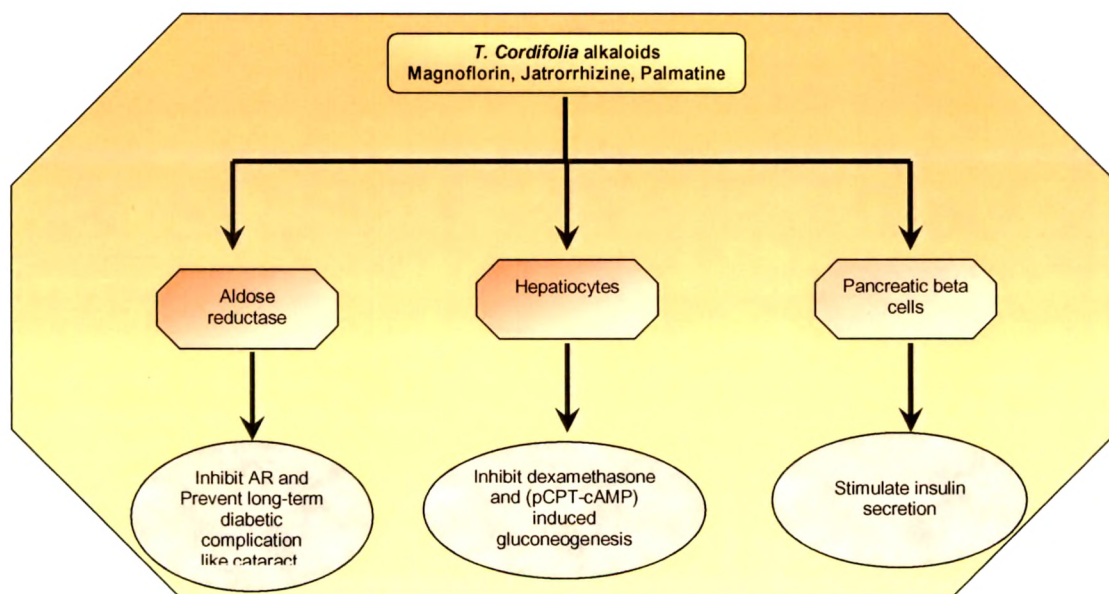


Figure 124 Mechanism of action of alkaloids of *T. cordifolia*.

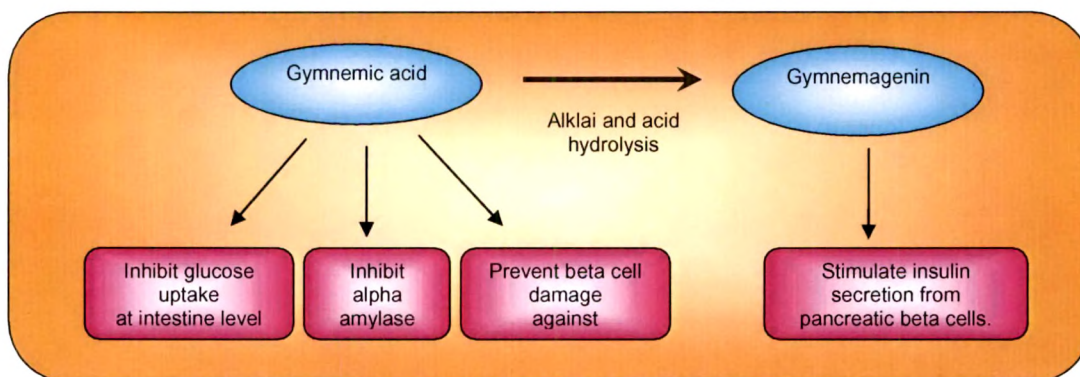


Figure 125 Mechanism of action of gymnemic acid and gymnemagenin.

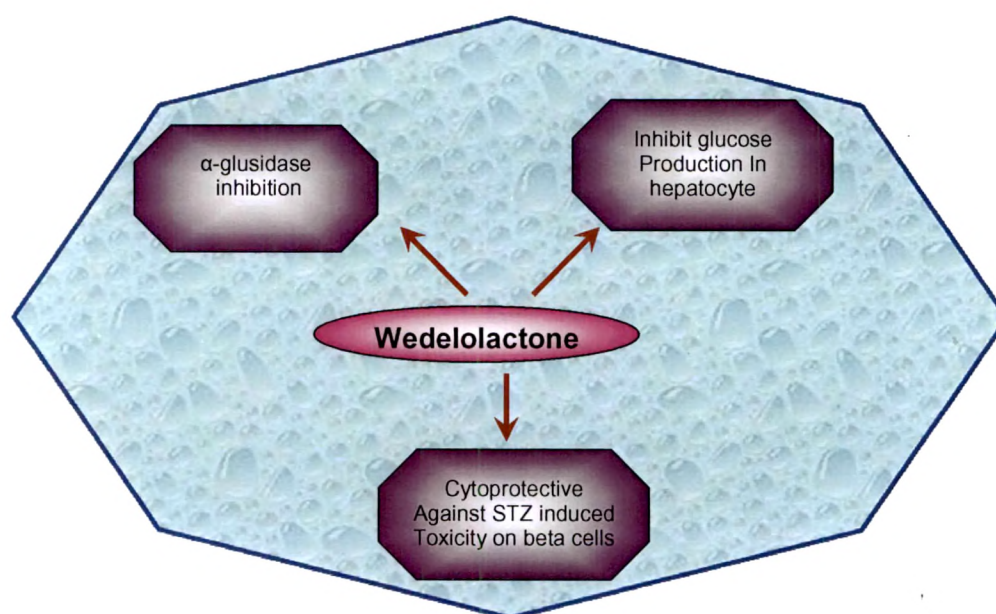


Figure 126 Mechanism of action of wedelolactone.

An alkaloid TCA (magnoflorine) was shown insulin secretion in RINm5F cells only in hyperglycemic condition where as TCY (jatrorrhizine) and TCB (palmatine) were also found to be effective as an insulin secretagogue at 1.1 mM glucose level. Magnoflorine in *In vivo* study restore the normoglycemic condition in 60 min after high dose glucose administration. Result of *in vivo* studies strongly justifies the hypoglycemic effect of TC alkaloid fraction in rats. A conclusion can be drawn that TC alkaloid fraction is effective as hypoglycemic and its activity is insulin secreting and not insulin like. The major contribution for this effect is of magnoflorine.

Gymnemic acid was found effective as inhibitor of glucose uptake at intestinal brush border membrane. A decreased glucose uptake is most probable by binding with the sodium-dependent glucose transporter 1, SGLT1. Thus may lead to wash out of glucose from the body. It may be one of the mechanisms for the hypoglycemic phenomenon after administration of these extracts noted by various investigators in animals or subjects. Gymnemic acid also showed a moderate inhibition of alpha amylase activity with IC_{50} value 74.63 $\mu\text{g/ml}$. It also exhibits some kind of protective action against oxidative stress induced damage of pancreatic cells. Gymnemic acid and gymnemagenin both were studied for their insulin secreting activity. Gymnemagenin was found to raise insulin secretion by 1.5 times as compare to control at the concentration of 100 $\mu\text{g/ml}$. *In vivo* results showed a negative result for gymnemagenin being insulin secretagogue but eventually showed significant hypoglycemic action in hyperglycemic rat. The results are indicative of gymnemagenin being a hypoglycemic agent which may act via some other mechanism.

Amongst the studied protocols, *Eclipta alba* phenolics fraction and sterol fraction were screened. Sterol fraction was found to have a great inhibitory effect on alpha amylase. A coumarin isolated from sterol fraction was identified as an active molecule responsible for this effect. Later on this molecule (EA002) found to have cyto-toxicity in MTT assay. Phenolic fraction showed inhibition of an enzyme alpha glucosidase with a great extent. A major coumestan from this fraction, wedelolactone was studied for the same activity and found to have potency as much as the positive control voglibose (IC_{50} value of wedelolactone was 1.0 $\mu\text{g/ml}$ and of voglibose was 1.23 $\mu\text{g/ml}$). Kinetic studies on enzymatic reaction indicated that the inhibition by wedelolactone was of competitive type. Phenolic fraction and wedelolactone were also possessed cyto protective activity when studied for MTT assay using STZ as standard toxicant. Wedelolactone showed to inhibit gluconeogenesis in rat hepatocytes. It does not show any action as insulin secreting agent *in vitro*.

For evaluation of synergetic effect, these bio markers in their combination were studied on biological models like effect on hepatic gluconeogenesis, insulin secreting activity *in vitro* and *in vivo*, and hypoglycemic activity *in vivo*. Results are discussed in above section where the combination in all cases possessed better activity as compare to equivalent amount of bio-marker alone. Thus, lower amounts of bio-markers are necessary to achieve the same effect in the case of a present synergism. The achieved synergy effect can amount to doubling or even greater multiplication of the expected effect. Connected with this option of dose

reduction, one can expect that at correctly chosen combination of natural products could have a better therapeutic efficacy than that of singular form. Studied marketed formulations have not found potent action in any particular model for biological activity. Most of the studied formulations did not show presence of bio-markers in detectable amount. Being multi-component systems all formulations may have multi target effects generated by various extracts with various constituents directed to different targets of biological systems. However, it was very much difficult to assign the therapeutic synergy effects to define combinations of bioactive compounds and to determine the molecular-biological mechanisms underlying the therapeutic equivalence. Nevertheless, it can be suggested that this conspicuous therapeutic equivalence must be due to synergy effects, as evidenced by various pharmacological investigations performed to prove the clinical efficacy of these formulations.